Ashutosh Kumar Shukla *Editor*

Spectroscopic Techniques & Artificial Intelligence for Food and Beverage Analysis

Springer

Spectroscopic Techniques & Artificial Intelligence for Food and Beverage Analysis

Ashutosh Kumar Shukla
Editor

Spectroscopic Techniques & Artificial Intelligence for Food and Beverage Analysis

Springer

Editor
Ashutosh Kumar Shukla
Department of Physics
Ewing Christian College
Prayagraj, Uttar Pradesh, India

ISBN 978-981-15-6494-9 ISBN 978-981-15-6495-6 (eBook)
https://doi.org/10.1007/978-981-15-6495-6

This Springer imprint is published by the registered company Springer Nature Singapore Pte Ltd.
The registered company address is: 152 Beach Road, #21-01/04 Gateway East, Singapore 189721, Singapore

To my parents

Preface

Spectroscopic techniques are potential tool to analyze the quality of food and beverages. Such techniques coupled with mathematical modeling and artificial intelligence offer enhanced spectral data analysis experience. This volume is a collection of five chapters and presents the current trends and practices dealing with spectral data analysis applying spectroscopic techniques equipped with artificial intelligence.

Chapter 1 by Jorge O. Caceres reviews the recent advances made by his group in the field of LIBS applications in food analysis. This chapter presents the new possibilities that LIBS can open up with the combination of mathematical modeling. Chapter 2 by Gunawan Indrayanto and Abdul Rohman presents food composition analysis using FTIR spectroscopy in combination with multivariate analysis. This chapter covers basics, instrumentation, sample preparation techniques, statistical analysis, and chemometrics with relevant examples. Chapter 3 by M. Moncada-Basualto and C. Olea-Azar presents a review of the spectrophotometric methods and electron spin resonance spectroscopy to determine antioxidant capacity of food. Chapter 4 by Grzegorz Piotr Guzik and Wacław Stachowicz describes the principles and details of thermoluminescence detection and talks about the procedural details to enhance the effectiveness of the technique. This chapter illustrates the application to different vegetable stuff. Chapter 5 by Sylvio Barbon Junior, Everton José Santana, Amanda Teixeira Badaró, Nuria Aleixos Borrás, and Douglas Fernandes Barbin describes multi-target regression methods as potential tool to enhance spectral data analysis. The presentation style in individual chapters is so as to introduce the novice researchers with the fundamentals and at the same time include the latest updates for the professionals.

I sincerely thank Dr. Naren Aggarwal, Editorial Director—Books, Asia, Medicine and Life Sciences, Springer for giving me the opportunity to present this book to the readers. I also thank Madhurima Kahali, Editor—Books, Medicine and Life Sciences, Springer and Mr. Selvakumar Rajendran, Production Editor (Books), Springer for their support.

Prayagraj, India — Ashutosh Kumar Shukla

Contents

1 Laser Induced Breakdown Spectroscopy in Food Analysis 1
Jorge O. Caceres

2 The Use of FTIR Spectroscopy Combined with Multivariate Analysis in Food Composition Analysis 25
Gunawan Indrayanto and Abdul Rohman

3 Spectrophotometric Methods and Electronic Spin Resonance for Evaluation of Antioxidant Capacity of Food 53
Mauricio Moncada-Basualto and Claudio Olea-Azar

4 Thermoluminescence the Method for the Detection of Irradiated Foodstuffs 77
Grzegorz Piotr Guzik and Wacław Stachowicz

5 Advantages of Multi-Target Modelling for Spectral Regression 95
Sylvio Barbon Junior, Everton José Santana, Amanda Teixeira Badaró, Nuria Aleixos Borrás, and Douglas Fernandes Barbin

About the Editor

Ashutosh Kumar Shukla is an Associate Professor of Physics at Ewing Christian College, University of Allahabad, India. In addition to journal publications, he also has a textbook and many edited volumes on, e.g. Medicine, Food Science, and Crude Oil to his credit. He has successfully completed research projects and presented his findings at various international events. He serves on the reviewer panel for numerous international journals, is a member of the International EPR Society (IES), and is a web member of the International Society of Magnetic Resonance (ISMAR).

Laser Induced Breakdown Spectroscopy in Food Analysis

1

Jorge O. Caceres

Abstract

The adulteration, quality control, food safety, and traceability are serious problems in the food industry and hold great importance for the customers. During the last years, laser induced breakdown spectroscopy (LIBS) analysis by direct measurement of the optical emission from laser-induced plasma has been the subject of research in food analysis, mainly because this technique presents a fast and cost effective method. The purpose of this article is to present an overview of the progress made by our research group in food analysis. Specific examples are given to illustrate the ability of this technique to carry out a rapid, qualitative, and quantitative analysis of different food samples. The implementation of combination of LIBS technique with mathematical modeling concretely neural networks algorithms, which have opened up new possibilities, are also discussed with available experimental data and relevant results.

Keywords

Food analysis · Laser induced breakdown spectroscopy (LIBS) · Wine analysis · Honey adulteration · Oils · Milk

1.1 Introduction

Laser induced breakdown spectroscopy (LIBS) analyzes a sample by direct measurement of the atomic emission of the elements from a laser-induced plasma

J. O. Caceres (✉)
Laser Chemistry Research Group, Department of Analytical Chemistry, Faculty of Chemistry, Complutense University of Madrid, Madrid, Spain
e-mail: jcaceres@ucm.es

A. K. Shukla (ed.), *Spectroscopic Techniques & Artificial Intelligence for Food and Beverage Analysis*, https://doi.org/10.1007/978-981-15-6495-6_1

generated by the ablation of the sample, providing an immediate spectral fingerprint which is representative of its elemental composition [1]. LIBS provides several advantages over conventional methods for elemental analysis by (a) eliminating the sample preparation step for analysis; (b) performing the analysis in any state of matter (solid, liquid, gas); (c) providing a fast analysis in a few seconds; (d) requiring a very small amount of sample, in the order of micrograms, that is vaporized from the surface of the sample; and (e) providing simultaneous detection of all elements without bias, including those present in molecules (which are atomized during the process) [2]. Although there is a loss of molecular information in plasma, this technique has provided excellent results for the identification of many polymer organic compounds [3] or bacterial samples [1, 4]. In these studies, emission lines of C, H, N, O and intensity ratios such as C/H, C/O, and C/N have been used for the classification of organic explosives [5, 6]. Given these advantages of detection of compounds of organic origin, LIBS has drawn attention to the food analysis in different types of samples such as wine [7], milk [2, 8], bread [9, 10], meat [11] vegetables [12, 13] tea samples [14], and trace elements in seafood [15].

The purpose of this paper is to briefly review the work done and recent advances made by our research group particularly in food analysis. The review covers studies with specific examples to illustrate LIBS ability to carry out a rapid qualitative and quantitative analysis of different food samples. The implementation of combination of LIBS technique with mathematical modeling concretely neural networks algorithms is also discussed along with available experimental data and relevant results.

LIBS qualitative analysis methods developed rely on performing an instantaneous identification of the sample using a unique feature of LIBS, which is its ability to generate a spectral "fingerprint" of the sample from the emission spectra, corresponding to of the nature of the sample and its composition. Thus, LIBS provides a unique spectrum, representative of the sample under analysis, which can be analyzed by multivariate data analysis techniques or neural networks (NNs) algorithms. Using a correlation procedure, the developed LIBS-NN system can be trained by supervised algorithms in order to recognize spectra of test sample from a set of different samples, evaluating the similarity of unknown test spectra against a reference spectral library of classified samples. The choice of NNs as classification method has been made due to its significant identification capability with a relatively simple implementation [16].

1.2 Experimental LIBS Set-Up

The LIBS technique and the methodology used in the present work together with the most significant experimental conditions have been previously described [1]. Each study has its own measurement parameters. Thus, only the experimental conditions relevant to this work are presented here and should be considered as a guide to the experimental system that can be used. LIBS measurements were obtained using a Q-switched Nd: YAG laser (Quantel, Brio model) operating at 1064 nm, with a pulse

duration of 4 ns full width at half maximum (FWHM), 4 mm beam diameter, and 0.6 mrad divergence. Samples were placed over an X–Y–Z manual micro-metric positionator with a 0.5 μm stage of travel at every coordinate to ensure that each laser pulse impinged on a fresh position. The laser beam was focused onto the sample surface with a 100 mm focal-distance lens, producing a spot of 100 μm in diameter. The best signal-to-background ratio was achieved at 42 mJ of pulse energy with a repetition rate of 1 Hz. The laser crater profile was measured by means of a confocal microscope after laser pulse irradiation on a fresh position. A narrow crater was created with a diameter of 450 μm and 140 μm in depth. Emission from the plasma was collected with a 4-mm aperture, and 7 mm focus fused silica collimator placed at 4 cm from the sample, and then focused into an optical fiber (1000 μm core diameter, 0.22 numerical aperture), coupled to a spectrometer. The spectrometer system was an EPP2000, StellarNet (Tampa, FL) with a gated CCD detector. A grating of 300 l/mm was selected; a spectral resolution of 0.5 nm was achieved with a 7 μm entrance slit. The wavelength range used was from 200 to 1000 nm. Therefore, 2048 data points were recorded for each sample. The detector integration time was set to 1 ms to prevent the detection of bremsstrahlung, the detector was triggered by a 2 μs delay time between the laser pulse and the acquired plasma radiation using a digital delay generator (Stanford model DG535). The spectrometer was computer-controlled using an interface developed in Matlab.

1.3 Neural Network Theory

Chemometric methods used for the classification of samples in the studies included have been widely described in the literature; therefore, a brief description is only presented here. There is a wide range of chemometric approaches for the purpose of developing classification models in the sample discrimination processes [17–20]. Nevertheless, it is not a straightforward task to choose an appropriate method in each case and this selection process involves a careful study of the raw data and the results required in order to achieve a satisfactory classification result. An appropriate chemometric method must be able to perform a classification when all the samples presented for the training of the model are tested and classified correctly (high sensitivity), as well as the unknown samples of the same class not included in the training step are also correctly classified (high generalization ability). Furthermore, in order to obtain a robust classification, the model must be able to classify a sample that does not belong to any class as unassigned and not classify it incorrectly as one of the classes/samples used in the training of the model (high robustness). Different chemometric methods have been employed in LIBS data analysis to perform reliable classification for various types of samples [21–26], even at remote sites such as rock classification on Mars. However, none of these works includes a complete analysis of the performance of these methods evaluating sensibility, generalization ability, and robustness with very similar samples. In the studies carried out by our group [26], special care was taken to deal with and include all these classification parameters. Some examples of such studies in food analysis are commented herein.

1.3.1 Neural Network Model

Home-made neural network software was developed that was specifically designed and optimized to deal with the problem of sample classification. The NNs model was based on a multilayer perceptron, feedforward, supervised network consisting of several neurons (information processing units) arranged in two or more layers receiving information from all of the neurons of the previous layer. The connections are controlled by a weight that modulates the output of the neuron before inputting its numerical content into a neuron in the next layer. The process that optimizes the weights, i.e., the learning or training process was based on a back-propagation (BP) algorithm [27, 28]. The inputs from each neuron are added by an activation function, and the result is transformed by a transfer function that limits the amplitude of the neuron output. In this work, the hyperbolic tangent sigmoid function was used as the NN transfer function. Every NN model was estimated using Matlab software (Mathworks, 2010a).

The NN topology consists of three layers (input, hidden, and output), which is widely used to model systems with a similar level of complexity [29]. As mentioned the conditions were those used in our studies, in particular, the input layer consisted of 2048 nodes (spectral response in the 200–1000 nm wavelength range). The number of neurons in the hidden layer was kept around 10 in all of the studies, in order to avoid overfitting of the models. The output layer that provides the classification results comprised of J neurons (where $J =$ number of reference samples used). The value obtained for the J neurons provided an estimation of the similarity between the reference sample spectra and the testing sample spectrum.

1.3.2 Neural Network Model Training

Since supervised learning has been used for creating the NNs models, for the optimization of the weight matrix, input and output data that adequately characterized the system to be modeled was used. The spectral data of the training library was randomly divided as a part of the training process into two subsets: 80% (64 spectra) for training and 20% (16 spectra) for self-validation of the model. Once the training and self-validation process was carried out, the models were validated by testing the spectra from the samples.

The identification process of the NNs model is based on their ability to detect the degree of similarity of the new spectrum to each reference spectra used to train the NN model in the training process. During the training process, each class of sample was associated with an identification number in the output layer. Therefore, correct identification is obtained if the output from the NN model for the test samples of the same classis matched with the identification number assigned to the sample at the training step. An identification number of “Zero” was always used to indicate no match at all.

NN training was achieved by applying the BP algorithm based on the conjugate gradient method [30], one of the general-purpose second-order techniques that helps minimizes the goal functions of several variables. Second order indicates that such methods use the second derivatives of the error function, whereas a first-order technique, such as standard back-propagation, uses only the first derivatives. To determine when the training should be stopped, an early stopping criteria based on performance improving (error rate) of the validation set [31]. The number of epochs was not relevant in this case. To avoid an overfitting of the NN model, the learning process was repeated until a minimum of the mean square error (MSE) of the verification data, defined in Eq. (1.1), was reached:

$$\mathrm{MSE} = \frac{1}{N}\sum_{k}^{N}(r_k - y_k)^2 \tag{1.1}$$

where N, y_k, and r_k are the number of input data, the response from each output neuron, and the observed output response, respectively. A detailed description of the calculation process is provided in the literature [27, 31].

1.3.3 Neural Network Model Validation

The parameter, accuracy (A), was used to assess the classification performance of the created models along with the relative frequency of correct and incorrect classification (Eq. (1.2)) and was evaluated [1, 32].

$$A = \frac{\mathrm{TP} + \mathrm{TN}}{\mathrm{TP} + \mathrm{TN} + \mathrm{FP} + \mathrm{FN}} \tag{1.2}$$

In a classification process the output has only two possibilities: positive (P) or negative (N). There are therefore four possible results from this binary classifier. If the output is P, a true positive (TP) or false positive (FP) is observed if the actual value is P or N, respectively. Conversely, a true negative (TN) or a false negative (FN) is observed if the predicted output is N and the actual value is N or P, respectively [1].

In order to measure the sensitivity and generalization ability of the NN model, "success rate" has been used, which has been determined by calculating the percentage of samples correctly classified over the total number of test spectra. In all studies the sensitivity, also taken as internal validation, was evaluated by the capacity of the model to provide correct classification for the test library of the samples used in calibration, whereas the generalization ability was measured as the percentage of correctly classified samples of the same or similar class that were not used in the training of the model. Another very important feature of the classification models is the robustness, which is measured by the ability to assign as "unknown" giving an output of zero to samples of unknown origin. The success of robustness

test lies in when the test samples of a completely class that was not included in the training step are considered as an outsider and not belonging to any of the classes of training data set [21]. Thus, the robustness of the model, also considered as independent external validation, was performed by removing one class from the training set and assessing the results for the excluded class.

To consider a sample correctly classified, the prediction of the model must match with the actual class by an arbitrary threshold of spectral correlation (SC) (Eq. (1.3)) higher than 90% and less than 20% to the other classes, otherwise is considered incorrectly classified. A sample was classified as unknown when the SC was less than 90% for all classes.

$$\mathrm{SC} = \frac{100}{N} \sum_i \delta_i \tag{1.3}$$

where δ_i is the number of spectra classified correctly and N is the total number of spectra.

1.4 Results

1.4.1 Wine Analysis

The certification of the protected designation of origin (PDO) is one of the most important parameters to be controlled in order to protect the production and origin of agroalimentary products. Since the introduction of European regulations control [33] on this matter, different strategies have been designed by the wine companies for the confirmation of the authenticity of wines in order to bring improvement in the PDO controls. Basically the parameters that are considered for the determination of the quality of wine products include the type of grape, harvest, geographical origin, and vintage; however, it is not a straightforward task to recognize these indicators on the consumers' end. Therefore, the only and clear sign of quality that is used by the companies for the promotion of their products at the market is PDO, and this parameter finally influences the final decision by the consumers [34].

The adulteration in case of wine products is done by the addition of any external substance to the natural wine changing its composition and features. The adulteration may occur in many ways; however, this is mostly done by addition of water and sugar, mixing with lower quality wines and label replacing [35]. Water makes 81%, while ethanol makes between 11 and 15% of wine. The key compounds that are two types of flavonoids, anthocyanins and flavanols, provide color and astringency, and are also responsible for the organoleptic properties and quality of wine. Other organic compounds in small amounts, such as acids, alcohols, phenols, nitrogenous compounds, and inorganic substances, represent the remaining 7%, making wine a complex sample and difficult sample to analyze [36, 37].

The sensorial analyses together with chemical assays, and mineral content analysis may not be adequate for determining the PDO of wine [35]. Chromatographic techniques on the other hand [38–40] require to conduct separate analysis of each component in the wine being slow and expensive process. The identification of grape variety by means of isotopic analysis [41, 42], nuclear magnetic resonance (NMR) [43, 44], or ADN/aRNA [45] techniques are generally used. These techniques perform the identification based on their capacity of generating a fingerprint of wine sample and produce accurate results, but require a large amount of sample and expensive consumables which increases the cost and duration of the analysis.

Here we evaluate the laser induced breakdown spectroscopy (LIBS) technique for the discrimination and the determination of geographical origin of red wines. LIBS technique is based on the interaction of a laser beam with a material target generating a plasma, the emission of the plasma contains spectroscopic information of excited atoms and ions present in the sample and reflecting its elemental composition [46]. The elemental composition of wine is generally related to soil composition, grape variety, climate conditions, yeasts, and winemaking [39]. The analysis of these LIBS spectral fingerprints by the supervised classification models NN has already shown successful results in many areas of knowledge for sample classification [16, 26, 47, 48].

Although LIBS analysis does not require sample preparation, however in some cases avoiding a sample preparation goes in detrimental of the technique limiting its analytical performance. The change of the physical state of the sample transforming the liquid into solid has already been described as sample preparation [49]. The liquid-to-solid process increases the time of analysis and introduces changes in chemical composition but on the other hand offers significant improvements in the increase of the ablation rate, higher plasma temperature, and electron density as well as a better laser-to-solid interaction [50–52]. In addition, the avoiding of inherent drawbacks of manipulating liquid samples such as splashing and surface ripples helps obtaining lower limits of detection, better repeatability, and sensitivity [53, 54]. Different liquid-to-solid matrix conversion protocols have been described in the literature involving precipitation, filtering, and pellets formation procedures [53, 55, 56]. Herein, the transformation of the liquid wine sample into gels by adding a natural collagen and its subsequent drying in an air assisted oven has been used as a new sample preparation protocol.

In this work we work on the identification of the adulteration of wines collected from Spanish local markets and evaluate the capacity of LIBS coupled with NN to detect the PDO of wines with negligible compositional and spectral differences and to improve the recognition capacity of extremely similar samples that have fewer physical and spectral differences between them.

1.4.1.1 Wine Samples

Thirty-eight Spanish red wines from eleven protected designation of origin, three foreign red wines, and four table wines were purchased in retail stores. Main Spanish wine regions were selected including La Mancha, Ribera de Duero, Rioja, Valdepeñas, Vinos de Madrid, Cariñeña, Ribeiro, Ribera del Guadiana, Navarra,

Somontano, and Toro. The foreign wines with origin from Germany, France, and Italy were also included in the study. Most of the wines included in the study were elaborated with Tempranillo grapes, although Cabernet Sauvignon, Garnacha, Tinta de Toro, and Syrah were also considered. All samples belong to the 2011 vintage and were not affected by aging period (young wine). Table 1.1 shows sample information including sample ID, commercial brand, and type of grapes.

Sample Preparation A gel of wine sample was made using a commercial collagen. For this purpose, 50 mL of wine sample were poured into a beaker and 1 g of collagen gel was added and dissolved in the wine sample. 2.4 ml of this solution were allowed to stand for 15 min until the gel was formed in a square petri dish of 4 $\times$ 4 cm. The gelled sample was introduced in a forced ventilation oven at 35 $\pm$ 2 °C during 12 h to evaporate the water, obtaining a dry solid sample, which was completely flat with a thickness of approximately 0.35 mm. Figure 1.1 shows an example of dry gel and the craters formed by single laser shots. In this process not only LIBS analysis was simplified but also pre-concentration of the sample (pre-concentration factor of 1:5) was done which improved the limits of detection. All samples were prepared into gels at the same time so that same conditions could be maintained and making sure that the wine components were not degraded or oxidized in the process of jellification.

1.4.1.2 Wavelength Range Selection

In case of LIBS spectra the intensity value at each wavelength is referred to as variable. Each spectrum was composed by 2048 variables taking into account the CCD pixels. For the NN analysis a reduction in the number of variables used as inputs was done, which has brought important advantages in the classification process, enhancing the robustness of the models, and being more efficient in the discrimination process, without a loss of meaningful information. Since the organic nature of the gel may affect C, H, N, O signals, the main emission lines from the mineral elements of wine, Mg, Ca, K, and Na were selected in seven wavelength ranges resulting into 355 variables (Table 1.2). Furthermore, the emission lines for these elements in the selected wavelengths intervals were not observed in the pure gel. The selection of several ranges may not describe the data fully; however, it describes the trend in PDO instead of the particular wine. The reduction of variables decreases the discrimination power of the NN model but increase the ability to generalize.

1.4.1.3 LIBS Analysis

The samples were measured directly in air at room condition. Each LIBS spectrum was acquired from a single-shot measurement and a total of 100 spectra were recorded for each wine sample by moving the sample stage about 0.25 mm to expose a fresh portion of the sample surface and avoiding areas irradiated by previous shots. For the samples M1, D1, R1, V1, and VM1, four data sets of 100 spectra were obtained: the first data set (training library) was used to create the NN model, whereas the last three data sets (replicate libraries) were used for validation purpose.

Table 1.1 Samples used in the study

PDO	Sample ID	Commercial brand	Grape variety	Vintage
La Mancha	M1	Libertario	Tempranillo, Garnacha	2.011
	M2	Vereda Mayor	Tempranillo	2.011
	M3	Don Lucio	Tempranillo	2.011
	M4	Fidencio	Tempranillo, Garnacha	2.011
	M5	Monte Don Lucio	Cabernet sauvignon	2.011
Ribera del Duero	D1	Dehesa	Cabernet sauvignon	2.011
	D2	Valpincia	Tempranillo	2.011
	D3	Barón de Santuy	Tempranillo, Cabernet	2.011
	D4	Mayor de Castilla	Tempranillo	2.011
	D5	Sangre de Castilla	Tempranillo	2.011
Rioja	R1	Viña Espolón	Tempranillo, Garnacha	2.011
	R2	Antaño	Tempranillo, Garnacha	2.011
	R3	Solar Viejo	Tempranillo, Garnacha	2.011
	R4	Barón de Urzande	Tempranillo, Garnacha	2.011
	R5	Castillo de Albali	Tempranillo	2.011
Valdepeñas	V1	Vega del Cega	Tempranillo	2.011
	V2	Calle Real	Tempranillo	2.011
	V3	Viña Albali	Tempranillo, cabernet	2.011
	V4	Señorío de Los Llanos	Tempranillo	2.011
	V5	Tanis	Tempranillo	2.011
Vinos de Madrid	VM1	Puerta de Alcalá	Tempranillo, syrah	2.011
	VM2	Vega Madroño	Tempranillo, Garnacha	2.011
	VM3	Alma de Valdeguerra	Tempranillo	2.011
	VM4	Puerta de Hierro	Tempranillo	2.011
	VM5	Jesús Díaz	Tempranillo, syrah	2.011
Cariñena	CR	Castillo de Aguaron	Garnacha, syrah	2.011
Ribeiro	RB	Pazo	Tempranillo, cabernet	2.011
Ribera del Guadiana	RG	5 Viñas	Tempranillo, Garnacha	2.011
Navarra	NV	Diácono	Tempranillo, Garnacha	2.011
Somontano	SM	MonteSierra	Tempranillo, cabernet	2.011
Toro	TR	Cermeño	Tinta de Toro	2.011
Table wine	TW1	Conde Noble	Mixture	2.011
	TW2	Don Simon	Mixture	2.011
	TW3	Eroski	Mixture	2.011
	TW4	Viñas Altas	Mixture	2.011
Chianti	CH	Corte Alle Mura	Sangiovese	2.011
Dornfelder	DR	Dornfield	Dornfelder	2.011
Valle central	VC	Cimarosa	Cabernet sauvignon	2.011

All spectra were normalized in order to avoid data variations as a result of variations in the laser pulse energy. The normalization was done by the intensity of one specific spectral line, i.e., K (I) 766.49 nm [57]. The spectral information of each sample was

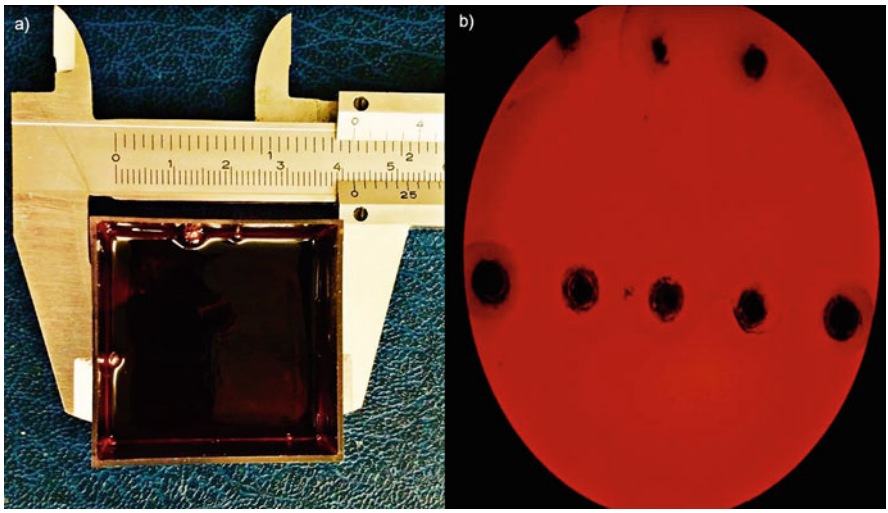

Fig. 1.1 (**a**) Sample after preparation. (**b**) Dry gel of wine sample with visible laser spots

Table 1.2 Wavelength range considered for wine analysis

Element	Wavelength range (nm)
Mg	271–291
Ca	311–340, 390–429, 513–524
Na	581–598
H_α	640–675
K	760–783

obtained in less than 2 min considering the integration time of the spectrometer and the frequency of laser pulses that was fixed to 1 Hz (Fig. 1.2).

1.4.1.4 Sensitivity Tests

For the training of the NN model, the training library samples M1, D1, R1, V1, and VM1 were used, producing an input matrix with 355 rows (number of variables) and 500 columns (5 × 100 spectra of each PDO). After the learning process of NN model is done, new spectra are presented for the classification. For the first validation procedure, three replicate samples of the wines used in training step were prepared and measured at the same condition, generating three new data sets used to validate the model. Although the same wine is considered to produce the replicates, each replica was prepared in different gels, assessing possible sample preparation differences. These data sets were not presented to the NN for training and are individual set of spectra. Table 1.3 gives the results of the sensitivity analysis for NN prediction of wine replicates. The model is considered sensitive if the correct classification is high and the misclassification rates are low. A high sensitivity is achieved for all replicates with an average correct classification rate of 99.2% along with a negligible rate of incorrect classification and misclassification.

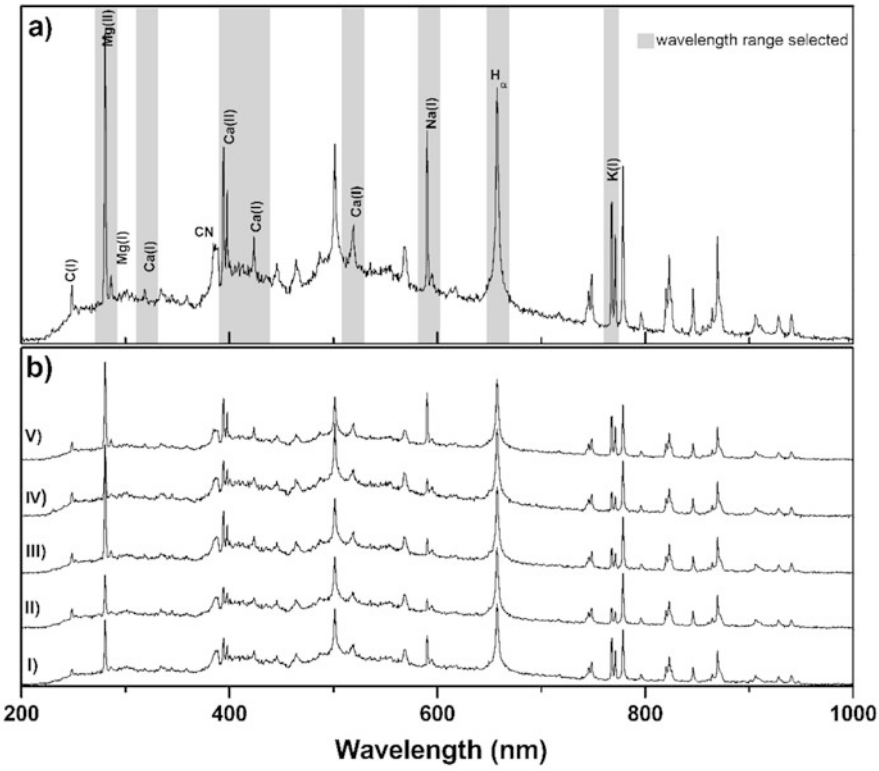

Fig. 1.2 (**a**) LIBS spectrum of Rioja PDO with the assignation of emission lines and selected the wavelength ranges as inputs to the NN have been highlighted in gray color. (**b**) Typical spectrum of (**I**) dry gel, (**II**) M1 (La Mancha: Libertario), (**III**) D1 (Ribera del Duero: Dehesa), (**IV**) R1 (Rioja: Viña Espolón), (**V**) V1 (Valdepeñas: Vega del Cega), (**VI**) VM1 (Vinos de Madrid: Puerta de Alcalá) within the spectral range of 200–1000 nm

This demonstrated that the model was able to classify new spectra belonging to the samples used for training despite the intrinsic sample-to-sample variability in the preparation of each gel.

1.4.1.5 Generalization Ability Test

Validation procedures assessing the generalization ability of the model must be performed. This is done as a second validation, where the same NN model as discussed in the previous section was used. In order to estimate the generalization ability of the model, four different wine brands belonging to the PDOs used in the training were tested to obtain the prediction result. The results are presented in Table 1.4, showing an average of 98.6% of correct classification, without any wine unclassified or misclassified. Therefore, all wine samples were correctly assigned to their respective classes showing a high generalization ability and showing that the model was flexible and lacked overfitting. A high rate in the correct classification

Table 1.3 Classification results to sensitivity test (internal validation)

	Predicted group membership (spectral correlation, %)					
Sample	La Mancha	Ribera del Duero	Rioja	Valdepeñas	Vinos de Madrid	Unclassified
M1-replicate 1	100	0	0	0	0	0
M1-replicate 2	99	0	1	0	0	0
M1-replicate 3	99	1	0	0	0	0
D1-replicate 1	0	100	0	0	0	0
D1-replicate 2	0	98	0	0	0	0
D1-replicate 3	0	100	0	0	0	0
R1-replicate 1	0	0	100	0	0	0
R1-replicate 2	0	1	99	0	0	0
R1-replicate 3	0	1	98	0	1	0
V1-replicate 1	0	0	0	100	0	0
V1-replicate 2	0	1	0	99	0	0
V1-replicate 3	1	1	0	98	0	0
VM1-replicate 1	0	0	0	0	100	0
VM1-replicate 2	0	0	0	0	99	1
VM3-replicate 3	1	0	0	0	99	0

Table 1.4 Classification results for the generalization ability test

	Predicted group membership (spectral correlation, %)					
Sample ID	La Mancha	Ribera del Duero	Rioja	Valdepeñas	Vinos de Madrid	Unclassified
2M2	98	0	1	1	0	0
2M3	100	0	0	0	0	0
2M4	98	1	0	1	0	0
2M5	99	1	0	0	0	0
2D2	2	98	0	0	0	0
2D3	0	99	1	0	0	0
2D4	1	98	1	0	0	0
2D5	0	100	0	0	0	0
2R2	0	0	100	0	0	0
2R3	1	0	98	0	0	1
2R4	1	1	97	0	1	0
2R5	0	2	97	1	0	0
2V2	0	0	0	100	0	0
2V3	2	1	0	97	0	0
2V4	1	0	0	98	0	1
2V5	0	0	0	100	0	0
2VM2	1	0	0	1	98	0
2VM3	0	0	0	0	99	1
2VM4	0	0	1	1	98	0
2VM5	0	0	0	0	100	0

and low rate of incorrect classification and misclassification were sought, which means that the model was able to generalize and correctly classify other spectra than those with which it was trained.

1.4.1.6 Robustness Test

The robustness of the NN model was assessed, evaluating the response of the model to detect samples completely external and independent of the training set. For this purpose, thirteen wine samples were measured and introduced into the NN model. Six wines with Spanish PDO, four table wines, and three foreign wines were considered. A robust model suggests a high capacity to detect unknown samples "correctly as unknown,", without decreasing the predicted accuracy of the known samples. Table 1.5 presents the NN model classification results when completely unknown samples were introduced to the model. The NN model classified correctly these wine samples as unknown. None of the samples was classified as belonging to other classes, providing a high robustness. Only in case of TW3 a spectral correlation of 70% was obtained in the La Mancha class which can be attributed to the fact that in the elaboration of table wines a variety of grapes are used, which in many cases come from the La Mancha region. However, the SC is lower than

Table 1.5 Classification results to the robustness test (external validation)

	Predicted group membership (spectral correlation, %)					
Sample ID	La Mancha	Ribera del Duero	Rioja	Valdepeñas	Vinos de Madrid	Correctly as unknown
CR	5	0	5	0	0	✓
RB	0	0	8	0	0	✓
RG	4	0	2	0	0	✓
NV	2	0	0	2	0	✓
SM	7	3	0	0	5	✓
TR	40	0	2	0	3	✓
TW1	32	0	0	0	0	✓
TW2	12	0	32	0	0	✓
TW3	70	0	0	0	10	✓
TW4	22	0	0	0	8	✓
CH	0	0	0	7	0	✓
DR	0	8	0	2	0	✓
VC	0	0	0	7	0	✓

the fixed threshold value and therefore classified as unknown to the model. This highlights the robustness of NN in dealing with samples of unknown classes.

The results were satisfactory and the proposed methodology was used for the analysis of red wines. The wavelength ranges selected, only considering the major elements of the wine, together with NN analysis is enough to perform successful classification of wines which is interesting as it was done without performing any quantification of the elements. The selected intervals provide a characteristic fingerprint of the sample considering the peak profiles that include information from the plasma which is useful in the classification process. Having the capacity to model complex non-linear input–target relationships, NN analysis was able to recognize the PDO pattern and classify correctly all the wines tested, maximizing inter-PDO differences and minimizing intra-PDO variability. All validation procedures have produced successful results. A high sensitivity and generalization ability were achieved with an average of 99.2% and 98.6% of correct classification, respectively, with a robustness of the 100%.

Thus, this work offers the possibility to perform red wine classification based on LIBS measurement combined with multivariate chemometric method (NN). This LIBS/NN methodology was able to distinguish between geographically close regions. From the legal point of view, this methodology seems to be sufficiently reliable to be used in quality control procedures as a screening tool. Methodologically, the developed LIBS-NN system provides a simple and fast way of identifying the PDOs without carrying out cumbersome analysis on experimental as well as mathematical scale.

1.4.2 Olive Oils Analysis

The adulteration and traceability of olive oils are some of the grave issues faced by olive oil industry. Here, a similar method based on laser induced breakdown spectroscopy (LIBS) and neural networks (NNs) has been developed and applied to the identification, quality control, trace ability, and adulteration detection of extra virgin olive oils [16].

Moreover, the usefulness of the developed method was demonstrated. Thus, this model was found to be appropriate and useful in the identification of these chemical compounds on line, for quality and control processes in the food industry, with adequate accuracy and without pretreatment of samples. In addition, single-shot measurements were sufficient for clear identification of the olive oils studied. Taking this into account, the optimized NN model provides reliable results (sample identification) for all samples analyzed. This result is the best indicator of the capacity of the methodology presented.

1.4.3 Milk Studies

This study focuses on the quantification of melamine in adulterated toddler milk powder. It is based on two methodologies developed; univariate analysis using CN emission band and multivariate calibration NN model obtaining correlation coefficient (R^2) values of 0.982 and 0.999, respectively. The results of the use of LIBS technique coupled with chemometric analysis are discussed in terms of its potential use in the food industry.

Due to its nutritional value, milk is counted as one of the most consumed foods containing the main ingredients to sustain life, especially in early stages such as toddlerhood and early childhood, where it is the principal intake. In 2016, the world milk production reached 816 million tons/year where the European states took the lead among the major milk exporters with 19.2 million tons [58]. This shows a great economic importance of milk products which resultantly makes milk as one of the main targets of adulteration. The adulteration consists of the addition of any substance to the natural milk, which changes its composition and may occur in many different forms. The most common practice is the addition of water to raw milk, mixing milk of different animal species, fat replacement, and modification of the protein or nitrogen content by introducing an adulterant as melamine ($C_3H_6N_6$). In the latter case, where melamine is used as an adulterant, its detection becomes a difficult job in routine analysis is that base on the measurement of nitrogen content of the milk. This occurs because the non-protein nitrogen cannot be detected by usual procedures for protein determination [59–61]. Therefore, it is needed to develop the methods that are simple, sensitive, and reliable to perform such analyses with the possibility to be employed for an on-line analysis.

LIBS technique has not been sufficiently explored in food control analysis and only few studies have been carried out till this time [10, 62–64]. The combination of LIBS with chemometric methods offers the possibility to be used in a fast, automatic, and on-line manner as has already been demonstrated with successful results for sample classification and quantification [7, 16, 26, 47, 48, 65].

A wide study on the formation of CN fragments presents in the plasma and its correlation with the carbon content of the sample is shown by Baudelet et al. [66]. In the case of the milk analysis by LIBS, G. Bilge et al. [62] demonstrate that LIBS in combination with multivariate methods can be successfully used to distinguish between skimmed milk powders and whey powders, and also to quantitatively determine the adulteration ratio of skimmed milk powder and sweet/acid whey powder. The quantification of melamine in toddler milk powder samples was performed, particularly observing the CN band emission correlating it to adulteration ratios. Conventional univariate calibration curve and a multivariate NN quantification procedure have also been compared.

1.4.3.1 Quantitative Analysis: Adulteration with Melamine

A commercial toddler milk sample was adulterated with different amounts of melamine at concentrations between 1% and 6% to plot the calibration curve. The

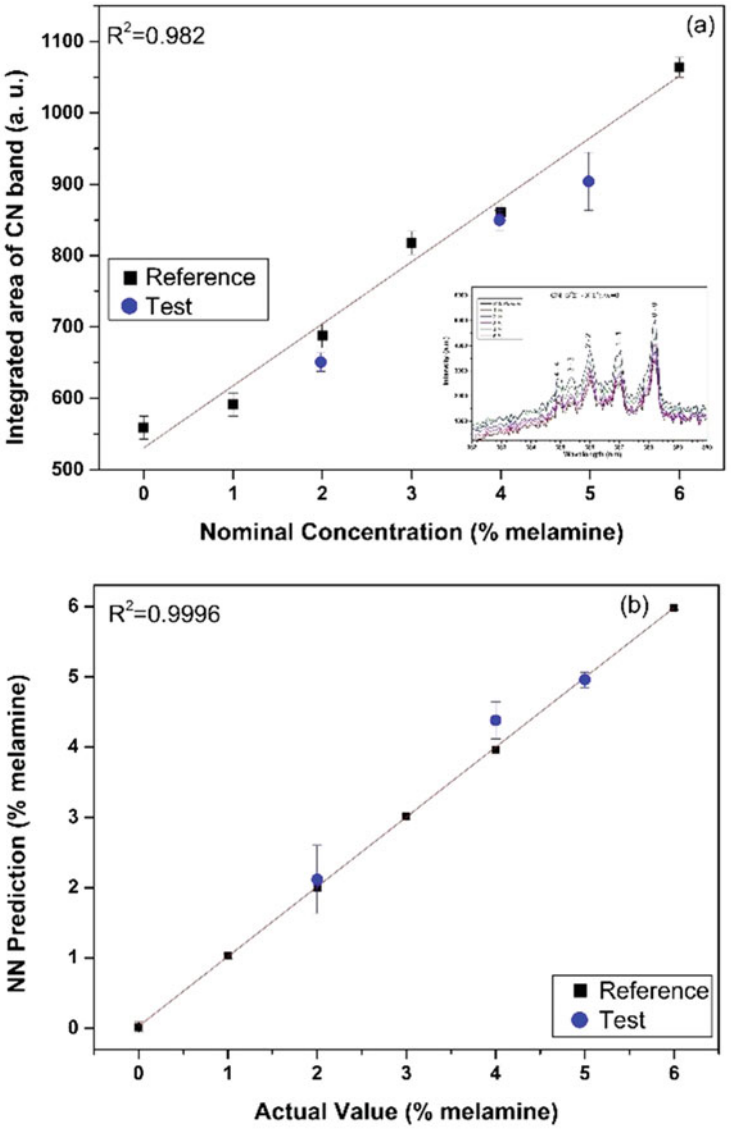

Fig. 1.3 (**a**) Spectral magnification on CN molecular band at different adulteration ratios and conventional calibration curve for melamine quantification by integration of the CN band (**b**) multivariate NN calibration model of adulterated milk powder (from (2))

validation sets comprised of samples at concentrations of 2, 4, and 5%. CN band emissions were used for the quantification of melamine in the milk samples. Figure 1.3a shows the CN spectral emission of milk adulterated with melamine at different concentrations, also demonstrating the variation in the intensity. Considering the

Table 1.6 Statistical results of the quantification test for melamine adulteration by LIBS

	Univariate method	NN model
Correlation coefficient (R^2)	0.982	0.999
Mean prediction error, MPE (%)	24	5
Standard deviation (%)	2.2	0.3

nature and composition of melamine ($C_3H_6N_6$), an increase in the CN molecule signal with increasing concentrations of melamine was observed.

Two calibration procedures were used for quantification purpose. Firstly, a conventional calibration curve was calculated by integrating the CN emission band in the spectral range between 382 and 389 nm. Figure 1.3a shows the correlation between the integrated area and the nominal adulterated ratio. Each point represents the value averaged of 30 LIBS spectra (10 for each of the three replicates at the same adulteration percentage) and the error bars show the relative standard deviation (RSD) between the three measurements. Black squares represent reference values, whereas blue circles the test value. The regression coefficient value was found to be 0.982.

A multivariate prediction curve using NN (Fig. 1.3b) was also studied. For this purpose, the same wavelength ranges, as in the qualitative analysis, were used as input to the NN model. In this case, an improvement in the correlation coefficient was observed, obtaining a value of 0.999 (see Table 1.6) and showing a perfect agreement between the actual and NN predicted concentration.

To compare both methods (univariate and multivariate), the mean prediction error (MPE) was calculated following Eq. (1.4) [67]:

$$\mathrm{MPE} = \frac{1}{N}\sum_{i=1}^{N}\frac{|\, r_i - y_i \,|}{r_i} \times 100 \tag{1.4}$$

where N is the total number of spectra, r_i the prediction output, and y_i the actual value. A MPE of 24% and 5% was obtained for the univariate and multivariate methods, respectively. Table 1.4 shows an overview of the quantification parameters, it is clear that the multivariate NN approach provided better results for the quantification of adulterated milk samples.

Taken together, these results seem to indicate that NN is more accurate than the conventional univariate method. This can be attributed to NN being able to model complex non-linear structure of the data. Although owing to its various functions and architecture, it may be difficult to implement NNth another standard chemometric methods, the results obtained in this study demonstrate that LIBS combined with NN offers significant advantages in the quantitative analysis as well as for the classification purpose.

1.4.4 Honey Adulteration

Honey is the third most adulterated product in the world and a non-negligible percentage of honey consumed in Europe contains adulterants and/or contaminants. This was confirmed in the report presented by European Commission, March 1, 2018, on the perspectives and challenges for the beekeeping sector of the European Union (2017/2115 (INI). In addition, massive imports of honey from other countries into Europe have caused significant economic losses for producers which represent over 620,000 beekeepers [68]. Beekeeping sector is significant for the EU and contributes around EUR 14.2 billion to the economy every year. This fact combined with the suspicion of adulteration and agrochemical contamination, calls for new approaches for honey testing, with the aim of implementing new methods of control. One of the most common forms of honey adulteration is the addition of rice syrup or corn syrup in it. Being a highly complex sample, it becomes really challenging to detect adulteration in it. Furthermore, there is no single available method that can simultaneously detect all forms of honey adulteration [69]. The real-time detection is not simple and requires very complex instrumentation and high technical level of the operators. On the other hand, the contamination of honey with heavy metals or another environmental contaminant through bees is a problem that is difficult to detect with current methods and technology.

Honey adulteration and agrochemical contamination resulting from the environment or originating from chemical products used for the treatment of varroosis sector are two major challenges faced by EU countries in the beekeeping sector. Honey is a natural product that has been valued for its sweetening properties since ancient times and has a long history of medicinal use [70]. Honey consumption has increased during the past decades due to consumers' preference for natural and pure products with no additives or preservatives [71]. Therefore, limited production and complex composition of honey combined with relatively high prices can be counted as major incentives provided for honey adulteration, thereby affecting consumers and honey producers [69].

LIBS technique offers instant spectra acquisition, minimal sample treatment, simplicity, versatility, experimental flexibility portability of the set-up and cost effectiveness provide an excellent combination of features to LIBS as an analytical tool for analysis of a wide range of food samples. In honey analysis, preliminary results that have been obtained show that LIBS offers the expected results by distinguishing between pure honey and adulterated honey (Fig. 1.4). In addition, excellent difference is observed between honey with protected designation of origin (PDO) and honey with protected geographical origin (PGO).

1.5 Conclusions

Laser induced breakdown spectroscopy (LIBS) technique has been evaluated to be applied for a real world application for a fast and robust control of adulteration

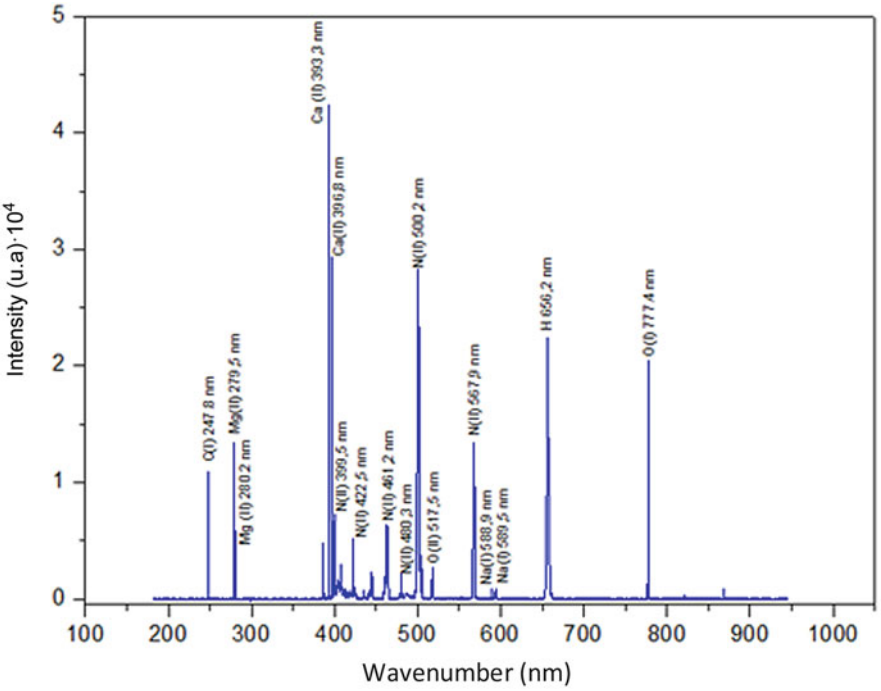

Fig. 1.4 Typical spectrum of a sample of pure honey obtained in air and in the environmental conditions of the laboratory. The assignment of the emission lines to the majority elements is shown

of olive oils, wine, milk, and honey. The results obtained indicate that although the intensity of the spectra can change from pulse to pulse and from day to day, it does not affect the system's ability to identify the sample. Despite that there are not significant/notable variations in the spectra of the samples from which the all samples can easily be discriminated. From a mathematical point of view, each sample can be discriminated based on its complete spectral fingerprint. The full sets of variables (intensities at each wavelength) that constitute the sample spectrum are vital in the process of comparison performed by the NN, which constitutes the basis of their ability to carry out the difference. The NN is able to compute internal parameters (weights and bias) in the training process for categorizing a given set of input variables as belonging to particular sample, with a high tolerance for noise and the presence of outliers.

The LIBS/NN combination allowed to clearly distinguish between the wine and milk and honey as well as differentiating the pure samples with a 100% of correct classification in all cases. On the other hand, the quantification of melamine in toddler powdered milk sample showed that the multivariate analysis by NN quantitative model produced better results than conventional calibration. It has been demonstrated that the emission band of the CN correlates to the molecular nature

and concentration of melamine. Although the methodology calls for further studies to increase the reliability and accuracy, the developed LIBS/NN methodology provided a sensitive and robust analysis to detect and quantify melamine in powdered milk sample or honey samples. The results show that LIBS/NN combination, along with its speed of analysis, reduced cost, and ease of use has the potential to serve as a useful screening tool in the quality control of food, both quantitatively and qualitatively.

References

1. Marcos-Martinez D, Ayala JA, Izquierdo-Hornillos RC, de Villena FJM, Caceres JO (2011) Identification and discrimination of bacterial strains by laser induced breakdown spectroscopy and neural networks. Talanta 84(3):730–737
2. Moncayo S, Manzoor S, Rosales JD, Anzano J, Caceres JO (2017) Qualitative and quantitative analysis of milk for the detection of adulteration by Laser Induced Breakdown Spectroscopy (LIBS). Food Chem 232:322–328
3. Lasheras RJ, Bello-Gálvez C, Rodríguez-Celis EM, Anzano J (2011) Discrimination of organic solid materials by LIBS using methods of correlation and normalized coordinates. J Hazard Mater 192(2):704–713
4. Manzoor S, Moncayo S, Navarro-Villoslada F, Ayala JA, Izquierdo-Hornillos R, de Villena FJM et al (2014) Rapid identification and discrimination of bacterial strains by laser induced breakdown spectroscopy and neural networks. Talanta 121:65–70
5. Lucena P, Gaona I, Moros J, Laserna JJ (2013) Location and detection of explosive-contaminated human fingerprints on distant targets using standoff laser-induced breakdown spectroscopy. Spectrochim Acta Pt B 85:71–77
6. Lucena P, Doña A, Tobaria LM, Laserna JJ (2011) New challenges and insights in the detection and spectral identification of organic explosives by laser induced breakdown spectroscopy. Spectrochim Acta Pt B 66(1):12–20
7. Moncayo S, Rosales JD, Izquierdo-Hornillos R, Anzano J, Caceres JO (2016) Classification of red wine based on its protected designation of origin (PDO) using laser-induced breakdown spectroscopy (LIBS). Talanta 158:185–191
8. Lei WQ, El Haddad J, Motto-Ros V, Gilon-Delepine N, Stankova A, Ma QL et al (2011) Comparative measurements of mineral elements in milk powders with laser-induced breakdown spectroscopy and inductively coupled plasma atomic emission spectroscopy. Anal Bioanal Chem 400(10):3303–3313
9. Mehder AO, Gondal MA, Dastageer MA, Habibullah YB, Iqbal MA, Oloore LE et al (2016) Direct spectral analysis and determination of high content of carcinogenic bromine in bread using UV pulsed laser induced breakdown spectroscopy. J Environ Sci Health B 51(6):358–365
10. Bilge G, Boyacı İH, Eseller KE, Tamer U, Çakır S (2015) Analysis of bakery products by laser-induced breakdown spectroscopy. Food Chem 181:186–190
11. Leme FO, Silvestre DM, Nascimento AN, Nomura CS (2018) Feasibility of using laser induced breakdown spectroscopy for quantitative measurement of calcium, magnesium, potassium and sodium in meat. J Anal At Spectrom 33(8):1322–1329
12. de Oliveira DM, Fontes LM, Pasquini C (2019) Comparing laser induced breakdown spectroscopy, near infrared spectroscopy, and their integration for simultaneous multi-elemental determination of micro- and macronutrients in vegetable samples. Anal Chim Acta 1062:28–36
13. Juvé V, Portelli R, Boueri M, Baudelet M, Yu J (2008) Space-resolved analysis of trace elements in fresh vegetables using ultraviolet nanosecond laser-induced breakdown spectroscopy. Spectrochim Acta Pt B 63(10):1047–1053

14. Wang J, Shi M, Zheng P, Xue S (2017) Quantitative analysis of lead in tea samples by laser-induced breakdown spectroscopy. J Appl Spectrosc 84(1):188–193
15. Chen C-T, Banaru D, Sarnet T, Hermann J (2018) Two-step procedure for trace element analysis in food via calibration-free laser-induced breakdown spectroscopy. Spectrochim Acta Pt B 150:77–85
16. Caceres JO, Moncayo S, Rosales JD, de Villena FJM, Alvira FC, Bilmes GM (2013) Application of laser-induced breakdown spectroscopy (LIBS) and neural networks to olive oils analysis. Appl Spectrosc 67(9):1064–1072
17. Zhang T, Tang H, Li H (2018) Chemometrics in laser-induced breakdown spectroscopy. J Chemom 32(11):e2983
18. Brereton RG (2009) Chemometrics for pattern recognition. Wiley, Chichester, p 513
19. Kuncheva LI (2004) Combining pattern classifiers: methods and algorithms, 1st edn. Wiley, Hoboken, p 376
20. Ballabio D, Todeschini R (2009) Multivariate classification for qualitative analysis. In: Sun D-W (ed) Infrared spectroscopy for food quality analysis and control. Academic, San Diego, pp 83–104
21. Sirven JB, Salle B, Mauchien P, Lacour J-L, Maurice S, Manhes G (2007) Feasibility study of rock identification at the surface of Mars by remote laser-induced breakdown spectroscopy and three chemometric methods. J Anal At Spectrom 22(12):1471–1480
22. Yueh F-Y, Zheng H, Singh JP, Burgess S (2009) Preliminary evaluation of laser-induced breakdown spectroscopy for tissue classification. Spectrochim Acta Pt B 64(10):1059–1067
23. Myakalwar AK, Sreedhar S, Barman I, Dingari NC, Venugopal Rao S, Prem Kiran P et al (2011) Laser-induced breakdown spectroscopy-based investigation and classification of pharmaceutical tablets using multivariate chemometric analysis. Talanta 87:53–59
24. Vítková G, Novotný K, Prokeš L, Hrdlička A, Kaiser J, Novotný J et al (2012) Fast identification of biominerals by means of stand-off laser-induced breakdown spectroscopy using linear discriminant analysis and artificial neural networks. Spectrochim Acta Pt B 73:1–6
25. Dingari NC, Barman I, Myakalwar AK, Tewari SP, Kumar GM (2012) Incorporation of support vector machines in the LIBS toolbox for sensitive and robust classification amidst unexpected sample and system variability. Anal Chem 84(6):2686–2694
26. Moncayo S, Manzoor S, Navarro-Villoslada F, Caceres JO (2015) Evaluation of supervised chemometric methods for sample classification by laser induced breakdown spectroscopy. Chemom Intell Lab Syst 146:354–364
27. Demuth HB, Beale MH, Hagan MT (2007) Neural network toolbox for use with MATLAB: User's guide 9th for version 6.0 (Release 2008a): Math Works
28. Maren AJ, Harston CT (1990) Handbook of neural computing applications. Academic, San Diego
29. Sirven JB, Bousquet B, Canioni L, Sarger L, Tellier S, Potin-Gautier M et al (2006) Qualitative and quantitative investigation of chromium-polluted soils by laser-induced breakdown spectroscopy combined with neural networks analysis. Anal Bioanal Chem 385(2):256–262
30. Møller MF (1993) A scaled conjugate gradient algorithm for fast supervised learning. Neural Netw 6(4):525–533
31. Bishop CM (1996) Neural networks for pattern recognition. Oxford University Press, Cambridge
32. Jiang Y, Cukic B, Ma Y (2008) Techniques for evaluating fault prediction models. Empir Softw Eng 13(5):561–595
33. Regulation (EU) No 1151/2012 of the European Parliament and of the Council of 21 November 2012 on quality schemes for agricultural products and foodstuffs: EUR-Lex - 32012R1151 - EN - EUR-Lex. Cited Feb. 2016. Available from http://eur-lex.europa.eu/legal-content/EN/TXT/?qid=1453324214582&uri=CELEX:32012R1151
34. Luykx DMAM, van Ruth SM (2008) An overview of analytical methods for determining the geographical origin of food products. Food Chem 107(2):897–911
35. Schlesier K, Fauhl-Hassek C, Forina M, Cotea V, Kocsi E, Schoula R et al (2009) Characterisation and determination of the geographical origin of wines. Part I: overview. Eur Food Res Technol 230(1):1–13

36. Aceto M, Abollino O, Bruzzoniti MC, Mentasti E, Sarzanini C, Malandrino M (2002) Determination of metals in wine with atomic spectroscopy (flame-AAS, GF-ASS and ICP-AES); a review. Food Addit Contam 19(2):126–133
37. Larsen FH, van den Berg F, Engelsen SB (2006) An exploratory chemometric study of 1H NMR spectra of table wines. J Chemom 20:198–208
38. Serrano-Lourido D, Saurina J, Hernández-Cassou S, Checa A (2012) Classification and characterisation of Spanish red wines according to their appellation of origin based on chromatographic profiles and chemometric data analysis. Food Chem 135(3):1425–1431
39. Makris DP, Kallithraka S, Mamalos A (2006) Differentiation of young red wines based on cultivar and geographical origin with application of chemometrics of principal polyphenolic constituents. Talanta 70(5):1143–1152
40. Jaitz L, Siegl K, Eder R, Rak G, Abranko L, Koellensperger G et al (2010) LC–MS/MS analysis of phenols for classification of red wine according to geographic origin, grape variety and vintage. Food Chem 122(1):366–372
41. Geana EI, Popescu R, Costinel D, Dinca OR, Stefanescu I, Ionete RE et al (2016) Verifying the red wines adulteration through isotopic and chromatographic investigations coupled with multivariate statistic interpretation of the data. Food Control 62:1–9
42. Wang D, Zhong Q, Li G, Huang Z (2015) Rapid method for the determination of the stable oxygen isotope ratio of water in alcoholic beverages. J Agric Food Chem 63(42):9357–9362
43. Brescia MA, Caldarola V, De Giglio A, Benedetti D, Fanizzi FP, Sacco A (2002) Characterization of the geographical origin of Italian red wines based on traditional and nuclear magnetic resonance spectrometric determinations. Anal Chim Acta 458(1):177–186
44. Geana EI, Popescu R, Costinel D, Dinca OR, Ionete RE, Stefanescu I et al (2016) Classification of red wines using suitable markers coupled with multivariate statistic analysis. Food Chem 192:1015–1024
45. Martins L, Goncalves P, De PGP, inventors; Universidade De Tras-Os-Montes E Alto Douro; Martins Lopes, Paula Filomena; Goncalves Pereira, Maria Leonor; De Pinho Guedes Pinto, Henrique, Assignee (2011) Method and kit for DNA extraction from Vitis Vinifera L. and for amplification and detection of grapevine varieties or cultivars in musts or wines patent WO2011067630 (A1)
46. Miziolek AW, Palleschi V, Schechter I (2008) Laser Induced Breakdown Spectroscopy (LIBS). 1 ed. New York, USA: Cambridge University Press
47. Huang Y, Kangas LJ, Rasco BA (2007) Applications of artificial neural networks (ANNs) in food science. Crit Rev Food Sci Nutr 47(2):113–126
48. Curteanu S, Cartwright H (2011) Neural networks applied in chemistry. I. Determination of the optimal topology of multilayer perceptron neural networks. J Chemom 25(10):527–549
49. Jantzi SC, Motto-Ros V, Trichard F, Markushin Y, Melikechi N, De Giacomo A (2016) Sample treatment and preparation for laser-induced breakdown spectroscopy. Spectrochim Acta Pt B 115:52–63
50. Sobral H, Sanginés R, Trujillo-Vázquez A (2012) Detection of trace elements in ice and water by laser-induced breakdown spectroscopy. Spectrochim Acta Pt B 78:62–66
51. Caceres JO, Tornero López J, Telle HH, González UA (2001) Quantitative analysis of trace metal ions in ice using laser-induced breakdown spectroscopy. Spectrochim Acta Pt B 56(6):831–838
52. Zhu D, Wu L, Wang B, Chen J, Lu J, Ni X (2011) Determination of Ca and Mg in aqueous solution by laser-induced breakdown spectroscopy using absorbent paper substrates. Appl Opt 50(29):5695–5699
53. Díaz Pace DM, D'Angelo CA, Bertuccelli D, Bertuccelli G (2006) Analysis of heavy metals in liquids using laser induced breakdown spectroscopy by liquid-to-solid matrix conversion. Spectrochim Acta Pt B 61(8):929–933
54. St-Onge L, Kwong E, Sabsabi M, Vadas EB (2004) Rapid analysis of liquid formulations containing sodium chloride using laser-induced breakdown spectroscopy. J Pharm Biomed Anal 36(2):277–284

55. Gondal MA, Hussain T, Yamani ZH, Baig MA (2006) Detection of heavy metals in Arabian crude oil residue using laser induced breakdown spectroscopy. Talanta 69(5):1072–1078
56. Gondal MA, Siddiqui MN, Nasr MM (2010) Detection of Trace Metals in Asphaltenes Using an Advanced Laser-Induced Breakdown Spectroscopy (LIBS) Technique. Energy Fuel 24(2):1099–1105
57. US Department of Commerce N. NIST Atomic Spectra Database 2015. updated 2015/06/05/Cited2014/04/24/. Available from http://physics.nist.gov/PhysRefData/ASD/lines_form.html; http://www.nist.gov/pml/data/asd.cfm
58. Griffin M (2016) Food outlook - milk and milk products. Available from http://www.fao.org/
59. Cremers DA, Radziemski LJ (2013) Handbook of laser-induced breakdown spectroscopy, 2nd edn. Wiley-Blackwell, Oxford
60. Gottfried JL, Frank CDL, Miziolek AW (2009) Discrimination of explosive residues on organic and inorganic substrates using laser-induced breakdown spectroscopy. J Anal At Spectrom 24(3):288–296
61. Grégoire S, Motto-Ros V, Ma QL, Lei WQ, Wang XC, Pelascini F et al (2012) Correlation between native bonds in a polymeric material and molecular emissions from the laser-induced plasma observed with space and time resolved imaging. Spectrochim Acta B At Spectrosc 74–75:31–37
62. Bilge G, Sezer B, Eseller KE, Berberoglu H, Topcu A, Boyaci IH (2016) Determination of whey adulteration in milk powder by using laser induced breakdown spectroscopy. Food Chem 212:183–188
63. Bilge G, Velioglu HM, Sezer B, Eseller KE, Boyaci IH (2016) Identification of meat species by using laser-induced breakdown spectroscopy. Meat Sci 119:118–122
64. Mbesse Kongbonga YG, Ghalila H, Onana MB, Ben LZ (2014) Classification of vegetable oils based on their concentration of saturated fatty acids using laser induced breakdown spectroscopy (LIBS). Food Chem 147:327–331
65. Torrecilla JS, Cámara M, Fernández-Ruiz V, Piera G, Caceres JO (2008) Solving the spectroscopy interference effects of β-carotene and lycopene by neural networks. J Agric Food Chem 56(15):6261–6266
66. Baudelet M, Boueri M, Yu J, Mao SS, Piscitelli V, Mao X et al (2007) Time-resolved ultraviolet laser-induced breakdown spectroscopy for organic material analysis. Spectrochim Acta B At Spectrosc 62(12):1329–1334
67. Cámara M, Torrecilla JS, Caceres JO, Sánchez Mata MC, Fernández-Ruiz V (2010) Neural network analysis of spectroscopic data of lycopene and β-carotene content in food samples compared to HPLC-UV-Vis. J Agric Food Chem 58(1):72–75
68. European-Commission. Detailed information on honey production, national apiculture programmes, budget and legal bases. Available from https://ec.europa.eu/agriculture/honey_en
69. Du B, Wu L, Xue X, Chen L, Li Y, Zhao J et al (2015) Rapid screening of multiclass syrup adulterants in honey by ultrahigh-performance liquid chromatography/quadrupole time of flight mass spectrometry. J Agric Food Chem 63(29):6614–6623
70. Ulberth F (2016) 26 - advances in testing for adulteration in honey. In: Downey G (ed) Advances in food authenticity testing. Woodhead Publishing, Cambridge, pp 729–753
71. Cabañero AI, Recio JL, Rupérez M (2006) Liquid chromatography coupled to isotope ratio mass spectrometry: a new perspective on honey adulteration detection. J Agric Food Chem 54(26):9719–9727

The Use of FTIR Spectroscopy Combined with Multivariate Analysis in Food Composition Analysis

2

Gunawan Indrayanto and Abdul Rohman

Abstract

Infrared spectroscopy, one of the vibrational spectroscopies, has emerged as rapid and powerful analytical technique for identification and quantitative analysis of food component. FTIR spectra is fingerprint analytical technique, therefore, by selecting the specific region, some analytical purposes can be achieved such as identification, confirmation and quantitative analysis of analyte(s) of interest in food samples. Equipped with some sampling technique such as attenuated total reflectance and combined with chemometrics software such as principal component analysis for classification and multivariate calibration for multicomponent analysis, FTIR spectroscopy has been successfully used for compositional analysis of food. The method is rapid with minimum or without sample preparation and is not involving the extensive solvents and reagents.

Keywords

FTIR spectroscopy · Food composition · Fingerprint technique · Chemometrics · Authentication analysis

G. Indrayanto
Faculty of Pharmacy, Universitas Surabaya, Surabaya, East Java, Indonesia

A. Rohman (✉)
Department of Pharmaceutical Chemistry, Faculty of Pharmacy, Universitas Gadjah Mada, Yogyakarta, Indonesia
e-mail: abdul_kimfar@ugm.ac.id

A. K. Shukla (ed.), *Spectroscopic Techniques & Artificial Intelligence for Food and Beverage Analysis*, https://doi.org/10.1007/978-981-15-6495-6_2

2.1 Introduction

Infrared (IR) spectroscopy is analytical technique related to interaction studies between analytes and electromagnetic radiation. This interaction can be in the form of transmission, absorption, scattering and reflection of light due to incident light in the spectral range corresponding to infrared region into samples. The frequencies or wavelengths, at which the samples absorb IR radiation and their corresponding intensities (either transmittance or absorbance), are recorded into IR spectrum [1]. IR spectroscopy is the most vibrational spectroscopic techniques widely applied in food analysis [2], which measure the vibrational energy levels in a compound [3]. IR spectroscopy is one of fingerprint analytical techniques, commonly applied in wide application in food science. Fourier transform infrared (FTIR) spectroscopy is an ideal technique for characterization and identification, confirmation, and quantitative analysis of food components [4].

There are two types of spectrometer, namely dispersive instrument and Fourier-transformed spectrophotometer based on interferometer. FTIR spectroscopy offer some advantages in identification and quantitative analyses including fast spectral data acquisition, without or minimal sample preparation, non-destructive in which the analysed samples by FTIR spectroscopy can be analysed using other methods like chromatographic-based techniques, high-throughput, low cost, applicable for a wide range of physical sample types (liquid, semi-solid and solid samples). Besides, IR spectroscopy can be used for analysis of multiple analytes, especially in combination with multivariate analysis [5]. FTIR spectroscopy can be used in the wide range of wavenumbers region which provide excellent resolution of spectra along with the large number of peaks, which can be correlated with the presence of certain analytes in the samples [6]. Due to its versatility with minimum use of solvents, FTIR spectroscopy is considered as green analytical techniques which are more environmentally friendly [7].

However, FTIR spectroscopy also has some drawbacks. The environment condition could affect the nature of spectra, therefore the temperature and humidity must be controlled. The FTIR spectra may vary which make the spectral interpretation more complicated [8]. The spectral data obtained are frequently complex which need sophisticated statistical tools known as chemometrics. The advance development of multivariate calibration can assist the resolving unique spectral patterns, improving instrument sensitivity, and monitoring the analyte characteristics in the analysed samples [9].

2.2 Infrared Spectroscopy

In analytical chemistry, infrared spectroscopy is considered as powerful technique for analysing inorganic and organic samples, in the form of gases, liquids, and solids either qualitatively or quantitatively. IR spectroscopy is based on the vibrations (stretching or bending) of chemical bonds within the molecules at specific frequen-

cies. The vibrations can be described by the laws of physics (Hooke laws). The chemical bonds can absorb IR radiation; they are excited to a higher energy level which make the vibration of bonds at specific frequency. At ambient temperature, molecules are in the levels of zero energy [10].

The region of IR radiation can be categorized in three regions, near-infrared (NIR), mid-infrared (MIR) and far-infrared (FIR). NIR corresponds to wavenumbers of 14,000–4000 cm^{-1} (or wavelength of 800–2500 nm), MIR corresponds to 4000–400 cm^{-1} (or wavelength 2500–50,000 nm) and FIR corresponds to 400–50 cm^{-1} (or wavelength 50,000–1,000,000 nm). Among these regions, MIR is the most widely used for the analytical purposes including qualitative analysis, confirmation and quantitative analyses of food composition within the analysed samples [11]. FTIR spectra are fingerprint spectra and can be used to characterize the chemical compounds. FTIR spectra can be obtained using the modes of absorbance or transmittance. The energy at any peak in IR spectrum corresponds to the vibrational frequency of functional groups present in the sample molecule [12].

2.2.1 Infrared Absorption Process

IR spectroscopy is mainly related to the molecular vibrations. The molecular absorption of EMR in IR region can cause the transition between the ground (lowest) state and the rotational and vibrational energy levels in the molecules [13]. As other absorption processes in spectroscopic techniques, the absorption of IR radiation is *a quantized process*, meaning that functional groups in molecule samples only absorbed IR radiation at selected frequencies (energies) which corresponds to energy changes in the order of 2–10 kcal/mol. Radiation in this range corresponds to the stretching and bending vibrations of the chemical bonds in the most covalent molecules [1], corresponding to the energy levels of chemical bonds. According to Hooke's law, the frequencies of stretching and bending vibrations are affected by (a) the mass of the atoms, in which the higher the mass the lower the frequency, (b) the geometrical shape of the molecules, (c) the bonds stiffness and (d) the periods of the associated vibrational coupling.

To absorb IR radiation, bonds in the molecule must have dipole moment such as CH_2. The modes of vibration can be either stretching (change in bond length) or bending (change in bond angle). Stretching can be symmetrical (in plane) or asymmetrical (out of plane), and the bending vibration is identified as rock or deformation when moved in the same or in opposite direction, respectively [14]. Figure 2.1 illustrates the vibration modes of methylene ($–CH_2–$) group. The modes of vibration can be either stretching (in which bond length is observed) or bending (in which bond angle is changed). Stretching can be symmetrical (in plane) or asymmetrical (out of plane). The bending vibration is identified as rock or deformation when moved in the same or in opposite direction, respectively. The modes of vibration can be either stretching (in which bond length is observed) or bending (in which bond angle is changed). Stretching can be symmetrical (in

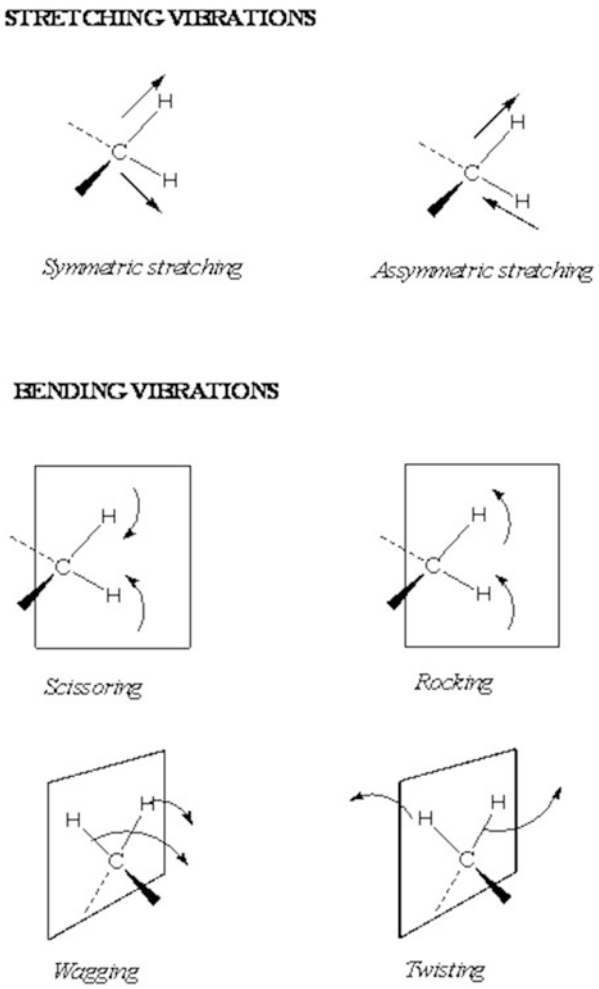

Fig. 2.1 The vibration modes (stretching and bending) in CH_2 group. Adapted from [1]

plane) or asymmetrical (out of plane). The bending vibration is identified as rock or deformation when moved in the same or in opposite direction, respectively [15].

2.2.2 Instrumentation

The instrument systems of infrared spectrometers can be in the form of dispersive and Fourier-transformed using interferometer [16]. The dispersive type has not been widely used in chemical analyses because some difficulties were met in sample handling. Dispersive instrument is also not equipped with software to treat the

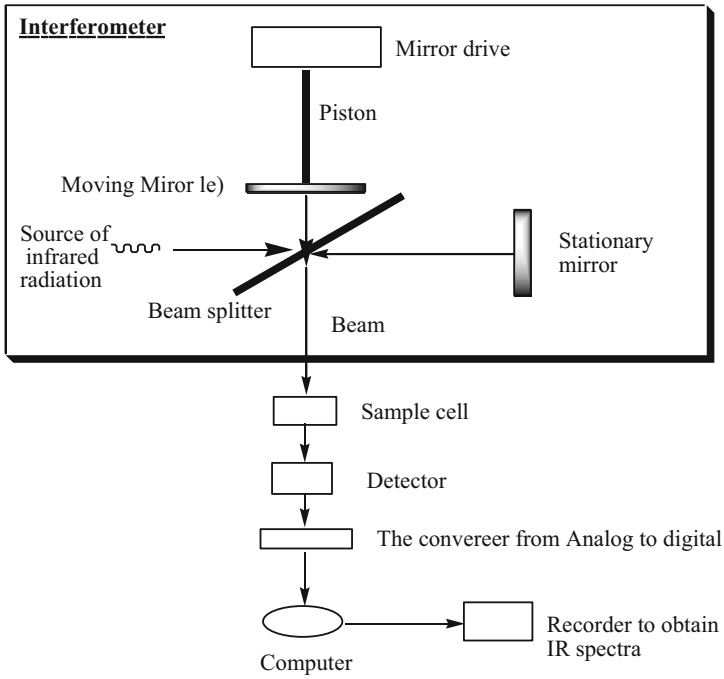

Fig. 2.2 Schematic of FTIR spectrophotometer. Adapted from [20]

spectral acquisition and processing systems. Therefore, in the last decades, FTIR instrument has replaced dispersive instrument and has appeared to become an important method for certain analytical purposes [17].

FTIR spectrophotometers are based on interferometer, therefore, they differ fundamentally from dispersive spectrometer. The Michelson interferometer is typically used in most FTIR spectrophotometers (Fig. 2.2). Michelson interferometer is normally composed of two mirrors, namely moving mirror and stationary mirror. In interferometer, the moving mirror will travel at constant velocity. The beam splitter made from KBr coated with Ge is located between two mirrors [18]. Beam splitter will divide the radiation beam into two parts, one part will be transmitted into a moving mirror while the part one is reflected into stationary mirror. When the radiation beams are reflected back, they will recombine to produce constructive/destructive interference patterns. After the IR energy has been selectively absorbed by a sample located between the beam splitter and the detector, the fluctuations in the energy intensities will reach to detector and then will be digitalized in real time, yielding an interferogram [19].

The obtained interferogram encompasses all requisite information during FTIR spectra of the analysed sample; however, interferogram outputs are in the time domain. The interferogram in time domain is then converted to frequency domain

using Fourier transformation for producing conventional FTIR spectrum. Fourier transformation is a mathematical algorithm typically applied during the decoding interferogram to obtain interpretable information related to individual frequencies in FTIR spectrum. Wavelength accuracy is necessary in order to obtain correct and highly resolved spectra. It is dependent on knowing the exact position of the moving mirror and is achieved using an internal reference laser (He-Ne), which monitors the position of the moving mirror during the scan. This leads to the precise scanning and to accurate spectrum collection in relation to the wavelength position, which is a key determinant for quantitative spectroscopy [1].

Because of its rapidity in scanning of FTIR spectra and its capability to provide sensitive response, FTIR spectrophotometers are the instrument choice for analysis of samples. FTIR instruments have distinct advantages over dispersive spectrometers, namely: (a) Fellgett advantage capable of providing better speed and sensitivity; (b) Jacquinot advantage by increasing the optical throughput; (c) dispersion or filtering of slits is not needed; (d) Connes advantage as shown by the presence of internal laser reference; (e) simpler mechanical design; (f) the contributions of stray light and light emission are eliminated and (g) FTIR instrument is easily connected and compatible with powerful data recording [21]. The significant advantage of FTIR instrument is the multiplexing advantage, in which all frequencies corresponding to absorption of chemical bonds can be measured simultaneously, as a consequence, whole FTIR spectra of analysed samples can be obtained in a single scanning. In addition, the signal of FTIR spectrophotometer has excellent sensitivity as indicated by higher ratio of signal to noise (S/N) that of dispersive instrument. Another important factor in the success of FTIR spectroscopy is the sophisticated software of chemometrics included in the instrument which facilitates spectral scanning and spectral treatments like derivatization and smoothing.

2.2.3 Sampling Preparation Techniques for Infrared Spectroscopy

Because of the large diversity of uses of IR spectroscopy in analysing and characterizing of food samples, a large number of sample preparation techniques have been developed and marketed over the years. Different sampling techniques have been used for obtaining better quality spectra, and new sensitive techniques have been developed and used in order to evaluate previously intractable samples. They can be divided into a few categories, namely transmission, internal reflectance, external reflectance, diffuse reflectance, photoacoustic detection and gas chromatography-infrared (GC/IR) [22]. According to USP 42 general method <854> Mid-Infrared Spectroscopy [23], the most common sample preparation techniques for FT-IR spectroscopy are by using potassium bromide disk, mineral oil mulls, self-supported polymer film, capillary film, liquid and solutions in transmission cells, gases, attenuated total reflectance, diffuse reflection and microscope sampling. In principle those techniques can be separated into transmission-, attenuated total reflectance (ATR)-, and diffuse reflectance-technique [24].

2.2.3.1 Transmission Technique

By transmission technique, the sample is placed precisely into sample holder. IR beam is passed through the holder containing the analysed samples, and the transmitted light is detected and recorded as IR spectrum. Samples should be first prepared as pellet, mull and film, before the measurement can be performed. The transmission techniques can be used alone, or in combination or with using accessories e.g. liquid-, gas-cells, microscope or gas chromatography. Many types of samples such as solid powders, liquids, gas, polymer film, can be analysed by using this technique [24]. Powdered organic and inorganic sample (1–2 mg) should be well mixed with 150 mg alkali halide (e.g. potassium bromide, potassium chloride and caesium iodide), finely pulverized to get homogenous mixture, and put in die to get pellet. In order to get transparent pellets, a power of around 8 tons is applied under a vacuum of several mmHg for several minutes. The pellet is then inserted into a sample holder in the spectrometer for analysis [23, 25, 26]. For preparing mull, 10–20 mg sample were pulverized in mortar then grinded with saturated hydrocarbon mineral oil (liquid paraffin, Nujol), to obtain a suspension, then the suspension was transferred into the cell (potassium bromide, sodium chloride, silver bromide or caesium iodide). Liquid paraffin exhibits absorption near 3000–2800 cm, 1460 cm, 1375 cm and 730 cm. Liquid sample can be measured by dropping it into the transmission cell, while gaseous sample can be analysed by the gas cell. Sample as thin film can be prepared by either melting or dissolved by solvents; this thin film method usually is used for analysing the polymers [27]. FT-IR spectrophotometer can be connected to a GC-IR module that contains liquid-nitrogen cooled MCT-A detector for performing GC-FT-IR analysis [28].

Some advantages of the transmission method are economical, well established, excellent spectral information and can well applied for quantitative work [24]. The disadvantages of transmission method that generally using alkali halide pellets or cells are hygroscopic; it needs skilled analyst and time consuming for preparing, liquid cells need to be filled without air bubble, homogenization of sample and alkali halide is difficult to achieve for some substances/materials like rubbers or other elastomers [29]. The other limitation of this technique is related to the sample thickness (except for gaseous samples), because the amount of IR energy absorbed by the sample is proportional to its thickness. Consequently, beyond a certain thickness, the sample will not transmit any IR radiation in the regions of the spectrum where it is strongly absorbing; therefore, no signal will reach the detector. The thickness is arranged in such a way that gives the absorbance value of 0.1–0.8 [30]. In order to overcome those disadvantages, a relatively new method of attenuated total reflectance (ATR) mode has been developed.

2.2.3.2 Attenuated Total Reflectance

For its simplicity, the sampling technique of ATR is widely used for analysis of the analysed samples. ATR is considered as one type of Internal Reflection Spectroscopy (IRS). The sample is positioned in good contact against special ATR crystal called an internal reflectance element (IRE) [31]. The basic principle of ATR

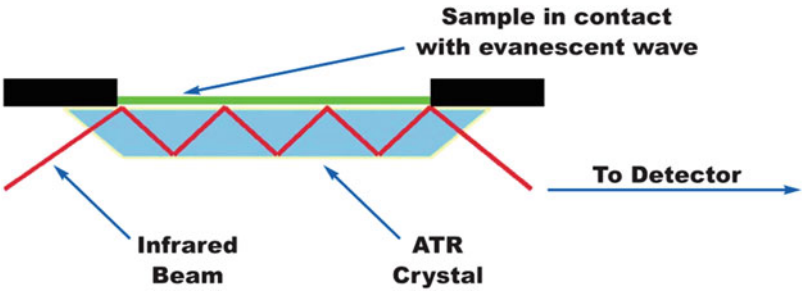

Fig. 2.3 A multiple reflection of attenuated total reflectance (ATR) system. (Courtesy of PerkinElmer, Shelton, CT 06484, USA) [29]

is shown in Fig. 2.3. An infrared beam enters the ATR crystal which has high refractive index at certain angle (usually 45°). The fraction of the light wave that reaches into the sample is called the evanescent wave. This wave will penetrate only a few microns (0.5–5 μ) beyond the crystal surface and then penetrate into the sample. In those spectral regions, the evanescent wave will be attenuated due to absorption of IR light by the analysed sample. After multiple internal reflections, the IR beam exits from the crystal and is then directed into the detector and recorded to get IR spectra. The system then produces an absorption infrared spectrum. During ATR scanning, the sample must be in good contact with ATR crystal surface. All sorts of samples can be placed directly on the surface of an ATR crystal, afterward measurements can be directly performed, and typically it needs only within seconds [29]. In order to attain the success of ATR, some conditions must be fulfilled namely [1] the sample must be on direct contact with ATR crystal, because the evanescent wave or bubble only extends beyond the crystal of 0.5–5 μ and [2] the refractive index of ATR crystal must be higher than that of the analysed sample. Usually, refractive index values of ATR crystals are between 2.38 and 4.01 at 2000 cm^{-1} [32].

There are some common crystals materials for ATR i.e. zinc selenide (ZnSe), germanium (Ge), silicon, diamond and KRS-5 (thallium iodide or thallium bromide). ZnSe (refractive index 2.43; spectral range 20,000–500 cm^{-1}) is a relatively low-cost ATR crystal and is perfect for analysing liquids and soft sample (gels). ZnSe can be used between pH 5 to pH 9. Due to relatively easily to scratches of the ZnSe crystal, care must be taken when cleaning it. Germanium (refractive index 4.01; spectral range 5000–600 cm^{-1}) is used to analyse highly absorbing samples like carbon-black coloured rubbers. Ge has a much better working pH range. Ge can be used for analysing weak acids and alkalis. Diamond (refractive index 2.40; spectral range 40,000–100 cm^{-1}) is the best ATR crystal material due to is robustness and chemically inert. The drawback of diamond is relatively more expensive compared to two other crystals. The ATR crystal must be always cleaned, usually by using a solvent soaked in piece of tissue (MeOH, Water, Isopropanol) [29, 33].

ATR technique provides a simple and convenient means of acquiring the IR spectra of a wide variety of samples; many of them are not readily convenient to IR analysis using conventional transmission measurements [34]. Some advantages of ATR are minimal or without sample preparation, fast and easy to clean up, analysis of sample in their natural states and excellent for thick or strongly absorbing samples [24]. According to our experience almost all kind of samples can be well analysed using ATR i.e. drug raw materials, drug preparations, powdered herbal drugs, dried leaves, plastics, liquids, etc.

2.2.3.3 Diffuse Reflection Infrared Fourier Transform Spectroscopy (DRIFTS)

By this method sample was mixed 90–99% with an IR diluent transparent matrix (e.g. as KBr). DRIFTS can be applied of both powdered organic and inorganic (<10 μm). The IR radiation will interact with the sample particles and then will reflect off their surfaces, causing the light to diffuse, or scatter, as it moves throughout the analysed sample. The scattered light is then directed into the detector. The advantages of this method are almost no sample preparation, no need to form KBr pellets and relatively fast [23, 24]. The original DRIFTS spectrum is recorded as diffuse reflectance (R%) vs. wave numbers, which is the ratio of single beam spectrum of the sample to that of non-absorbent references. Since R% is not linear with concentrations, generally it is converted to log (1/R) for NIR spectra, while for MIR it should be converted to Kubelka-Munk function. For sample with a higher absorption index, larger particle size and higher refractive index, interference of specular reflection becomes more significant [27].

2.2.3.4 FT-IR Microscopy

FT-IR Microscopy (FT-IR-M) comprises a FT-IR spectrometer, an infrared detector and an optical microscopy. The microscope must be free from any glass lenses, as glass can absorb all IR light. Therefore, the optical elements used are gold- or aluminium-coated mirrors, or some other windows with IR transparent [35]. The central elements of an infrared microscope are a pair of reflective condensing objectives with a Schwarzschild/Cassegrain design, which focus/collect light to/from samples, allowing both transmission and reflection spectroscopy [36]. Typically, FT-IR-M can be measured using either transmission-, or reflection-mode [37, 38]. The infrared pathway in a PerkinElmer Spotlight 200 FT-IR-M system was illustrated by Fig. 2.4 (in transmittance form) and Fig. 2.5 (in reflectance form) [39]. The quality of the FT-IR-M spectra was affected by spatial resolution, signal-to-noise ratio and the spectra artefacts, which could be defined as the variation of absorbance or location of spectral bands due to non-chemical effects [38]. Two types of MIR array detectors commercially available for FT-IR-M are linear and focal plane array (FPA). FPA detector can be used from near infrared to 900 cm^{-1}, while a 16 pixels linear array can be used for measurement to lower wavenumbers (720 cm^{-1}) [37]. New FPA detector is comprised of a matrix of 16 × 16 up to 128 × 128 detector elements; this allows user to acquire up to 16,000 pixels/spectra simultaneously [40]. The relatively new Linear Array Detector (LAD), capable of incorporating

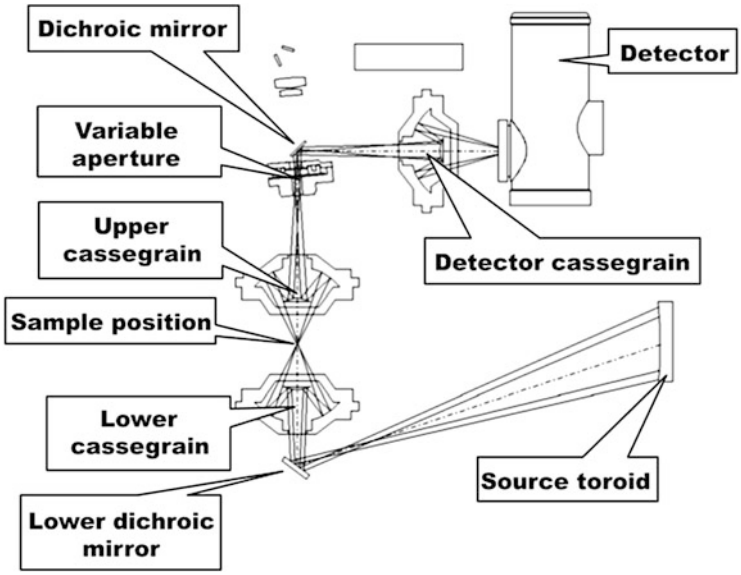

Fig. 2.4 Path of the infrared beam for collecting an image in transmittance in spotlight 200 FT-IR microscopy system. Light from the spectrophotometer is reflected off the toroid onto the lower dichroic mirror which sends it through lower Cassegrain; the upper dichroic mirror reflects the beam onto the detector Cassegrain; the detector Cassegrain focuses onto the detector (Courtesy of PerkinElmer, Shelton, CT 06484, USA) [41]

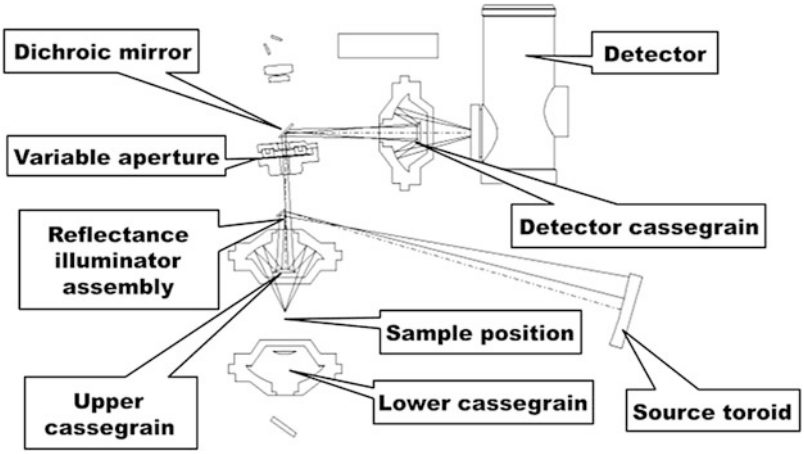

Fig. 2.5 Path of the infrared beam for collecting IR spectra in reflectance in spotlight 200 FT-IR microscopy system. The toroid moves to send the beam to the reflectance illuminator assembly dichroic mirror, which sends it to through upper Cassegrain; The beam reflected off sample and back through to the other side of Cassegrain toward the remote aperture; the detector Cassegrain focuses onto the detector (Courtesy of PerkinElmer, Shelton, CT 06484, USA) [41]

high-quality mercury cadmium telluride (MCT) is arranged as 16 gold-wired IR detector elements. MCT has been already patented by Perkin Elmer, and MCT detector can measure up to wavenumbers of 580 cm^{-1} [39]. The spatial resolution is depended to its numerical aperture (NA), while the smallest distance (δ) at which two points of the analysed sample can still be separated is inversely proportional to NA ($\delta = 0.61\ \lambda/NA$).

Because the numerical aperture of the objective mirror in FTIR microscopes is about 0.6, then δ value is equal to wavelength λ [40]. For transmission mode sample can be placed directly on sample windows that employ IR transparent materials (NaCl or BaF_2); BaF_2 is preferred due to its low water solubility. If the sample is too thick it can be flattened by using a roller blade or a micro compression cell; other method for transmittance mode is by placing the sample in two diamond windows, or as a thin section that can be obtained by microtome. ATR FT-IR-M is frequently used for reflectance mode by using a micro-ATR objective; Germanium (5500–600 cm^{-1}) and Silicon (7800–800 cm^{-1}) are generally used as ATR objective crystal materials [41–43]. Recently Agilent developed a Laser Direct Infrared Imaging System (LDIR); this LDIR can relatively collect data faster compared to conventional FT-IR-M [44]. The main advantage of applying FT-IR-M is non-invasive; it does not need staining or labelling of the sample; the molecules are identified based on their characteristic IR vibrations. FT-IR-M delivers the group of compound information of the targeted area. Therefore FT-IR-M is also called as *chemical imaging* method [40].

2.2.3.5 Two-Dimension FT-IR Correlation Spectroscopy (2D FT-IR)

Sometimes it is very difficult to differentiate different samples by carrying out a conventional FT-IR only (absorbance- or transmission-mode) due to their close similarity. To overcome this problem, the conventional FT-IR spectra can be converted to their second derivative infrared spectra, and/or performing a 2D FT-IR [26]. 2D FT-IR can be prepared by using a KBr pellet, which will be perturbed by some physical or chemical stimulus using a special device; these stimuli will induce a dynamic 2D spectrum. A physical thermal stimulus was usually used for preparing a 2D FT-IR spectrum [45]. As example, 2D FT-IR spectra of some *Polygonum minus* can be prepared by using a thermal stimulus at certain range of temperatures (e.g. 40–120 °C, interval of 10 °C) [46]. The dynamic 2D infrared spectra can be obtained by plotting absorbance intensities and variables (wave number and perturbations); the spectra can be shown as three-dimensional spectra or as a contour plot. Two-dimension (2D) correlation infrared spectra, synchronous and asynchronous 2D, can be directly observed. A synchronous 2D FT-IR spectra of powdered *Curcuma longa* (KBr pellet) which was prepared at our laboratory was presented in Fig. 2.6 (unpublished work).

In synchronous FTIR spectrum, peaks presented the coincidence of the spectral intensity's differences (increase or decrease) at corresponding variables wave numbers v_i and v_j during perturbations. The synchronous correlation intensity of wave numbers (v_i, v_j) characterizes the degree of coherence between two signals that are measured concurrently. This intensity becomes maximum if the variations

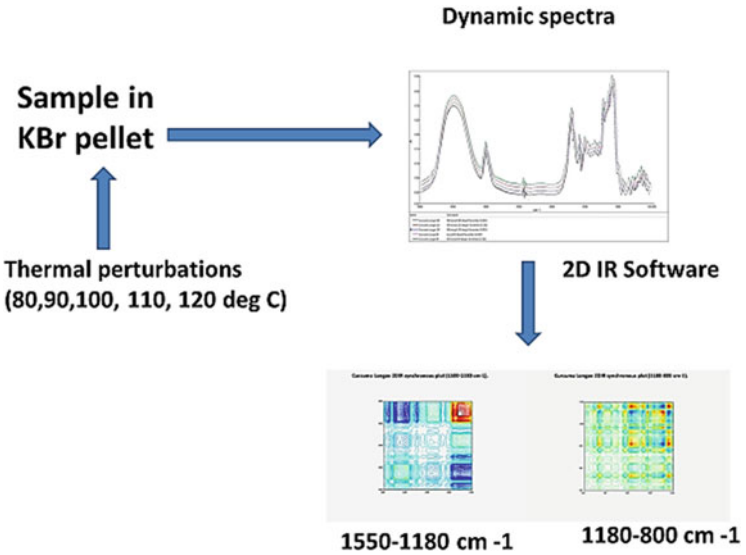

Fig. 2.6 How to generate two-dimension (2D) correlation spectrum of powdered *Curcuma longa* by using five levels thermal perturbations (unpublished results)

of the two dynamic IR signals are totally in phase with each other, and minimum if they are antiphase. IR signals which are nearly orthogonal to each other should yield almost no synchronous correlation intensity. A cross peak (at v_i, v_j) was observed if the spectral intensities at v_i and v_j changed instantaneously when perturbation was applied. The cross peak is positive if the intensities of v_i and v_j both increase (or decrease) along the perturbation, otherwise the cross peak is negative. 2D FT-IR spectrum is symmetric with respect to the diagonal line in the synchronous spectra. The variation of the spectra intensity at a variable is always the same as itself so there are only positive peaks that defined as auto peaks along the diagonal of the 2D synchronous spectrum. An auto peak characterizes the overall susceptibility of the spectral signal to change intensity when an external perturbation is applied [26, 45].

The asynchronous spectra afford the sequence of the spectral intensities' variations at different wave numbers v_i and v_j during the perturbations. The asynchronous correlation intensity on the other hand will characterize the coherence degree between signals measured at two different instances, which are separated by a correlation time. The asynchronous correlation intensity will be maximum if the dynamic signals are orthogonal to each other, and will be minimum when the signals are exactly in phase or antiphase with each other. A cross peak at v_i, v_j is detected if the spectral intensities at v_i changed before or after the variations of v_j. No diagonal peaks are observed in asynchronous 2D correlation spectrum [26, 45].

2.3 Chemometrics

The success of FTIR spectroscopy for analysis of food composition is supported by statistical analysis and chemometrics. Fortunately, some sophisticated instruments were equipped with statistical and chemometrics software [47]. Chemometrics, also known as multivariate data analysis (MDA), is a branch of chemistry which apply mathematics and statistics sciences to treat chemical data either qualitative or quantitative data (pH, concentrations, weights, etc.). Some topics are covered in chemometrics, namely descriptive statistics, the experimental design, process optimization, signal detection and signal processing, multivariate calibration, classification modelling and analytical quality assurance [48]. Chemical data typically include properties and values of numerous compounds as determined by instrumental methods and having various sources of variance. Accordingly, statistical evaluation of such data should use one or more multivariate data statistics (chemometrics). Multivariate statistics allows the simultaneous analysis of several independent variables (factors) against several dependent variables or responses [49].

Chemometrics is exploited for multivariate data collection and analysis protocols, calibration modelling, classification and cluster modelling, signal correction and compression, method optimization and statistical process control. Singh et al. [50] stated that chemometrics is useful means for the real-time in-process testing and is a valuable process analytical tool. In general, chemometrics or MDA are categorized in two classes: (a) chemometrics for qualitative data analysis intended for identification or classification purposes using pattern recognition methods and (b) multivariate calibration intended for facilitating the quantitative analytical purposes.

In analytical purposes, the most widely uses of MVA in FTIR spectra include confirmation, qualitative analysis, purity test and quantitative analysis of food components are (a) FTIR spectra processing by applying some pre-treatment spectra of mean centring, Savitzky-Golay derivatization, smoothing, etc. Spectra pre-treatment can enhance the accuracy and robustness of spectra resulting in reliable data, while spectra derivatization (1st, 2nd, 3th or higher order) can enhance the resolution of overlapping peaks [51–53]; (b) pattern recognition either unsupervised such as principal component analysis and cluster analysis or supervised like discriminant analysis with its algorithm variations; (c) multivariate calibrations (MC) using several algorithms including principle component regression and partial least square; (d) experimental design typically used for optimization of analytical conditions during food analysis [55]. Some methods such as analysis of variance and response surface methodology are widely used for optimization of factors affecting food analysis [54].

The steps of analytical procedures which involved FTIR spectroscopy and chemometrics techniques in food analysis can be briefly described as: (a) definition of food analysis problems, i.e. confirmation, identification (qualitative analysis) or quantitative analysis, (b) sampling process, (c) acquisition of FTIR spectra using

FTIR spectrophotometer, (d) pre-treatment (processing) of FTIR spectral data, (e) selection of chemometrics models, (f) selecting calibration and validation sets of samples, (g) the chemometrics model optimization in calibration using selected variables, namely absorbance values at specific wavenumbers region, (h) validation of chemometrics model and (i) making conclusion of chemometrics models [56]. All these steps can be assisted using sophisticated statistics software, among these are Minitab®, Unscrambler®, SIMCA® SIRIUS®, Matlab® and Pirouette®, Grams® 32 [57, 58]. Currently, free interface software of Chemoface has been developed by Prof. Cleiton A. Nunes et al. for chemometrics analysis [59].

2.4 Applications of FT-IR for Food Analysis

Some books and review articles, which described and discussed the general application of FT-IR for the analysis and quality control of food preparations, have been published in the last ten years. In 2009, Sun [27] edited a book entitled "Infrared Spectroscopy for Food Quality Analysis and Control", this book consisted of seven chapters on fundamental/instrumentation, and eight chapters for applications, which were comprised of meat, fish, milk, cereal, fruit and vegetable, fruit juice, wine and beer, egg and related products. Sun et al. [26] published a nice book that discussed in detail the methods and application of FT-IR for the analysis of complex mixtures of foods and traditional Chinese medicines. Rodriguez-Saona and Allendorf [60] wrote a review article on the application of FT-IR combined with MVA for the authentication and detection of food's adulterants. A mini review on the application of mid-infrared as a tool for phenotyping tool of milk trait has been published by Marchi et al. [61]. Khan et al. [62] described the application of FT-IR for identification of food's adulterants in honey, milk, wines, fat and oils. A review article on the application of FT-IR for detecting specific regulated or toxic plant in plant food supplements and herbal drugs has been published by Deconinck et al. [63]. Su and Sun [64] published a review article on the application of FT-IR, Raman and hyperspectral imaging techniques for quality determinations of powdery foods (e.g. milk, tea, cocoa, coffee, soybean floor, wheat flour, culinary powder). Application of FT-IR for checking the quality and safety of fat and oils was recently reviewed by Li et al. [65]. FTIR and its combination with various techniques (NIR, MS) for detecting food adulterants has been reviewed by Valand et al. [66]. Furthermore, Rohman [5] published mini review on the application of FT-IR for traceability and authentication of meat and meat products.

The objectives of the applications of FT-IR, 2D FT-IR combined with multivariate analysis (MVA) or chemometrics for analysis of food, which were described and discussed in books and article, which were cited in this present chapter, can be been summarized in Box 2.1. Our experiences showed that all kind of raw material (RM) from plant origin (including leaves, fruits, beans, herbs, etc.), meats and related animal products can be analysed by FT-IR. Sun et al. [67] and Sun et al. [26] have outlined *a tri-level infrared identification* for qualitative analysis by using FT-IR. Sample usually could be identified or differentiated by comparing

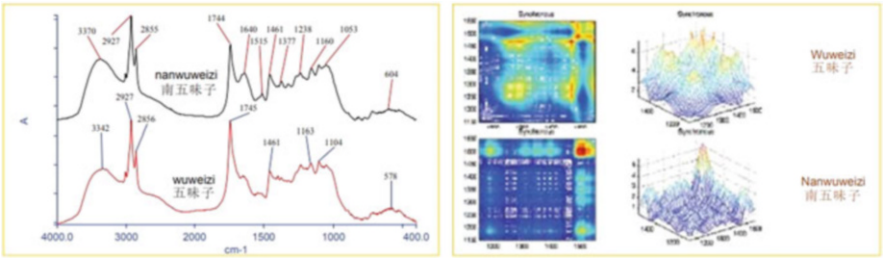

Fig. 2.7 By using two-dimension Fourier transform infrared (2D FT-IR) sample of Wuweizi (*Schisandrae chinensis* Fructus) and Nanwuweizi (*Schisandrae sphenantherae* Fructus) (Courtesy of PerkinElmer, Shelton, CT 06484, USA) [39]

their FT-IR spectra, and this is known as primary identification. The secondary step of identification is based on the second derivative infrared spectroscopy (SD-IR); some overlapped peaks, which were observed in the primary identification could be well differentiated by using SD-IR. In case, it was not possible for identification of a sample by using primary- and secondary-step, due to almost similar observed spectra, a two-dimensional correlation infrared (2D-IR) spectroscopy method can be applied; this 2D-IR is known as a tertiary step of identification method. Figure 2.7 showed the FT-IR spectra of the two fruits, which were similar, so the differentiation of those two fruits was difficult, but by using 2D FT-IR, both fruits can be easily discriminated. For identification and classification purposes by using primary and secondary identification methods, generally MVA was applied for data evaluations (e.g. PCA, PLS-DA, SIMCA). See Sect. 2.3.

Quantitative analysis by FT-IR can be performed by construction of a linear regression between concentrations of standard against the ratio of intensities of two specific wave number of the absorption FT-IR spectra; concentration of sample can be calculated from the linear calibration regression curve [26]. Quantitative analysis of the sample can be also done also using MVA (PLS); this will be discussed in section Chemometrics. It is very important to note, that before any data collections, method validation should be first performed. This present review will be focused on the application of FT-IR for analysing for fat, oil, fruits, beans and related products which appeared in the last ten years.

2.4.1 Application of FT-IR for Fruits, Beans and Related Products

The objective of application of FTIR spectroscopy in combination with multivariate data analysis (MVA) in food analysis is compiled in Box 2.1. Furthermore, Table 2.1 summarized publications that reported the application of FT-IR for analysing fruits, beans and related products. As shown in the table, ATR method was the most used method, this could be due to its simplicity of the method. Almost all publication used MVA for evaluations the FT-IR data.

Table 2.1 Application of FT-IR for analysing fruit, beans, nectar and its related preparations

Material	IR method	Sample for analysis	Measured/specific bands (cm^{-1})	Chemometrics[a]	Objective	Ref. (application[b])
Nectars	ATR	Nectars transferred to ATR surface	1200–900	PLS, OPS, GA	Quantification of a certain nectars in original- and adulterant-sample	[71] (b, h)
Fruits, vegetables	ATR	100 mesh powdered raw material (RM) and alcohol insoluble solids (ASI) transferred to ATR surface	1740 (neutral sugars); 1075, 1440–1450, 1616 and 1740 (pectin); 895, 1035–1041 and 1160–1163 (cellulose); 1035–1041 (lignin)	ANOVA, PCA, PLS	Determination of cell wall composition based on certain group of compounds	[72] (f)
Citrus fruits	ATR	Supernatant of MeOH extracts was dispensed into a 384-well zinc selenide (ZnSe) plate, and dried at 37 °C	1800–800	PCA, PLS-DA, PLS	Determination of total carotenoids, flavonoids and phenolic compounds in fruits	[73] (f)
Citrus fruits	ATR	Supernatant of MeOH extracts was dispensed into a 384-well zinc selenide (ZnSe) plate, and dried at 37 °C	950–1100, 1300–1500, and 1500–1700	PCA, PLS-DA, HCA	Discrimination of Citrus lines, and prediction sugar and acid content in fruits	[74] (a, f)
Drink fruit juices	ATR	Water solutions of sugars and Juices	900–1400	PCA, PLS	Prediction of sugars and acid contents	[74] (f)
Pineapple (*Ananas comosus* L.) by-products (core and shell)	ATR	Lyophilized pineapple by-product	4000–600	PCA, PLS	Determination of phenolic content and antioxidants in treatment's pineapple	[75] (a, f)
Mangoes fruit	DRIFFT	Approximately 2 mg of homogenized freeze-dried mango pulps were transferred to the DRIFT sample holder cup	1500–750	PCA, PLS	Determination of glucose and sucrose	[76] (f)

Tomato fruit	ATR	Whole tomato fruit was placed on the sample stage for analysis, with no more than 0.1 kg of applied pressure	1800–900	PCA-LDA	Determination of ripening processes of the tomato	[77] (a)
Mango fruit	DRIFFT	2 mg of freeze-dried mango samples transferred to the DRIFT sample holder cup	1250–740, 780 (7-cis β-carotene); 2922, 2862 (α-tocopherol); 2933, 2940 (ascorbic acid)	Random Forest of 1st derivative spectra and ANOVA	Determination of β-carotene, α-tocopherol and l-ascorbic acid	[78] (f)
Red plum-, persimmon-, peach- and kiwi-fruits	ATR	Fruit extract (extractor: 50% methanol/water, or 1.2 mol/L HCl in 50 mL/100 mL methanol/water then heating at 90 °C for 3 h)	1800–600	NA	Qualitative identification of poly phenols. Using catechin as standard	[79] (f)
Grape, carob and mulberry *Pekmez* (juices)	ATR	Adulterated and pure grape, carob and mulberry pekmez samples	1500–800	PLS, PLS-DA	Discriminate original and adulterant's juices	[80] (b)
Coffee samples	Transmission, DRIFFT, ATR	Ground coffee (GC) and KBr (1/50) for pellet (transmission); 1 mg GC mixed with 150 mg KBr (Driff)	3200–700	PCA, HCA	Discrimination of defective and non-defective coffee samples	[81] (c)
Green coffee bean samples	ATR	Liquid-nitrogen frozen green coffee beans were finely ground using a mortar	4000–600, (2750–1775) was removed before evaluations	PCA, PLS	Distinguishing green coffee beans from different origins	[82] (a)
Ayocote bean starches	Transmission	Powered samples mixed with dry KBr	4000–500	NA	Studying the effect of thermal and extraction on the characteristic of bean starches	[83] (a, g)

(continued)

Table 2.1 (continued)

Material	IR method	Sample for analysis	Measured/specific bands (cm^{-1})	Chemometrics[a]	Objective	Ref. (application[b])
Nespresso® coffee pods and Americano coffee pods	ATR	Approximately (1 g) of the roasted and ground coffee was placed in the sampling accessory	1800–1550	PCA, HCA	Differentiating Espresso and Americano coffee pods	[84] (d)
Powdered rice beans 40 mesh	Transmission	Powdered rice beans mixed with KBr	4000–500	NA	Studying the effect of thermal and extraction on the characteristic of rice starches	[85] (a)
Beans	ATR, 2D	Placing the samples directly onto the attenuated total reflection (ATR) crystal	3700–700 4000–1000 (for 2D)	PLS, PLSR	Determination of protein, starch and total amylose in common beans correlation between MIR and NIR	[86] (f)
Honey samples	ATR	Samples were placed on diamond/ZnSe crystal plate	1800–750	PCA, HCA	Determination of honey floral source	[87] (a)
Flour of some wheat grains	NA	Flour of each wheat variety was collected. These flour samples were converted into pellets and pellets were cut into thin sections. These thin sections were oven dried and their spectra were recorded on FTIR	1640–3300 (moisture); 1600–1700, 1550–1570 (crude fat); 1600–1700, 1550–1570 (crude protein); 800–1500, 2800–3000, 3000–3600 (starch)	NA	Qualitative identification of wheat varieties	[88] (a)

Strawberry fruits	Transmission using gaseous cell, 2D FT-IR	Using special device gas sampling	4000–600	PCA, 2D software	Determination spoilage process of strawberries	[89] (a)
Fruits peel	Transmission	Special gas sampling system designed by the authors	2990–2830 and 1259–1227	PCA	Detection of pesticide (chlorpyrifos) residues on fruit peels	[90] (f)
Cocoa beans and chocolate produced	ATR	Freeze-dried chocolate and cocoa beans were transferred onto ATR crystal	4400–600	PCA, PLS, PLSR	Prediction of the total phenol content and total antioxidant	[91] (f)
Crude coffee oil	ATR	An aliquot of 1 ml of the oil sample in a thin film was used for FTIR	3050–2800 (hydrogen's stretching vibrations); 1780–1680 (carbonyl stretching vibrations)	ANOVA	Differentiating roasted coffee oil and heated roasted coffee oil	[92] (a, e)
Soybeans	ATR	Soybean powder was loaded onto ATR crystal	4000–400	PLS-DA, PLSR	Discrimination and prediction of the origin of Chinese and Korean soybeans	[93] (a)

[a] *PLS* partial least square, *OPS* ordered predictor selection, *GA* genetic algorithm, *ANOVA* analysis of variance, *PCA* principal component analysis, *PLS-DA* partial least square-discriminant analysis, *HCA* hierarchal cluster analysis, *PLSR* partial least square regression, *NA* not available

[b] See Box 2.1

Box 2.1 The Objectives of the Application of Combination FT-IR, 2D FT-IR and MVA for Food Analysis[a]

a. Identification of raw RM; discrimination of the same RM, which was based on variants, geographical origins, harvested time and treatments
b. Rapid identification of genuine and counterfeit products
c. Quality control of the products
d. Differentiate products from different manufacturers
e. Stability evaluation of the RM and related products
f. Performing qualitative and quantitative analysis of compounds or group of compounds in RM and/or products
g. Monitoring and analysing the manufacturing and extraction processes
h. Performing rapid qualitative identification of RM in various formulations of the product.

[a]Modified from PerkinElmer, Complete Solution for Traditional Medicine Research and Analysis [68]

The distribution of certain class compounds (e.g. lipids and or sugars) in the cross section of a tomato fruit can be clearly observed by using FT-IR-M. Figure 2.8 showed the distribution of the absorbance at 1740 cm^{-1} (C=O lipid) corresponding to the lipid distribution, while Fig. 2.9 showed the distribution of sugars or carbohydrate can be detected using absorbance at 1050 cm^{-1} (OH); the red area corresponds to a high concentration of lipid relative to the blue area. The distributions and relative concentrations of proteins, carbohydrates and the waxes/lipids in the cross section of a wheat stem can be also easily determined by using FT-IR-M [40]. This showed that FT-IR Microscopy can be well used for searching and determining the locations and distribution of a certain compound or group of compounds in certain tissue(s) or organ(s) of plant and animal. Unfortunately, there is not many works that have been published on the application of FT-IR-M for food analysis.

2.5 Advantages and Disadvantages of Infrared Spectroscopy in Food Analysis

Some advantages of the application of FT-IR in food analysis are: the FT-IR spectrometer is relative cheap, sample preparation is simple, sample also can direct to be measured without any sample preparation, a small of amount of sample is required, non-destructive method of analysis, less use of hazardous solvent and decreasing hazard to environmental and human, rapid detection, analysing time is relatively very fast, various sample analysis can be analysis (such as, solids, liquids, semi-solids, powder samples, herbs etc.), relatively low operational cost, FT-IR can be used for both quantitative and qualitative methods, repeatability of the measurements is relative good, by using standardized method good reproducibility

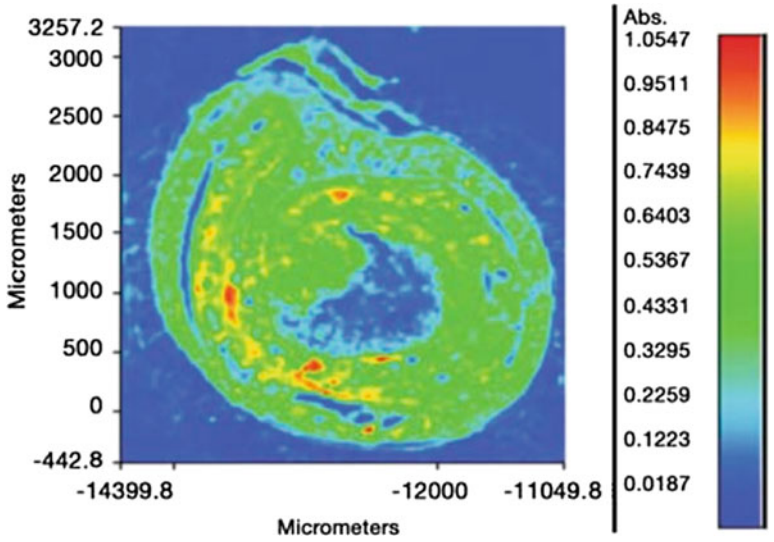

Fig. 2.8 Distribution of the absorbance at 1740 cm^{-1} corresponding to the lipid's distribution in the cross section of tomato (Courtesy of PerkinElmer, Shelton, CT 06484, USA) [39]

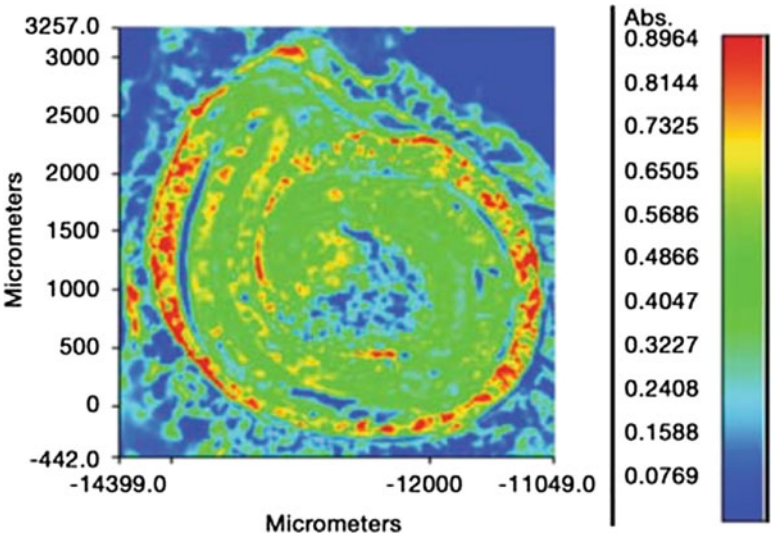

Fig. 2.9 Distribution of the absorbance at 1050 cm^{-1} corresponding to the sugar's distribution in the cross section of tomato (Courtesy of PerkinElmer, Shelton, CT 06484, USA) [39]

can be achieved. The disadvantages of FT-IR are: biological samples are difficult to analyse using FT-IR due to strong absorption of OH, FT-IR is sensitive to the environment change (CO_2 and water vapour can affect the spectra), FT-IR cannot detect atoms and monoatomic ions, elements or inert gas, FT-IR cannot detect

diatomic molecules such as nitrogen and oxygen [67, 69]. To overcome the problem of analysing biological fluids by FT-IR, Pupeza et al. [70] proposed a new method called Field-resolved infrared spectroscopy; detailed discussion of the new method can be referred in their recent publication.

2.6 Conclusion

Infrared spectroscopy method equipped with modern instrument and sampling handling technique such as attenuated total reflectance, Diffuse reflection infrared Fourier transform spectroscopy (DRIFTS), FTIR microscopy and Two-Dimension FT-IR Correlation Spectroscopy (2D FT-IR) is ideal technique for qualitative and quantitative analyses of food composition due to its capability to provide fingerprinting technique. FTIR spectroscopy is widely used for food composition analysis intended to confirmation and identification of raw materials, discrimination of food from different origin, authentication of food products as well as the monitoring and quality control of food production. In the future, the miniature of FTIR spectroscopy instrumentation makes this technique suitable for on-site application for rapid quality control.

Acknowledgements The authors are thankful to Dr. Teo Wei Boon (PerkinElmer, Singapore) for preparing 2D-FT-IR of *Curcuma longa* during short visit at the Faculty of Pharmacy, Airlangga University, Surabaya (2016), Dr. Robert Packer (PerkinElmer, Shelton, CA, USA) and Dr. Tan Boon Chun (PerkinElmer Selangor, Malaysia) for permission to reproduce some figures, Ms. Febry Ardiana (PT Bernofarm, Sidoarjo, Surabaya) for reference (USP 42, General method <854>) [23].

References

1. Pavia DL, Lampman GM, Kriz GS (2001) Introduction to spectroscopy, 3rd edn. Thomson Learning, Inc., Boston, p 579
2. Cozzolino D (2014) An overview of the use of infrared spectroscopy and chemometrics in authenticity and traceability of cereals. Food Res Int 60:262–265. https://doi.org/10.1016/j.foodres.2013.08.034
3. Teixeira AM, Sousa C (2019) A review on the application of vibrational spectroscopy to the chemistry of nuts. Food Chem 277:713–724. https://doi.org/10.1016/j.foodchem.2018.11.030
4. Tan HP, Ling SK, Chuah CH (2011) One- and two-dimensional Fourier transform infrared correlation spectroscopy of Phyllagathis rotundifolia. J Mol Struct 1006(1–3):297–302. https://doi.org/10.1016/j.molstruc.2011.09.023
5. Rohman A (2019) The employment of Fourier transform infrared spectroscopy coupled with chemometrics techniques for traceability and authentication of meat and meat products. J Adv Vet Anim Res 6(1):9–17
6. Moros J, Garrigues S, De Guardia M (2010) Vibrational spectroscopy provides a green tool for multi-component analysis. Trends Anal Chem 29(7):578–591. https://doi.org/10.1016/j.trac.2009.12.012
7. Gredilla A, De Vallejuelo SF, Elejoste N, De Diego A, Madariaga JM (2016) Trends in analytical chemistry non-destructive spectroscopy combined with chemometrics as a tool for green chemical analysis of environmental samples: a review. Trends Anal Chem 76:30–39. https://doi.org/10.1016/j.trac.2015.11.011

8. Li YS, Church JS (2014) Raman spectroscopy in the analysis of food and pharmaceutical nanomaterials. J Food Drug Anal 22(1):29–48. https://doi.org/10.1016/j.jfda.2014.01.003
9. Callao MP, Ruisánchez I (2018) An overview of multivariate qualitative methods for food fraud detection. Food Control 86:283–293
10. Pallone JAL, dos Caramês ET, Alamar PD (2018) Green analytical chemistry applied in food analysis: alternative techniques. Curr Opin Food Sci 22:115–121
11. Maree JE, Viljoen AM (2011) Fourier transform near- and mid-infrared spectroscopy can distinguish between the commercially important Pelargonium sidoides and its close taxonomic ally P. reniforme. Vib Spectrosc 55(2):146–152. https://doi.org/10.1016/j.vibspec.2010.10.005
12. Man YBC, Syahariza ZA, Rohman A (2011) Fourier transform infrared (FTIR) spectroscopy: development, techniques, and application in the analyses of fats and oils. In: Fourier transform infrared spectroscopy: developments, techniques and applications. Nova Science Publisher, New York
13. Chakraborty DS (2016) Instrumentation of FTIR and its herbal applications. World J Pharm Pharm Sci 5(3):498–505
14. Rohman A (2017) The use of infrared spectroscopy in combination with chemometrics for quality control and authentication of edible fats and oils: A review. Appl Spectrosc Rev 52:7
15. Ma G, Allen HC (2004) Handbook of Spectroscopy, Volumes 1 and 2 Edited by Günter Gauglitz (University of Tübingen) and Tuan Vo-Dinh (Oak Ridge National Laboratory). Wiley-VCH Verlag GmbH & Co. KGaA: Weinheim. 2003. 1168 pp. $435.00. ISBN: 3-527-29782-0. Vol. 126. J Am Chem Soc 34:8859–8860
16. Ballabio D, Todeschini R (2009) Infrared spectroscopy for food quality analysis and control multivariate classification for qualitative analysis. Infrared Spectrosc Food Qual Anal Control 2009:83–104
17. von Aulock FW, Kennedy BM, Schipper CI, Castro JM, Martin D, Oze C et al (2014) Advances in Fourier transform infrared spectroscopy of natural glasses: From sample preparation to data analysis. Lithos 206–207(1):52–64. https://doi.org/10.1016/j.lithos.2014.07.017
18. Hashimoto K, Badarla VR, Kawai A, Ideguchi T (2019) Complementary vibrational spectroscopy. Nat Commun 10(1):1–6. https://doi.org/10.1038/s41467-019-12442-9
19. Davis SP, Abrams MC, Brault JW (2001) Theory of the ideal instrument. Fourier Transform Spectrom 2001:29–39
20. Robertson M, Elements V, Table P, Library B, Society TR, Society TR et al (2004) Organic spectroscopic analysis
21. Baeten V, Dardenne P (2002) Spectroscopy: Developments in instrumentation and analysis. Grasas Aceites 53(1):45–63
22. Stuart BH (2004) Infrared spectroscopy: fundamentals and applications, vol. 8, Methods, p 224. Available from http://doi.wiley.com/10.1002/0470011149
23. United Stated Pharmacopeia (USP) 42, General method <854> mid infrared spectroscopy. https://online.uspnf.com/uspnf/document/GUID-21493947-8F57-4FC7-9338-FD47C1354A3A_4_en-US?highlight=854 © 2019 USPC. November 15, 2019
24. Thermo Scientific (2013) Introduction to FT-IR sample handling. Thermo Fish Sci Inc., Waltham, pp 1–8
25. Shimadzu. Measurement Methods for Powder Samples : SHIMADZU (Shimadzu Corporation). [cited 2020 Mar 21]. Available from https://www.shimadzu.com/an/ftir/support/ftirtalk/talk8/intro.html
26. Sun S-Q, Zhou Q, Chen J-B (2020) Infrared spectroscopy for complex mixtures: applications in food and traditional Chinese medicine. 2011 [cited 2020 Mar 21]. Available from http://books.google.es/books/about/Infrared_Spectroscopy_for_Complex_Mixtur.html?id=SUhIMwEACAAJ&pgis=1
27. Sun DW (2009) Infrared spectroscopy for food quality analysis and control. infrared spectroscopy for food quality analysis and control. Elsevier Inc., Amsterdam
28. Thermo Scientific (2019) Move from investigate to solve Forensics compendium. Move from investigate to solve Forensics compendium. Thermo Scientific, Waltham

29. PerkinElmer (2005) FT-IR Spectroscopy Attenuated Total Reflectance (ATR). PerkinElmer Life Anal Sci. pp 1–5. Available from http://www.utsc.utoronto.ca/~traceslab/ATR_FTIR.pdf
30. Griffiths PR, De Haseth JA (2006) Fourier transform infrared spectrometry, 2nd edn. Wiley, Hoboken, pp 1–529
31. Sciences N, Mada UG, Utara S, Mada UG, Utara S (2017) Attenuated total reflectance-FTIR spectra combined with multivariate calibration and discrimination analysis for analysis of patchouli oil adulteration. Indones J Chem 1:1–8
32. Smith BC (2002) Quantitative spectroscopy: theory and practice. Elsevier, Amsterdam, p 212
33. Bruker Optics Inc. Attenuated Total Reflection (ATR) – a versatile tool for FT-IR spectroscopy. Appl Note AN # 79. 2011. p 4
34. Van De Voort FR, Sedman J, Russin T (2001) Lipid analysis by vibrational spectroscopy. Eur J Lipid Sci Technol 103(12):815–826
35. Wellner N (2013) Fourier transform infrared (FTIR) and Raman microscopy: principles and applications to food microstructures. In: Food microstructures: microscopy, measurement and modelling. Elsevier Ltd, Amsterdam, pp 163–191
36. Infrared Microscopy Applications. [cited 2020 Mar 21]. Available from https://www.gia.edu/gia-news-research-Infrared-Microscopy-Applications
37. Kazarian SG, KLA C (2013) ATR-FTIR spectroscopic imaging: recent advances and applications to biological systems, vol 138. Royal Society of Chemistry, London, pp 1940–1951
38. Kimber JA, Kazarian SG (2017) Spectroscopic imaging of biomaterials and biological systems with FTIR microscopy or with quantum cascade lasers. Anal Bioanal Chem 409(25):5813–5820
39. Perkinelmer. Infrared Imaging and Microscopy Systems. [cited 2020 Mar 21]. Available from: https://www.perkinelmer.com/lab-solutions/resources/docs/BRO_Spotlight400A.pdf
40. Bruker Optics Inc. FT-IR microscopy - a powerful chemical imaging tool. [cited 2020 Mar 21]. Available from https://www.azom.com/article.aspx?ArticleID=5949
41. PerkinElmer, Inc. Spotlight 200 FT-IR microscopy system redefining IR microscopy. [cited 2020 Mar 21]. Available from www.perkinelmer.com
42. Maryse JEM. Application of FTIR microscopy to cultural heritage materials . 2009. [cited 2020 Mar 21]. Available from: http://amsdottorato.unibo.it/1404/
43. Prati S, Joseph E, Sciutto G, Mazzeo R (2010) New advances in the application of FTIR microscopy and spectroscopy for the characterization of artistic materials. Acc Chem Res 43(6):792–801
44. Paper W. Microplastics analysis doesn't need to be so hard simplify microplastics analysis through a rapid
45. Noda I (1990) Two-dimensional infrared (2D IR) spectroscopy: theory and applications. Appl Spectrosc 44(4):550–561
46. Khairudin K, Sukiran NA, Goh HH, Baharum SN, Noor NM (2014) Direct discrimination of different plant populations and study on temperature effects by Fourier transform infrared spectroscopy. Metabolomics 10(2):203–211
47. Rohman A, Arsanti L, Erwanto Y, Pranoto Y (2016) The use of vibrational spectroscopy and chemometrics in the analysis of pig derivatives for halal authentication. Int Food Res J 23:5
48. Daszykowski M, Walczak B (2006) Use and abuse of chemometrics in chromatography. TrAC - Trends Anal Chem 25(11):1081–1096
49. Granato D, Putnik P, Kovačević DB, Santos JS, Calado V, Rocha RS et al (2018) Trends in chemometrics: food authentication, microbiology, and effects of processing. Compr Rev Food Sci Food Saf 17(3):663–677
50. Singh SK, Jha SK, Chaudhary A, Yadava RDS, Rai SB (2010) Quality control of herbal medicines by using spectroscopic techniques and multivariate statistical analysis. Pharm Biol 48(2):134–141
51. Ferreira GWD, Roque JV, Soares EMB, Silva IR, Silva EF, Vasconcelos A et al (2018) Temporal decomposition sampling and chemical characterization of eucalyptus harvest residues using NIR spectroscopy and chemometric methods. Talanta 188:168–177

52. Lasch P (2012) Spectral pre-processing for biomedical vibrational spectroscopy and microspectroscopic imaging. Chemom Intell Lab Syst 117:100–114
53. Lai Y, Ni Y, Kokot S (2011) Discrimination of Rhizoma Corydalis from two sources by near-infrared spectroscopy supported by the wavelet transform and least-squares support vector machine methods. Vib Spectrosc 56(2):154–160. https://doi.org/10.1016/j.vibspec.2011.01.007
54. Singh I, Juneja P, Kaur B, Kumar P (2013) Pharmaceutical Applications of Chemometric Techniques. ISRN Anal Chem 2013:1–13
55. Leardi R (2009) Experimental design in chemistry: a tutorial. Anal Chim Acta 652(1–2):161–172
56. Krakowska B, Custers D, Deconinck E, Daszykowski M (2016) Journal of Pharmaceutical and Biomedical Analysis Chemometrics and the identification of counterfeit medicines — a review. J Pharm Biomed Anal 127:112–122. https://doi.org/10.1016/j.jpba.2016.04.016
57. Gad HA, El-Ahmady SH, Abou-Shoer MI, Al-Azizi MM (2013) Application of chemometrics in authentication of herbal medicines: a review. Phytochem Anal 24(1):1–24
58. Rodionova OY, Pomerantsev AL (2006) Chemometrics: achievements and prospects. Russ Chem Rev 75(4):271–287
59. Nunes CA, Freitas MP, Pinheiro ACM, Bastos SC (2012) Chemoface: a novel free user-friendly interface for chemometrics. J Braz Chem Soc 23(11):2003–2010
60. Rodriguez-Saona LE, Allendorf ME (2011) Use of FTIR for rapid authentication and detection of adulteration of food. Annu Rev Food Sci Technol 2(1):467–483
61. De Marchi M, Toffanin V, Cassandro M, Penasa M (2014) Invited review: mid-infrared spectroscopy as phenotyping tool for milk traits. J Dairy Sci 1:1171–1186
62. Khan U, Afzaal M, Arshad MS, Imran M (2018) Non-destructive analysis of food adulteration and legitimacy by FTIR technology. J Food Ind Microbiol 1(1):1–7
63. Deconinck E, Djiogo CAS, Bothy JL, Courselle P (2017) Detection of regulated herbs and plants in plant food supplements and traditional medicines using infrared spectroscopy. J Pharm Biomed Anal 142:210–217
64. Su W-H, Sun D-W (2018) Fourier transform infrared and Raman and hyperspectral imaging techniques for quality determinations of powdery foods: a review. Compr Rev Food Sci Food Saf 17(1):104–122
65. Li Q, Chen J, Huyan Z, Kou Y, Xu L, Yu X et al (2019) Application of Fourier transform infrared spectroscopy for the quality and safety analysis of fats and oils: a review. Rev Food Science Nutr 59:3597–3611
66. Valand R, Tanna S, Lawson G, Bengtström L (2020) A review of Fourier transform infrared (FTIR) spectroscopy used in food adulteration and authenticity investigations. Food Addit Contam 37:19–38
67. Sun S, Chen J, Zhou Q, Lu G, Chan K (2010) Application of mid-infrared spectroscopy in the quality control of traditional Chinese medicines. Planta Med 76:1987–1996
68. McGraw B (2015) Reversing the traditional drug development model. PerkinElmer, Waltham, pp 1–4
69. Cheng N (2013) Application of Fourier-transform infrared (FTIR) for quality control of Swiss cheese. Ohio State Univ 84:487–492
70. Pupeza I, Huber M, Trubetskov M, Schweinberger W, Hussain SA, Hofer C et al (2020) Field-resolved infrared spectroscopy of biological systems. Nature 577(7788):52–59
71. Miaw CSW, Assis C, Silva ARCS, Cunha ML, Sena MM, de Souza SVC (2018) Determination of main fruits in adulterated nectars by ATR-FTIR spectroscopy combined with multivariate calibration and variable selection methods. Food Chem 254:272–280
72. Canteri MHG, Renard CMGC, Le Bourvellec C, Bureau S (2019) ATR-FTIR spectroscopy to determine cell wall composition: application on a large diversity of fruits and vegetables. Carbohydr Polym 212:186–196
73. Song SY, Kim CH, Im SJ, Kim IJ (2018) Discrimination of citrus fruits using FT-IR fingerprinting by quantitative prediction of bioactive compounds. Food Sci Biotechnol 27(2):367–374

74. Song SY, Lee YK, Kim IJ (2016) Sugar and acid content of citrus prediction modeling using FT-IR fingerprinting in combination with multivariate statistical analysis. Food Chem 190:1027–1032
75. Santos DI, Neiva Correia MJ, Mateus MM, Saraiva JA, Vicente AA, Moldão M (2019) Fourier transform infrared (FT-IR) spectroscopy as a possible rapid tool to evaluate abiotic stress effects on pineapple by-products. Appl Sci 9(19):4141
76. Olale K, Walyambillah W, Mohammed SA, Sila A, Shepherd K (2017) Application of DRIFT-FTIR spectroscopy for quantitative prediction of simple sugars in two local and two Floridian mango (Mangifera indica L.) cultivars in Kenya. J Anal Sci Technol 8(1):1–13
77. Skolik P, Morais CLM, Martin FL, McAinsh MR (2019) Determination of developmental and ripening stages of whole tomato fruit using portable infrared spectroscopy and chemometrics. BMC Plant Biol 19(1):236
78. Olale K, Walyambillah W, Mohammed SA, Sila A, Shepherd K (2019) FTIR-DRIFTS-based prediction of β-carotene, α-tocopherol and l-ascorbic acid in mango (Mangifera indica L.) fruit pulp. SN Appl Sci 1(3):1–11
79. Park YS, Im MH, Ham KS, Kang SG, Park YK, Namiesnik J et al (2015) Quantitative assessment of the main antioxidant compounds, antioxidant activities and FTIR spectra from commonly consumed fruits, compared to standard kiwi fruit. LWT- Food Sci Technol 63(1):346–352
80. Yaman N, Velioglu SD (2019) Use of attenuated total reflectance—Fourier transform infrared (ATR-FTIR) spectroscopy in combination with multivariate methods for the rapid determination of the adulteration of grape, carob and mulberry PEKmez. Foods 8:7
81. Craig AP, Franca AS, Oliveira LS (2012) Evaluation of the potential of FTIR and chemometrics for separation between defective and non-defective coffees. Food Chem 132(3):1368–1374
82. Obeidat SM, Hammoudeh AY, Alomary AA (2018) Application of FTIR spectroscopy for assessment of green coffee beans according to their origin. J Appl Spectrosc 84(6):1051–1055
83. Bernardino-Nicanor A, Acosta-García G, Güemes-Vera N, Montañez-Soto JL, de los Ángeles Vivar-Vera M, González-Cruz L (2017) Fourier transform infrared and Raman spectroscopic study of the effect of the thermal treatment and extraction methods on the characteristics of ayocote bean starches. J Food Sci Technol 54(4):933–943
84. Monje AFB, Parrado LX, Gutiérrez-Guzmán N (2018) ATR-FTIR for discrimenation of espresso and Americano coffee pods. Coffee Sci 13(4):550–558
85. González-Cruz L, Montañez-Soto JL, Conde-Barajas E, de la Negrete-Rodríguez M, Flores-Morales A, Bernardino-Nicanor A (2018) Spectroscopic, calorimetric and structural analyses of the effects of hydrothermal treatment of rice beans and the extraction solvent on starch characteristics. Int J Biol Macromol 107(PartA):965–972
86. Plans M, Simó J, Casañas F, Sabaté J, Rodriguez-Saona L (2013) Characterization of common beans (Phaseolus vulgaris L.) by infrared spectroscopy: comparison of MIR, FT-NIR and dispersive NIR using portable and benchtop instruments. Food Res Int 54(2):1643–1651
87. Gok S, Severcan M, Goormaghtigh E, Kandemir I, Severcan F (2015) Differentiation of Anatolian honey samples from different botanical origins by ATR-FTIR spectroscopy using multivariate analysis. Food Chem 170:234–240
88. Amir RM, Anjum FM, Khan MI, Khan MR, Pasha I, Nadeem M (2013) Application of Fourier transform infrared (FTIR) spectroscopy for the identification of wheat varieties. J Food Sci Technol 50(5):1018–1023
89. Dong D, Zhao C, Zheng W, Wang W, Zhao X, Jiao L (2013) Analyzing strawberry spoilage via its volatile compounds using longpath Fourier transform infrared spectroscopy. Sci Rep 3:1
90. Xiao G, Dong D, Liao T, Li Y, Zheng L, Zhang D et al (2015) Detection of pesticide (Chlorpyrifos) residues on fruit peels through spectra of volatiles by FTIR. Food Anal Methods 8(5):1341–1346
91. Batista NN, de Andrade DP, Ramos CL, Dias DR, Schwan RF (2016) Antioxidant capacity of cocoa beans and chocolate assessed by FTIR. Food Res Int 90:313–319

92. Raba DN, Poiana M-A, Borozan AB, Stef M, Radu F, Popa M-V (2015) Investigation on crude and high-temperature heated coffee oil by ATR-FTIR spectroscopy along with antioxidant and antimicrobial properties. PLoS One 10(9):e0138080
93. Lee B-J, Zhou Y, Lee JS, Shin BK, Seo J-A, Lee D et al (2018) Discrimination and prediction of the origin of Chinese and Korean soybeans using Fourier transform infrared spectrometry (FT-IR) with multivariate statistical analysis. PLoS One 13(4):e0196315

Spectrophotometric Methods and Electronic Spin Resonance for Evaluation of Antioxidant Capacity of Food

3

Mauricio Moncada-Basualto and Claudio Olea-Azar

Abstract

"Antioxidant" is a popular term that applies to bioactive compounds that are not necessarily nutrients but can deliver added value to food. Therefore, the determination of the antioxidant capacity of foods has been of considerable interest for several decades.

The determination of antioxidant capacity of secondary metabolites present in food has been commonly associated with the health benefits of those who consume them. Currently there are numerous antecedents that discuss the potential benefits of these metabolites to health and how this term has been used by the advertising industry in the supply of food with added value. However, the fact that a food has an antioxidant capacity or not can account for its quality in terms of its organoleptic properties, their resistance to pathogens, among others. For the determination of antioxidant capacity there are several methodologies that allow obtaining information about the antioxidant power of food. In this chapter we will analyze the most used methods to determine the antioxidant capacity in food and raw materials.

Keywords

Antioxidant capacity · Antioxidant foods · Antioxidant capacity methods · HAT methods · SET methods

M. Moncada-Basualto · C. Olea-Azar (✉)
Departamento de Química Inorgánica y Analítica, Facultad de Ciencias Química y Farmacéuticas, Universidad de Chile, Santiago de Chile, Chile
e-mail: colea@uchile.cl

A. K. Shukla (ed.), *Spectroscopic Techniques & Artificial Intelligence for Food and Beverage Analysis*, https://doi.org/10.1007/978-981-15-6495-6_3

3.1 Introduction

Free radicals are highly unstable molecules that contain unpaired electrons, generated in vivo during metabolic processes. These molecules are neutralized by antioxidants, produced naturally by the body. However, environmental or behavioral stressors (pollution, exposure to sunlight, smoking cigarettes, excessive alcohol consumption, etc.) or simply a malfunction of the production of endogenous antioxidants can lead to excess free radicals, which results in oxidative stress. Oxidative stress can damage lipids, proteins, enzymes, carbohydrates, and DNA, preventing the normal functioning of the cell. These biochemical alterations build the molecular basis in the development of cancer, neurodegenerative and autoimmune disorders, cardiovascular diseases, and diabetes. Under such conditions, the external supply of antioxidants is essential to compensate for the harmful consequences of oxidative stress. Since antioxidants are naturally present in vegetables, a balanced diet helps the body prevent these diseases and deliver added value to plant products [1, 2].

At the end of the 19th century, antioxidant compounds were generally used in industrial processes against metal corrosion and rubber vulcanization. Later, the use in the prevention of rancidity caused by the oxidation of unsaturated fats became prevalent [3]. This is how the demand for raw materials of natural origin for production of food supplements, nutraceuticals and cosmetic products is growing. Raw extracts of fruits, herbs, vegetables, cereals, and other plant materials rich in phenolic compounds have an increasing interest in the food industry, as they hinder the oxidative degradation of lipids and, therefore, improve the quality of food and nutritional value [3–6].

3.2 Antioxidants in Food

The antioxidants present in food, also called dietetics, perform important functions in food and/or in mammals by counteracting oxidation processes and preventing chronic diseases related to oxidative stress. These compounds exert their activity through: (1) inhibition of free radicals, (2) inhibition of reactive oxygen/nitrogen species (ROS/RNS), or (3) chelating metals that catalyze oxidative reactions. For decades, studies have been conducted that indicate the antioxidant profiles of different foods. Different antioxidants of synthetic origin have been described that prevent rancidity in food caused by the oxidation of unsaturated fats. Likewise, naturally occurring antioxidants were discovered, isolated, and used for the same purpose [5].

Subsequently, synthetic antioxidants such as butylated hydroxytoluene (BHT), butylated hydroxyanisole (BHA), propyl gallate (PG), and ethoxyquin (EQ) were developed. These compounds or their combinations are commonly used in various foods to retard rancidity [7–9]. However, it has been reported that such antioxidants possibly increase health risks due to their toxicity and carcinogenicity, creating the need to identify natural sources that have antioxidant potential.

These sources contain different types of antioxidant compounds (tocopherols, ascorbic acid, carotenoids, and phenolic compounds). As a general classification, antioxidants were grouped into carotenoids (condensed tannins, xanthophylls, and carotenes), vitamins (ascorbic acid, tocopherols), flavonoids (flavones, isoflavones, flavonols, flavanols, flavanones), phenolic acids (hydroxybenzoic acid, acid hydroxycinnamic), sulfur-containing antioxidants, stilbenes, phenolic alcohols, tannins, lignans, and neoformed compounds (melanoidins) [5, 10–12].

- Tocopherols have been used to prevent the oxidation of lipids and prevent the oxidative destruction of carotenes due to their chain breaking activity [12, 13]. Their antioxidant mechanism could be summarized as: they are able to turn off lipid radicals and regenerate lipid molecules, and then produce a tocopheryl semiquinone radical that can form a stable tocopheryl quinone molecule and a regenerated tocopherol molecule. Natural sources of this type of compounds are nuts, vegetable oils, herbs, and spices [14]. The structure of tocopherols is described as a polar chromanol head group with a hydrophobic tail derived from isoprenoids. The number and substation of the methyl groups attached to the chromanol ring determined the types of tocopherols (α-, β-, γ-, or δ-) [14, 15].
- Carotenoids (xanthophylls and carotenes) are highly soluble compounds in lipophilic media, these contain 40-carbon terpenoids with a basic isoprene structural unit. These compounds have been used as lipid oxidation inhibitors when turning off singlet oxygen. In addition to its use potential scavenging of reactive oxygen species [16]. It was shown that β-carotene, α-carotene, lycopene, lutein, and cryptoxanthin constituted almost 90% of the carotenoids in the human diet. Green leafy vegetables, carrots, tomatoes, and cereals were found as the most common carotenoid sources [17].
- Ascorbic acid, also known as vitamin C, was described as one of the most important antioxidant compounds for human metabolism. The activity of this compound is characterized by being a radical chain terminator by transformation to non-toxic and non-radical products [18]. Ascorbic acid was observed to be capable of donating electrons to a wide variety of substrates such as superoxide radical anion, peroxide of hydrogen, hydroxyl radical, singlet oxygen, and oxide-reactive nitrogen [19].

Despite the above, compounds with highest antioxidant capacity are phenolic compounds and their derivatives. These correspond to most numerous groups of secondary metabolites of plants and are classified into flavonoids, phenolic acids, phenolic alcohols, stilbenes, lignans, and tannins. The antioxidant properties of these compounds are due to aromatic ring in its structure, which stabilizes the unpaired electron by delocalization. Additionally, the presence of substituents such as hydroxyl groups produces diversity in its structure and antioxidant capacity [20–22].

The largest group of phenolic compounds, flavonoids have variations of lateral groups in rings B and C that give rise to the diversity of flavonoid classes such as flavones, isoflavones, flavonols, flavanols, and flavonones. Several studies have

been carried out to elucidate the relationship between the structure of the phenolic compounds and their antioxidant capacity, and it was reported that the number of hydroxyl groups and the position of the substituents determine the antioxidant capacity [23, 24].

Phenolic acids consist of a benzene ring attached to a carboxylic group (benzoic acid) or a propenoic acid (cinnamic acid). They are classified according to their structure into hydroxycinnamic acids and hydroxybenzoic acids. Another group of phenolic compounds are stilbenes that are characterized by their antioxidant capacity. Resveratrol, one of the most common stilbenes in nature, has been reported to prevent oxidative stress in humans [25]. In addition, beneficial effects of stilbenes (especially resveratrol) have been associated with popular alcoholic beverages such as wine. However, it must be considered that it is not possible to absorb the recommended therapeutic dose by drinking only wine.

Likewise, it has been described that the fragments of peptides present in gelatin, egg yolk, meat, fish, chicken, and legumes have antioxidant capacity and are considered natural sources [26]. The antioxidant capacity of proteins is due to the elimination of free radicals by amino acid residues, as well as the chelation of pro-oxidative transition metals. The antioxidant capacity of the amino acids cysteine and methionine is due to the sulfhydryl groups that can eliminate free radicals [27].

Also, it has been described that antioxidant compounds could occur during food processing. Maillard reaction products (MRP), which occurred as a result of the reaction between carbonyl groups and amino groups, could exert antioxidant capacity in food systems [28–32]. The antioxidant mechanisms of melanoidins generated are: (1) capture of charged electrophilic metabolites, (2) elimination of oxygen radicals, (3) metal chelation, and (4) synergism [33].

Antioxidants in food are produced as a combination of two or more antioxidants. To understand their antioxidant effect, the effect was studied by combining α-tocopherol and flavonoids or ascorbic acid; evidencing a higher antioxidant capacity than the sum of its antioxidant effects due to the regeneration of α-tocopherol, an effect called synergism [34]. However, it was observed that some combinations of antioxidants such as α-tocopherol with rosemary extract or the combination BHA with peanut extract caused a decrease in antioxidant capacity than the simple addition of its individual effects, which is called antagonistic interaction [35, 36].

During the past decade, numerous studies focused on antioxidant synergy between ascorbic acid, tocopherols, carotenoids, and phenolic compounds have been conducted to understand the mechanism of synergy in food and simulated physiological conditions [37]. Antioxidant concentration was also considered determined the type of interaction (antagonistic or synergistic) with other antioxidants or their pro-oxidant effect. Due to the above, the favorable dose of antioxidants in the diet must be taken into account to maintain the balance between oxidants and antioxidants [5].

3.3 Methods for Determining Antioxidant Capacity

Quantification and determination of antioxidant capacity has become an area of interest for decades among food scientists. To date, many different analytical methods have been developed with various procedures that are mostly based on spectrophotometric techniques and electron spin resonance (ESR) [38].

These methodologies involve the following reaction mechanisms between antioxidants and free radicals:

1. Transfer of a hydrogen atom (HAT). In this HAT mechanism (Eq. (3.1)), an antioxidant H-atom (Fl-OH) is transferred to the free radical (R·) and forms a radical (Fl-O), which is more stable than R. This blocks the additional chain reaction. Greater stability of Fl-O represents a stronger antioxidant capacity of the antioxidant.

$$R^{\cdot} + Fl - OH \rightarrow RH + Fl - O^{\cdot} \tag{3.1}$$

2. Single-electron Transfer (SET), the antioxidant molecule could donate an electron to the free radical, thus becoming a radical cation (Eq. (3.2)); the latter can be done sequentially, either by transfer of an electron followed by proton transfer called SET-PT mechanism (Eq. (3.3)) and another mechanism referred to the loss of a proton followed by delivery of an electron called SPLET (Eq. (3.4)) [2, 39].

$$R^{\cdot} + Fl - OH \rightarrow R^{-} + Fl - OH^{\cdot +} \tag{3.2}$$

$$Fl - OH \rightarrow Fl - OH^{+} + e^{-} \tag{3.3}$$

$$Fl - OH^{+} \rightarrow Fl - O + H^{+}$$

$$Fl - OH \rightarrow Fl - O^{-} + H^{+} \tag{3.4}$$

$$Fl - O^{-} \rightarrow Fl - O + e^{-}$$

In first step of SET-PT, an electron was transferred from an antioxidant molecule to a free radical and followed by a detonation of the radical cation. As for SPLET, the first step was the detonation of the antioxidant, thus forming an anion, and then an electron was transferred from the anion to the free radical.

Based on these mechanisms, there are several methodologies that allow to determine the antioxidant capacity of both foods of natural origin and processed foods (Table 3.1) [40]. Due to different mechanisms involved in the determination of antioxidant capacity, the analysis of affected results by methodologies it is usually not comparable to each other.

Table 3.1 Methods for determining antioxidant capacity based on the mechanisms of hydrogen atom transfer and electron transfer

Hydrogen atom transfer methods (HAT)	Electron transfer methods (ET)
• Oxygen radical absorbance capacity (ORAC) method • Cellular antioxidant activity (CAA) assay • Scavenging of hydroxyl radical by ESR • ABTS radical scavenging method • Lipid peroxidation inhibition capacity (LPIC) assay • Total radical trapping antioxidant parameter (TRAP) • Inhibited oxygen uptake (IOC) • Crocin bleaching nitric oxide radical inhibition activity • Hydroxyl radical scavenging activity by p-NDA (p-butrisidunethyl aniline) • Scavenging of H_2O_2 • Scavenging of super oxide radical formation by alkaline (SASA)	• Ferric reducing antioxidant power (FRAP) • DPPH free radical scavenging assay • Total phenols by Folin–Ciocalteu • Trolox equivalent antioxidant capacity (TEAC) decolorization • Copper (II) reduction capacity • N,N-dimethyl-p-Phenylenediamine (DMPD) assay

The type of methodology to use depends on several factors, where the main ones are the chemical nature of the antioxidants that they want to analyze in a food and the way of extraction of said compounds from the food matrix.

Despite the above, it must be clear that antioxidant methodologies are complementary to each other and many times an attempt is made to find correlations between them. However, these may not correlate due to the nature of the trials.

Next, different methodologies used in determination of antioxidant capacity in foods or by-products associated with the nutritional quality of these will be described.

3.4 Hydrogen Atom Transfer Methodologies Used in Determining Antioxidant Capacity in Food

3.4.1 Oxygen Radical Absorbance Capacity (ORAC) Method

ORAC method is one of the most widely used tests; in fact, the ORAC fruit databases have been recently built to emphasize the benefits and establish the antioxidant capacity of foods rich in polyphenolic compounds [41]. Currently, it has been known that the ORAC index is strongly influenced by the type of probe used in the determination of antioxidant capacity [42]. Dorta et al. [43] indicated that the ORAC index is not directly related to the ability to eliminate free radicals, present in a sample, since its determination not only involves the concentration of antioxidant, but also the chemical nature of compound, and its possible interaction between the antioxidants present in a complex matrix.

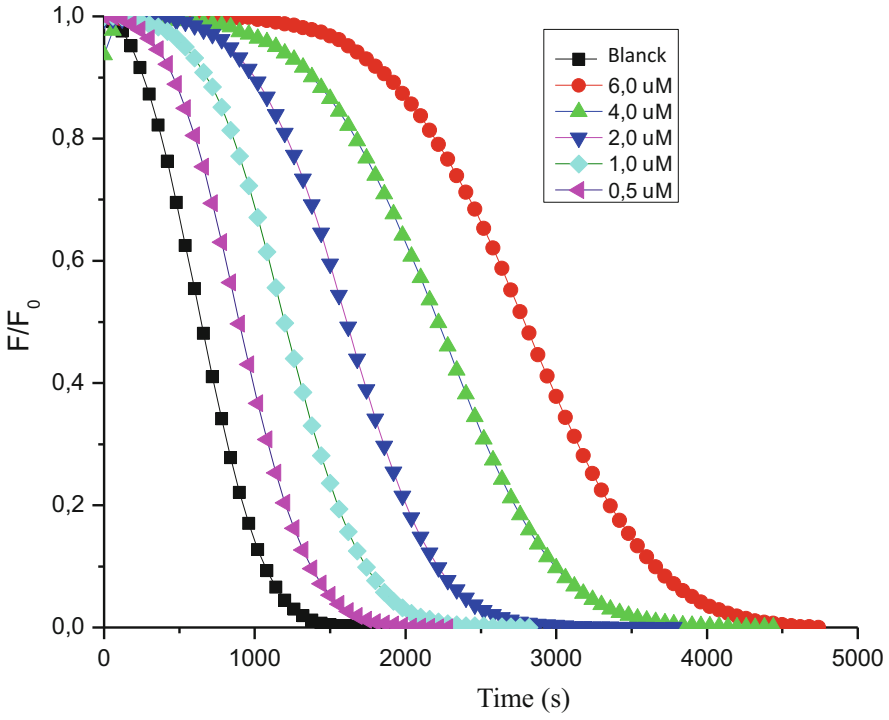

Fig. 3.1 FL fluorescence decay curve induced by AAPH in the presence of different Trolox concentrations

Method consists in transfer of hydrogen atoms of the antioxidant compound to the free radical generated by thermolysis at 37 °C of 2,2′-azo-bis- (2-amidino-propane) (AAPH). To demonstrate this reaction, probes of different nature are used, which reacts with the free radicals generated in the thermolysis once the antioxidant concentration decreases or if the reaction rate of the antioxidant is slower than that of the probe with the generated radical. Therefore, absorbance or fluorescence is recorded in this technique as a function of time at different concentrations of antioxidant (Fig. 3.1), depending on the type of probe [2, 43, 44].

Figure 3.1 shows the decay curve of the normalized fluorescence of the FL probe as a function of time, it can be shown that as the concentration of the antioxidant (Trolox) increases there is a time that no decrease in fluorescence is evidenced (induction time); this indicates that there is protection of the probe by the antioxidant until its concentration decreases and the reaction of the radicals with the probe begins.

Based on the above, the use of the probe in ORAC methodologies accounts for the antioxidant capacity in terms of reaction stoichiometry (ORAC-FL) or in terms of antioxidant reactivity (ORAC-PGR) [42, 45, 46]. This difference in profiles

must be seen because the thermolysis of the AAPH generates both radicals peroxyl ($ROO^{\bullet}$) as alkoxy ($RO^{\bullet}$), the latter being more reactive [43].

Zheng et al. [47] investigated the antioxidant activity of various spice extracts, which have been popularly described as medicinal agents, by the ORAC technique; determining that the diversity and complexity of the phenolic compounds present in the extracts are difficult to characterize and evaluate each of its antioxidant properties. Prior et al. [48] indicated that the ORAC test provides valuable results in the analysis of samples of natural products regarding antioxidant capacity, provided that the advantages, disadvantages, and deficiencies of the in vitro assay are understood. This test could represent a practical way to evaluate the potential that a certain food can have to contribute to the antioxidant state of the organism. However, for a full description of the antioxidant capacity it must be complemented with other techniques [49].

Another of the ORAC methodologies widely used and that reduces the problems regarding the type of radical generated is the use of Electronic Spin Resonance by means of the spin trapping technique. This technique involves the generation by thermolysis or photolysis of the radical $RO^{\bullet}$, which reacts with a spin trap (usually 5,5-dimethyl-1-pyrroline-N-oxide (DMPO)), generating a radical species with a longer life, which decreases its concentration based on the increase in antioxidant concentration (Fig. 3.2) [50–53].

$$RO^{\bullet} + DMPO \overset{kST}{\rightarrow} [DMPO - OR]^{\bullet} \tag{3.5}$$

$$RO^{\bullet} + AOH \overset{kAOH}{\rightarrow} Product \tag{3.6}$$

In ORAC-ESR methodology, the antioxidant capacity is evaluated in terms of reactivity of the competing compound of the spin trap as opposed to the ORAC-FL methodology.

In addition, other ORAC methodologies have been developed that involve other reactive oxygen species such as superoxide anion, hydroxyl, hydrogen peroxide, singlet oxygen, and peroxynitrite. The sum of the antioxidant capacity measured by these six radicals was described as ORAC Multiple Radicals [54]. However, it was found that these tests were inconvenient to determine the antioxidant capacity of foods, since some of them were not suitable for quantifying non-antioxidants. Enzymatic, some of them were difficult to apply and it was not practical to use in routine analysis by peroxyl radicals [5].

This methodology can be used to determine the quality of food or its durability. The oxidative rancidity of food includes the deterioration of proteins and lipids. In the case of meat, special attention has been paid to the oxidation of its proteins by peroxyl radicals [55], generating oxidation products (carbonyls), the consumption of tryptophan, and the formation of high molecular weight protein aggregates associated with meat digestibility [56, 57]. Oxidation of these proteins has been described as involving the formation of the perferrilmyoglobin radical, originating

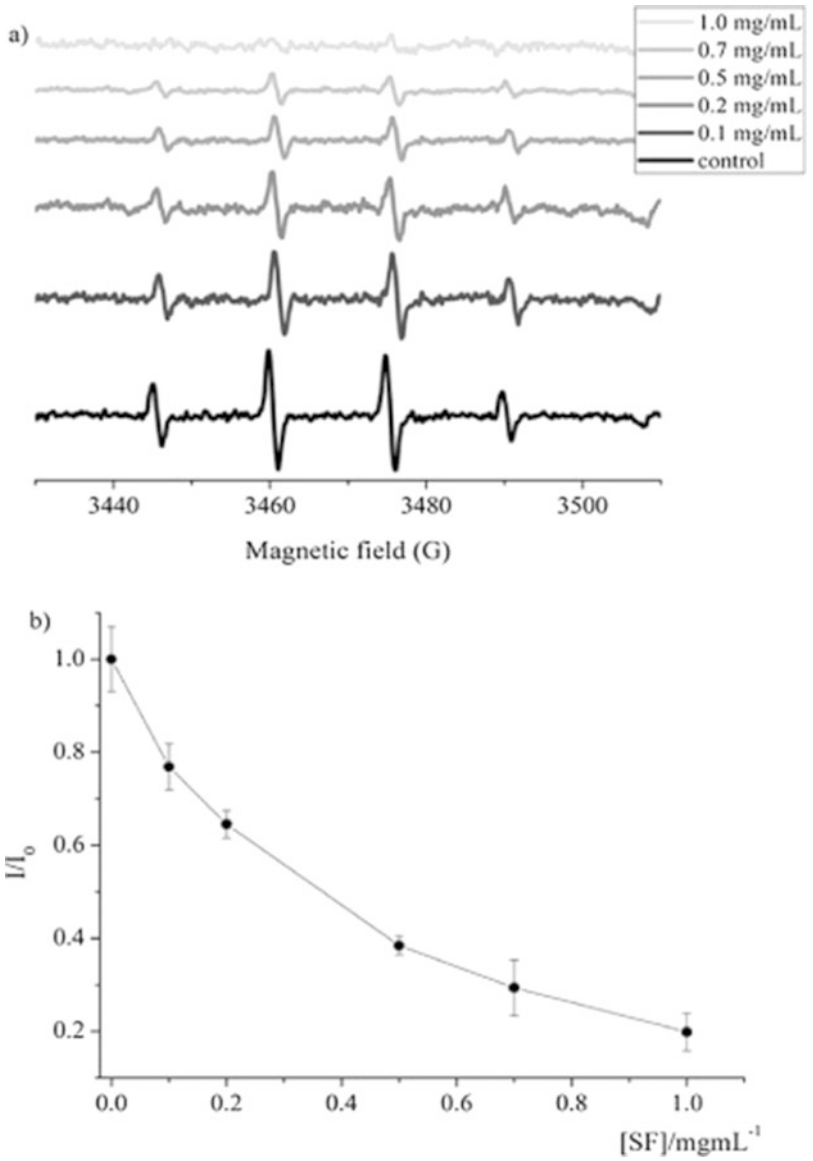

Fig. 3.2 (**a**) Decrease in the intensity of the ESR spectrum of the DMPO-RO spin adduct • as a function of sulfated fucan (antioxidant) concentration; (**b**) Relationship between normalized intensity in ESR spectra by adding sulfated fucan [50]

from of metmyoglobin. Based on the above, extracts of natural origin have been used to prevent the oxidation of meat products, due to the scavenging of peroxyl and perferrilmyoglobin radicals generated during lipid peroxidation [58, 59].

Along these lines, the use of food by-products has been the focus of attention in recent years, in order to deliver added value to these wastes. Thus, inhibition of peroxyl radical mediated oxidation of tryptophan residues in myofibrillar proteins by the use of mage by-products (seed, peel, and pulp) has been studied. These were studied using the ORAC-FL and ORAC-PGR tests. The data obtained using the ORAC-FL assay indicated similar values of antioxidant capacity of pulp, seed, and peel. However, by means of ORAL-PGR it was possible to differentiate the antioxidant activity of the samples, with the pulp being higher, followed by peel and finally seed. All extracts demonstrated inhibition capacity of peroxyl radical-mediated tryptophan oxidation and it was correlated with that determined by ORAC-PGR. The latter would indicate that the ORAC-PGR method could be used to predict this inhibitory effect [60].

3.4.2 Cellular Antioxidant Activity (CAA) Assay

Despite wide usage of these chemical antioxidant activity assays, their ability to predict in vivo activity is questioned for a number of reasons. Some are performed at nonphysiological pH and temperature and none of them considers the bioavailability, uptake, and metabolism of the antioxidant compounds. The protocols often do not include the appropriate biological substrates to be protected, relevant types of oxidants encountered, or the partitioning of compounds between the water and lipid phases and the influence of interfacial behavior. Biological systems are much more complex than the simple chemical mixtures employed, and antioxidant compounds may operate via multiple mechanisms. The different efficacies of compounds in the various assays attest to the functional variation. The best measures are from animal models and human studies; however, these are expensive and time-consuming and not suitable for initial antioxidant screening of foods and dietary supplements. Cell culture models provide an approach that is cost-effective, relatively fast, and address some issues of uptake, distribution, and metabolism.

Despite wide use of ORAC-FL, PGR, or EPR antioxidant assays, which involve the transfer of a hydrogen atom. There is evidence that indicates that these methods cannot correctly predict activity in in vivo systems, since this type of test, like others, may not contemplate physiological conditions, such as pH, temperature, bioavailability, absorption, and metabolism of antioxidant compounds. Where one of the most important factors is the bioavailability of the compounds, which implies the solubility in the physiological medium and the interaction with the lipid membrane that could limit the activity in the biological medium [2, 51, 61]. Therefore, the best measures of antioxidant capacity would be animal models and human studies; however, these involve large costs, time, and may not be adequate for the study of antioxidant compounds in food and dietary supplements [62]. It is then that cell models would provide a cost-effective approach to address some problems of absorption, distribution, and metabolism [61, 63].

Based on the above, a cellular antioxidant activity (CAA) assay has been developed to quantify the antioxidant activity of phytochemicals, food extracts,

and dietary supplements. This assay uses dichlorofluorescein as a probe that permeates cell membrane and is easily oxidized to a fluorescent probe, fluorescent dichlorofluorescein (DCF). The method determines the ability of antioxidants to prevent peroxyl radical-mediated DCF formation generated by 2,2′-azobis (2-amidinopropane) dihydrochloride (ABAP) thermolysis in mammalian cells. The area under curve between fluorescence intensity in cells treated with antioxidant compounds as a function of time. Control cells (without addition of antioxidant) indicates antioxidant capacity of the compounds inside treated cells (Fig. 3.3) [2, 51, 64]. The latter because cells are washed before formation free radicals. Therefore,

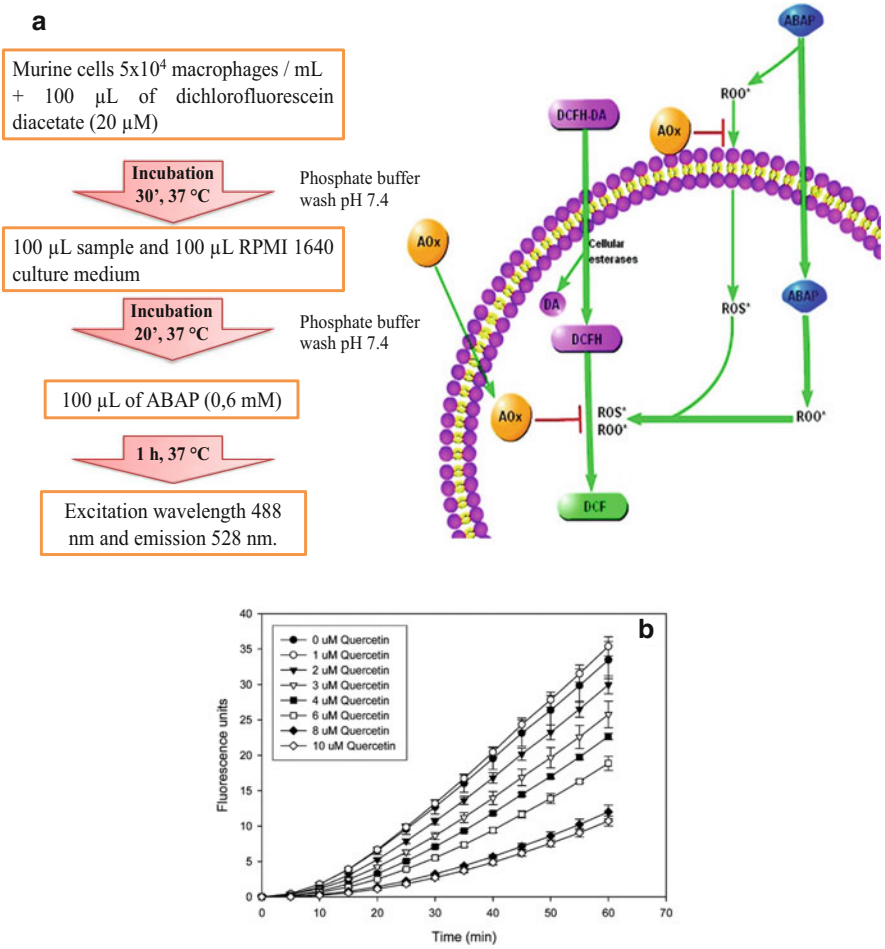

Fig. 3.3 (**a**) Proposed method and principle of the assay of cellular antioxidant activity (CAA) in murine RAW 264.7 cells. (**b**) Fluorescence intensity curve as a function of time for different concentrations of quercetin [61]

cellular antioxidant activity also informs the ability to traverse cell membranes of antioxidant compounds.

Wolfe et al. determined the antioxidant activity of selected phytochemicals and fruit extracts were evaluated and the results were expressed in micromoles of quercetin equivalents per 100 μmol of phytochemical or micromoles of quercetin equivalents per 100 g of fresh fruit. Quercetin had the highest CAA value, followed by kaempferol, epigallocatechin gallate (EGCG), myricetin, and luteolin among the pure compounds tested. Among the selected fruits tested, blueberry had the highest CAA value, followed by cranberry > apple = red grape > green grape. The CAA assay is a more biologically relevant method than the popular chemistry antioxidant activity assays because it accounts for some aspects of uptake, metabolism, and location of antioxidant compounds within cells.

Wolfe et al. [61] determined the cellular antioxidant activity of phytochemicals and fruit extracts. Activity results were expressed in micromoles of quercetin equivalents per 100 μmol of phytochemicals or 100 g of fresh sample. Quercetin had the highest CAA value, followed by kaempferol, epigallocatechin gallate (EGCG), myricetin, and luteolin among the tested antioxidants. Among fruits evaluated, bilberry had the highest CAA value, followed by the bilberry, apple; being the least active the green grape. The CAA assay is a more relevant method than the antioxidant capacity assays discussed above, since it involves aspects of absorption, metabolism, and location of antioxidant compounds within cells.

The high amount of bioactive compounds present in fruit co-products can be used as natural food additives, especially considering that agroindustrial waste is rich in dietary fibers (DF), among them pectins. Several efforts have been made for the harnessing of fruit industrial waste, and studies have already reported the utilization of peels from mango, yellow passion fruit, watermelon and Ponkan mandarin, pomace of grape, tomato, pumpkin, and carrot, among others for the production of pectin and other bioactive compounds [65, 66].

Food products may incorporate fiber-rich co-products as inexpensive, non-caloric bulking agents for partial substitute of flour, fat, or sugar, or as enhancers of water and oil retention and to increase emulsion or oxidative stabilities. Moreover, DF presents beneficial human health effects related to promoting better functioning of the digestive system, mainly due to increased satiety and the volume and weight of fecal matter. It also reduces the risk and occurrence of obesity, hyperglycemia, hypercholesterolemia, constipation, coronary heart disease, hemorrhoids, and colon cancer [67]. Furthermore, DF can be substrate for fermentation by bacteria in the large intestine, producing various end compounds (such as short chain fatty acids), energy, and biomass, leading to the maintenance of the gut microflora and improvement of the immune system [66].

Antioxidant capacity is another important DF benefit as it significantly contributes to positive health effects. Antioxidant DF can be defined as a product containing expressive amounts of natural antioxidants, such as phenolic compounds, associated with the fiber matrix.

Schneider et al. [66] studied the characterize DF obtained from guavira fruit pomace and investigate its antioxidant potential in a cell model. The DF were chem-

ically characterized as containing arabinan, highly methoxylated homogalacturonan and arabinogalactan. The cellular viability by MTT and DCFH-DA assay was performed to assess, respectively, changes in cell viability and the potential intracellular antioxidant activity against H_2O_2-induced oxidative stress in murine NIH 3T3 fibroblast. DF exhibited no effects on cell viability, moreover, when administered 48 h prior the induction of H_2O_2 toxic effects, it protected the cells, significantly increasing the cell viability compared to control. This protection may be related to the observed reduction of reactive oxygen species levels. Thus, the pre-treatment of cells with guavira DF for 48 h remarkably induced a cytoprotection against pro-oxidant conditions and may be a valuable functional compound recovered from an unexploited agroindustrial waste. These results demonstrated the protective effect of guavira DF against the oxidative stress induced by the H_2O_2 in NIH 3T3 cells.

3.4.3 Scavenging of Hydroxyl Radical by ESR

Since its development by Zavoisky in 1940 this non-destructive technique, which enables the detection and identification of paramagnetic species in different matrices, has been applied in several investigation fields such as food antioxidants [2]. One of most reactive radical species, which can be found in biological systems and has been used in the characterization of the antioxidant capacity of foods is hydroxyl radical [53].

The formation of hydroxyl radical can come from catalytic Fenton reactions, which involves the use of an active redox metal such as Fe^{+3} or non-catalytic in a basic medium. In both cases, hydrogen peroxide can be used; however, in the case of products of natural origin or food, the non-catalytic method is preferable (Eq. (3.7)), since Fe^{+3} can be chelated by polyphenolic compounds, reducing the scavenging capacity of the hydroxyl radical [68].

$$2H_2O_2 + OH^- \rightarrow OH^{\bullet} + O_2^{\bullet -} + H_2O \tag{3.7}$$

The hydroxyl-scavenging ability can be assessed by a non-catalytic and competitive Fenton system that uses DMPO or 5-diethoxyphosphoryl-5-methyl-1-pyrroline-N-oxide (DEPMPO) as the spin trap in basic media. The spin trap reacts with hydroxyl radicals to generate a spin adduct that shows a control signal, which is quantified by electron spin resonance (ESR, Fig. 3.4) [2, 68, 69].

Quantification can be performed based on percentage decrease of one of signals of formed spin adduct (area under the curve) or through a calibration curve with an antioxidant recognized by means of intensity of signals (Fig. 3.4). Figure 3.4 shows decrease in signal of spin adduct of hydroxyl radical in ESR spectra by adding increasing concentrations of a fucoidan (polysaccharide with antioxidant capacity) [50].

The determination of the antioxidant capacity through the elimination of the hydroxyl radical can explain the quality of the wine products. In particular, the loss of wine aroma can be explained by its aeration, since controlled oxidation in the

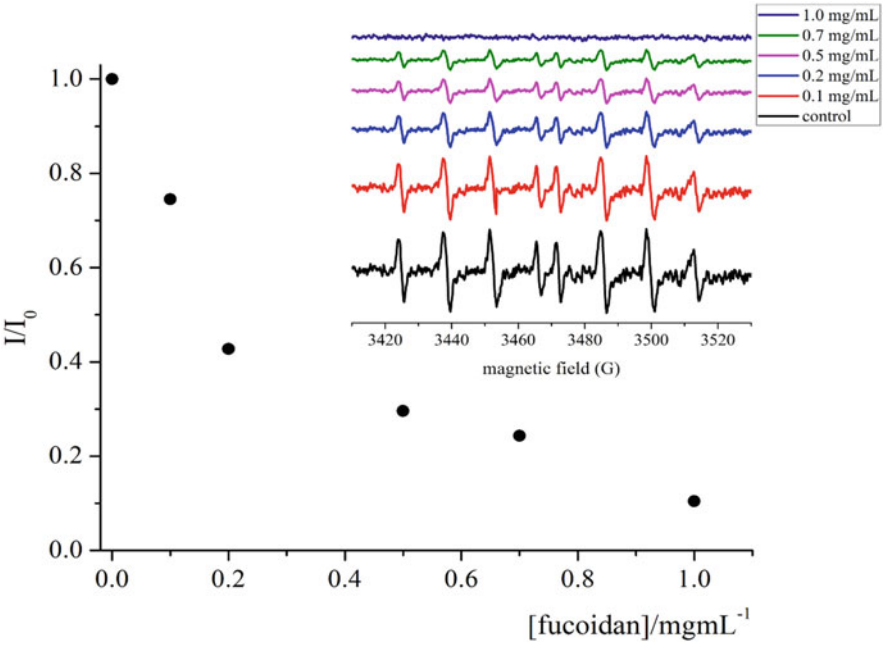

Fig. 3.4 Decrease in the intensity of the hydroxyl radical signals in the ESR spectra by the addition of fucoidan and Ratio between the normalized intensity in ESR spectra by the addition of fucoidan [50]

vinification and aging process is due to the reactions between molecular oxygen and phenolic compounds. Therefore, during aeration, the formation of quinones is stimulated, which in turn react with reduced sulfur volatiles such as hydrogen sulfide and alkyl thiols such as ethane thiol. This is a more likely explanation for the loss of aroma in this product [70, 71].

Espinoza et al. [69] studied four different types of Chilean wines (Cabernet Sauvignon, Merlot, Carmenere, and Syrah) examined for their free radical scavenging capabilities by electron spin resonance (ESR). Among the wines evaluated, Cabernet Sauvignon was the one that had the most activity against radicals. The presence of copper or iron added to the wines resulted in a reduced free radical scavenging capacity for all types of wines studied. The latter, probably due to the formation of coordination compounds between the phenolic compounds and metals present in the wine, which inactivate the redox capacity of the hydroxyl groups. Therefore, this methodology could explain the sensory quality of this type of product.

3.5 Electron Transfer Methodologies Used in Determining Antioxidant Capacity in Food

3.5.1 Total Phenols by Folin–Ciocalteu

Many procedures have been developed for the quantification of the total phenolic content in foods. Although separation methods such as high performance liquid chromatography are powerful techniques for identifying phenolic compounds in complex samples, their application to estimate total phenolic content may be inaccurate, time-consuming, and expensive [72].

For the quantification of total polyphenols, the methods available for the most part are based on colorimetric reactions, which allow their determination in the visible region [73]. Among which, one of the most used is the Folin–Ciocalteu (FC test); several studies have been able to correlate the content of polyphenols determined by this method with the antioxidant activity determined by electron transfer and hydrogen atom tests (ABTS + • and DPPH •, for example) [74]. For this reason, the method described by Singleton and Rossi has been proposed as a routine standardized method for measuring the measurement of antioxidant capacity of food products and/or dietary supplements [75]. In addition, the new designation "reducing capacity of FC reagents" was suggested [49].

Despite the above, it should be borne in mind that phenolic compounds within a sample of natural origin are not the only reducing species, since other reducing agents such as carbohydrates with terminal reducing ends can also reduce the reagent generating a false positive. For this reason, the inclusion of other methods of determining phenolic compounds is recommended for more exhaustive studies.

Magalhães et al. [72] described an automated procedure for the evaluation of the content of phenolic compounds and/or antioxidant capacity, which consists of the automated injection of the reagent and has been used for the determination in various food products, using as reference phenol. Different strategies were tried to mix the sample and the reagent, achieving a higher yield in the determination using 100 μL of sample + 100 μL of reagent. The application of the proposed method to compounds with antioxidant activity (both phenolic and non-phenolic) and to food samples and alcoholic beverages provided similar results to those obtained by the conventional batch method.

3.5.2 Ferric Reducing Antioxidant Power (FRAP)

The ferric reducing antioxidant power (FRAP) assay proposed by Benzie and Strain in 1996 monitors the reaction of Fe^{2+} with 2,4,6-Tripyridyl-s-Triazine (TPTZ) to form a violet-blue color with an absorbance maximum at 593 nm (Fig. 3.5) [2, 76]. Some FRAP assays employ phenanthroline, bathophenanthroline, ferricyanide, or ferrozine as a chromogenic ligand [77]. However, all FRAP assays detect compounds with a standard reduction potential (EO) below +0.77 and which reduce

$$[Fe(+3)(TPTZ)_2]^{3+} \xrightarrow[AOH]{} [Fe(+2)(TPTZ)_2]^{2+}$$

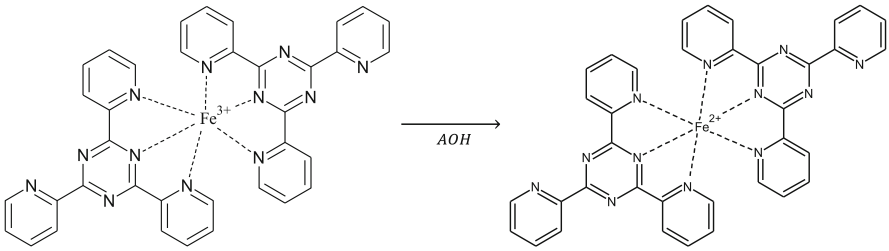

Fig. 3.5 Formation of the colored complex between Fe^{+2} and TPTZ, after the redox reaction between ferric ion and the antioxidant AOH

Fe^{3+} to Fe^{2+}. The characteristics of the TPTZ-FRAP assay have been compared with other total antioxidant capacity (TAC) assays [78]. FRAP assays are compatible with auto-analyzer and manual assay formats [79, 80].

Microplate-based FRAP (mFRAP) assays were introduced recently leading to improved sample throughput compared to the manual FRAP assay [81]. However, the optical pathlength for microplate readers is not fixed and results may be affected by changes of sample volume and composition. The pathlength dependence on sample volume leads to microplate results being less readily compared between different laboratories.

The FRAP assay has been applied widely in nutritional science. Apart from measuring the "total antioxidant content" of various foods, the FRAP assay has been used also to explore absorption of antioxidants from foods, such as soya milk, cocoa, and tea, and to investigate the effect of processing and cooking on the antioxidant content of foods. It is well recognized that transport to market, storage, and cooking practices affect the content of labile antioxidants in foods, and the World Health Organization (WHO) has taken this information into account in their recommendations for vitamin and mineral requirements in human nutrition. WHO recommendations for cooking foods containing labile antioxidants are to steam or stir fry. If water is used in the cooking of vegetables, it may be advisable to also consume the cooking water, as it contains antioxidants released from the food. The FRAP assay has also been used as part of a quality control system in the agri-food industry, and to assess the effect of genetic variation, season, growing conditions, and storage on the "total antioxidant content" of foods [78, 82, 83].

Dragović-Uzelac et al. [84] determined total antioxidant content of blueberries of the same cultivar grown in the same field can vary by up to 25% depending on the harvesting year, and variation of up to 47% in total antioxidant content is seen in different cultivars grown in the same area and harvested in the same year.

3.5.3 DPPH Free Radical Scavenging Assay

This assay uses the 2,2-diphenyl-1-picrylhydrazyl (DPPH) radical to assess the antioxidant capacity of pure compounds, natural extracts, or food. In this test, instead of evaluating the reactivity of antioxidants against radicals with low half-life times, X •, such as O_2 •-, HO •, LOO •, LO •, or NO •, the decrease in the intensity of the signal or area under the curve, it is evaluated against the stable radical DPPH, as shown in Fig. 3.6. This radical has a longer half-life, since it contains tri-nitrohydrazyl in its structure where the derailed electron is located between the group Hydrazyl NN limited by the two adjacent phenyl rings. Scavenging of this radical can be followed at a wavelength of 517 nm [85, 86].

The results obtained from this test can be expressed in terms of 50% inhibition of radicals (EC_{50}), through a calibration curve of a reference antioxidant such as trolox or by means of the scavenging percentage of the radical.

The DPPH assay was used to determine the antioxidant capacity of thiols, ascorbic acid, tocopherol, polyphenols, isoflavones, and aromatic amines. This methodology has been used to determine the antioxidant capacity of complex plant matrices, such as plant extracts and tomato seed oil, alcoholic beverages, among others. Furthermore, this methodology has been combined with HPLC for the detection of antioxidant secondary antioxidant metabolites. In addition, automated methods involving flow injection analysis with multiple syringes have been used to determine the antioxidant capacity of various food products with good reproducibility and detection limit [87–89].

The antioxidant capacity can be reported, as previously mentioned, as IC_{50} (that is, the concentration of AOH necessary to reduce 50% of the DPPH), a concentration equivalent to that of some reference antioxidant, percentage of

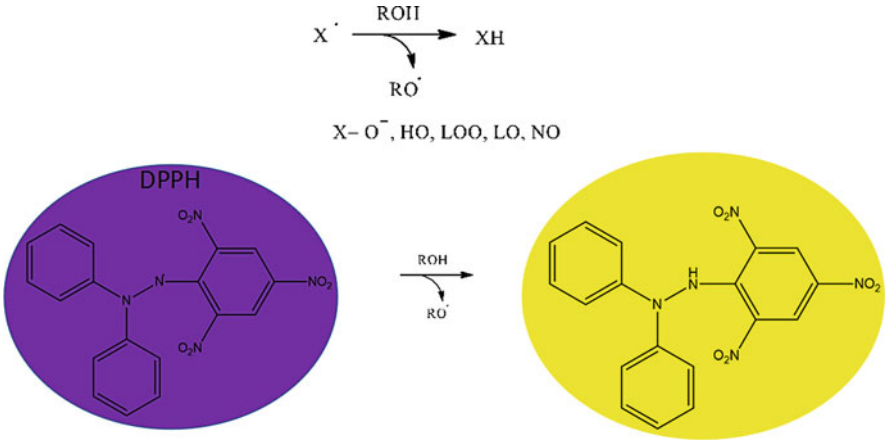

Fig. 3.6 Reaction of DPPH with antioxidant showing competition reaction with other reactive species

scavenging, among others. Due to the poor solubility of DPPH in water, studies are conducted on methanol. In this test, the presence of transition metals, solvent, incubation time, concentration, and molecular size of the antioxidant could affect the determination of antioxidant capacity. Likewise, the dependence of IC_{50} on various experimental conditions, the IC_{50} value for a particular antioxidant could vary from study to study and is therefore very qualitative and is only presented in terms of antioxidant capacity in relation to standards such as Trolox or ascorbic acid. Several recommendations have been suggested for an interpretation of the antioxidant capacity studied by the DPPH assay, such as: (1) measurement of the initial reaction rate (0–2 min), preferably using stopped flow mixture instead of the final absorbance after a long incubation that ignores effects of antioxidant concentration, reaction saturation, and effect of antioxidant molecular size; and (2) the use of an antioxidant concentration range instead of a single one to identify a valid linear response range, saturation levels, and differentiate reactivity patterns [90]. Interpreting the antioxidant capacity of complex mixtures as in Extracts should only reflect the general antioxidant capacity of the mixture by itself without reference to a particular component [85].

Different foods have different bioactive compounds with varied antioxidant capacities that can have different types of matrix interactions. When foods are consumed together, the total antioxidant capacity of food mixtures can be modified through synergistic, additive, or antagonistic interactions between these components, which in turn can alter their physiological impacts, considering that they may have different diffusion capacity in biological media. Wang et al. [91] investigated interactions and identified synergistic combinations. Eleven foods from three categories, including fruits (raspberry, blackberry, and apple), vegetables (broccoli, tomato, mushrooms, and purple cauliflower), and legumes (soybeans, adzuki beans, red beans, and black beans) were combined in pairs. The DPPH assay was used to determine the antioxidant capacity of individual foods and their combinations. The results indicated that within the same food category, 13, 68, and 21% of the combinations produced synergistic, additive, and antagonistic interactions, respectively.

On the other hand, while the combinations produced 21, 54, and 25% of synergistic, additive, and antagonistic effects, respectively, in all the food categories. The combination of specific foods in all categories (for example, fruits and vegetables) was more likely to generate synergistic antioxidant capacity than combinations with one food group. Also, the combination of raspberry and adzuki bean extracts demonstrated synergistic interactions. The results of this study suggest the importance of strategically selecting foods or diets to obtain maximum synergies, as well as for minimal antagonisms in antioxidant activity.

As described, the antioxidant methodologies are varied and useful for different food matrices. In addition, these are complementary to each other and can provide information about the nutritional quality that a food may have or the application of by-products that prevent the oxidation of a particular material or food. However, it should be borne in mind that all these methodologies have limitations. The main ones are due to the solubility of the probe, for example, DPPH which is insoluble

in an acid medium and partially soluble in hydroalcoholic mixtures. Also, many of these do not consider the bioavailability of antioxidant compounds, which is why all antioxidant methodologies are complementary but not necessarily correlated due to the antioxidant mechanism involved.

References

1. Amarowicz R, Pegg RB (2019) Natural antioxidants of plant origin. In: Advances in food and nutrition research. Academic, Cambridge
2. Pérez-Cruz K, Moncada-Basualto M, Morales-Valenzuela J, Barriga-González G, Navarrete-Encina P, Núñez-Vergara L, Squella JA, Olea-Azar C (2018) Synthesis and antioxidant study of new polyphenolic hybrid-coumarins. Arab J Chem 11:525–537
3. Harnly J (2017) Antioxidant methods. J Food Compos Anal 64:145–146
4. Granato D, Shahidi F, Wrolstad R, Kilmartin P, Melton LD, Hidalgo FJ, Miyashita K, Camp JV, Alasalvar C, Ismail AB, Elmore S, Birch GG, Charalampopoulos D, Astley SB, Pegg R, Zhou P, Finglas P (2018) Antioxidant activity, total phenolics and flavonoids contents: should we ban in vitro screening methods? Food Chem 264:471–475
5. Cömert ED, Gökmen V (2018) Evolution of food antioxidants as a core topic of food science for a century. Food Res Int 105:76–93
6. Al-Duais M, Müller L, Böhm V, Jetschke G (2009) Antioxidant capacity and total phenolics of Cyphostemma digitatum before and after processing: use of different assays. Eur Food Res Technol 228:813–821
7. Kraybill HR, Dugan LR, Beadle BW, Vibrans FC, Swartz V, Rezabek H (1949) Butylated hydroxyanisole as an antioxidant for animal fats. J Am Oil Chem Soc 26:449–453
8. Antonio Moreno, J.; López-Miranda, J.; Gómez, P.; Benkhalti, F.; El Boustani ES, Pérez-Jiménez, F. Efecto de los compuestos fenólicos del aceite de oliva virgen sobre la resistencia de las lipoproteínas de baja densidad a la oxidación. Med Clin 2003, 120, 128-131.
9. Kraybill HR, Dugan LR (1954) Antitoxidants, new developments for food use. J Agric Food Chem 2:81–84
10. Nicoli MC, Anese M, Parpinel MT, Franceschi S, Lerici CR (1997) Loss and/or formation of antioxidants during food processing and storage. Cancer Lett 114:71–74
11. Herbert V (1997) The value of antioxidant supplements vs their natural counterparts. J Am Diet Assoc 97:375
12. Halliwell B, Gutteridge JMC (2015) Ageing, nutrition, disease, and therapy: a role for antioxidants? In: Free radicals in biology and medicine, 5th edn. Oxford University Press, Oxford
13. Galleano M, Puntarulo S (1997) Dietary α-tocopherol supplementation on antioxidant defenses after in vivo iron overload in rats. Toxicology 124:73–81
14. Saini RK, Keum Y-S (2016) Tocopherols and tocotrienols in plants and their products: a review on methods of extraction, chromatographic separation, and detection. Food Res Int 82:59–70
15. Karmowski J, Hintze V, Kschonsek J, Killenberg M, Böhm V (2015) Antioxidant activities of tocopherols/tocotrienols and lipophilic antioxidant capacity of wheat, vegetable oils, milk and milk cream by using photochemiluminescence. Food Chem 175:593–600
16. Fiedor J, Burda K (2014) Potential role of carotenoids as antioxidants in human health and disease. Nutrients 6:466–488
17. Muller L, Caris-Veyrat C, Lowe G, Bohm V (2016) Lycopene and its antioxidant role in the prevention of cardiovascular diseases-a critical review. Crit Rev Food Sci Nutr 56:1868–1879
18. Davey MW, Montagu MV, Inzé D, Sanmartin M, Kanellis A, Smirnoff N, Benzie IJJ, Strain JJ, Favell D, Fletcher J (2000) Plant L-ascorbic acid: chemistry, function, metabolism, bioavailability and effects of processing. J Sci Food Agric 80:825–860

19. Carocho M, Ferreira ICFR (2013) A review on antioxidants, prooxidants and related controversy: Natural and synthetic compounds, screening and analysis methodologies and future perspectives. Food Chem Toxicol 51:15–25
20. Vuolo MM, Lima VS, Maróstica Junior MR (2019) Chapter 2 - phenolic compounds: structure, classification, and antioxidant power. In: Campos MRS (ed) Bioactive compounds. Woodhead Publishing, Cambridge, pp 33–50
21. Tsao R (2010) Chemistry and biochemistry of dietary polyphenols. Nutrients 2:1231–1246
22. Flora SJS (2009) Structural, chemical and biological aspects of antioxidants for strategies against metal and metalloid exposure. Oxidative Med Cell Longev 2:191–206
23. Chen G-L, Fan M-X, Wu J-L, Li N, Guo M-Q (2019) Antioxidant and anti-inflammatory properties of flavonoids from lotus plumule. Food Chem 277:706–712
24. Hernández-Rodríguez P, Baquero LP, Larrota HR (2019) Chapter 14 - flavonoids: potential therapeutic agents by their antioxidant capacity. In: Campos MRS (ed) Bioactive compounds. Woodhead Publishing, Cambridge, pp 265–288
25. Frombaum M, Le Clanche S, Bonnefont-Rousselot D, Borderie D (2012) Antioxidant effects of resveratrol and other stilbene derivatives on oxidative stress and *NO bioavailability: potential benefits to cardiovascular diseases. Biochimie 94:269–276
26. Rajapakse N, Mendis E, Jung W-K, Je J-Y, Kim S-K (2005) Purification of a radical scavenging peptide from fermented mussel sauce and its antioxidant properties. Food Res Int 38:175–182
27. Elias RJ, McClements DJ, Decker EA (2005) Antioxidant activity of cysteine, tryptophan, and methionine residues in continuous phase beta-lactoglobulin in oil-in-water emulsions. J Agric Food Chem 53:10248–10253
28. Baltes W (1982) Chemical changes in food by the maillard reaction. Food Chem 9:59–73
29. Hedegaard RV, Skibsted LH (2013) 16 - shelf-life of food powders. In: Bhandari B, Bansal N, Zhang M, Schuck P (eds) Handbook of food powders. Woodhead Publishing, Cambridge, pp 409–434
30. Manley D (2011) 11 - sugars and syrups as biscuit ingredients. In: Manley D (ed) Manley's technology of biscuits, crackers and cookies, 4th edn. Woodhead Publishing, Cambridge, pp 143–159
31. Pastoriza S, Quesada J, Rufián-Henares JA (2018) Lactose and oligosaccharides: maillard reaction. In: Reference module in food science. Elsevier, Amsterdam
32. Koubaa M, Roohinejad S, Mungure TE, Alaa El-Din B, Greiner R, Mallikarjunan K (2019) Effect of emerging processing technologies on maillard reactions. In: Melton L, Shahidi F, Varelis P (eds) Encyclopedia of food chemistry. Academic, Oxford, pp 76–82
33. Patrignani M, Rinaldi GJ, Rufián-Henares JÁ, Lupano CE (2019) Antioxidant capacity of Maillard reaction products in the digestive tract: An in vitro and in vivo study. Food Chem 276:443–450
34. Han RM, Li DD, Chen CH, Liang R, Tian YX, Zhang JP, Skibsted LH (2011) Phenol acidity and ease of oxidation in isoflavonoid/beta-carotene antioxidant synergism. J Agric Food Chem 59:10367–10372
35. Duh P-D, Yen G-C (1997) Antioxidant efficacy of methanolic extracts of peanut hulls in soybean and peanut oils. J Am Oil Chem Soc 74:745
36. Banias C, Oreopoulou V, Thomopoulos CD (1992) The effect of primary antioxidants and synergists on the activity of plant extracts in lard. J Am Oil Chem Soc 69:520–524
37. Wang S, Zhu F (2017) Dietary antioxidant synergy in chemical and biological systems. Crit Rev Food Sci Nutr 57:2343–2357
38. Alañón ME, Castro-Vázquez L, Díaz-Maroto MC, Gordon MH, Pérez-Coello MS (2011) A study of the antioxidant capacity of oak wood used in wine ageing and the correlation with polyphenol composition. Food Chem 128:997–1002
39. Pérez-Cruz F, Villamena FA, Zapata-Torres G, Das A, Headley CA, Quezada E, Lopez-Alarcon C, Olea-Azar C (2013) Selected hydroxycoumarins as antioxidants in cells: physicochemical and reactive oxygen species scavenging studies. J Phys Org Chem 26:773–783
40. Alam MN, Bristi NJ, Rafiquzzaman M (2013) Review on in vivo and in vitro methods evaluation of antioxidant activity. Saudi Pharm J 21:143–152

41. Speisky H, Lopez-Alarcon C, Gomez M, Fuentes J, Sandoval-Acuna C (2012) First web-based database on total phenolics and oxygen radical absorbance capacity (ORAC) of fruits produced and consumed within the south Andes region of South America. J Agric Food Chem 60:8851–8859
42. López-Alarcón C, Aspée A, Lissi E (2012) Influence of the target molecule on the ORAC Index. In: Emerging trends in dietary components for preventing and combating disease, vol 1093. American Chemical Society, Washington, DC, pp 417–429
43. Dorta E, Fuentes-Lemus E, Aspee A, Atala E, Speisky H, Bridi R, Lissi E, Lopez-Alarcon C (2015) The ORAC (oxygen radical absorbance capacity) index does not reflect the capacity of antioxidants to trap peroxyl radicals. RSC Adv 5:39899–39902
44. Dorta E, Aspée A, Pino E, González L, Lissi E, López-Alarcón C (2017) Controversial alkoxyl and peroxyl radical scavenging activity of the tryptophan metabolite 3-hydroxy-anthranilic acid. Biomed Pharmacother 90:332–338
45. Matos MJ, Pérez-Cruz F, Vazquez-Rodriguez S, Uriarte E, Santana L, Borges F, Olea-Azar C (2013) Remarkable antioxidant properties of a series of hydroxy-3-arylcoumarins. Bioorg Med Chem 21:3900–3906
46. Takashima M, Horie M, Shichiri M, Hagihara Y, Yoshida Y, Niki E (2012) Assessment of antioxidant capacity for scavenging free radicals in vitro: a rational basis and practical application. Free Radic Biol Med 52:1242–1252
47. Zheng W, Wang SY (2001) Antioxidant activity and phenolic compounds in selected herbs. J Agric Food Chem 49:5165–5170
48. Prior RL (2015) Oxygen radical absorbance capacity (ORAC): new horizons in relating dietary antioxidants/bioactives and health benefits. J Funct Foods 18:797–810
49. Huang D, Ou B, Prior RL (2005) The chemistry behind antioxidant capacity assays. J Agric Food Chem 53:1841–1856
50. Leal D, Mansilla A, Matsuhiro B, Moncada-Basualto M, Lapier M, Maya JD, Olea-Azar C, De Borggraeve WM (2018) Chemical structure and biological properties of sulfated fucan from the sequential extraction of subAntarctic Lessonia sp (Phaeophyceae). Carbohydr Polym 199:304–313
51. Moncada-Basualto M, Lapier M, Maya JD, Matsuhiro B, Olea-Azar C, Delogu G, Uriarte E, Santana L, Matos MJ (2018) Evaluation of trypanocidal and antioxidant activities of a selected series of 3-amidocoumarins. Med Chem 14:1–12
52. Matos JM, Mura F, Vazquez-Rodriguez S, Borges F, Santana L, Uriarte E, Olea-Azar C (2015) Study of coumarin-resveratrol hybrids as potent antioxidant compounds. Molecules 20:3290–3308
53. Villamena FA (2017) Chapter 5 - EPR spin trapping. In: Reactive species detection in biology. Elsevier, Boston, pp 163–202
54. Mullen W, Nemzer B, Ou B, Stalmach A, Hunter J, Clifford MN, Combet E (2011) The antioxidant and chlorogenic acid profiles of whole coffee fruits are influenced by the extraction procedures. J Agric Food Chem 59:3754–3762
55. Utrera M (2014) Fat content has a significant impact on protein oxidation occurred during frozen storage of beef patties. Lebensml-Wiss Technol 56:62–68
56. Soladoye OP, Juárez ML, Aalhus JL, Shand P, Estévez M (2015) Protein oxidation in processed meat: mechanisms and potential implications on human health. Compr Rev Food Sci Food Saf 14:106–122
57. Zhou F, Zhao M, Zhao H, Sun W, Cui C (2014) Effects of oxidative modification on gel properties of isolated porcine myofibrillar protein by peroxyl radicals. Meat Sci 96:1432–1439
58. Jongberg S, Lund MN, Skibsted LH, Davies MJ (2014) Competitive reduction of perferrylmyoglobin radicals by protein thiols and plant phenols. J Agric Food Chem 62:11279–11288
59. Rodriguez-Carpena JG, Morcuende D, Estevez M (2011) Avocado by-products as inhibitors of color deterioration and lipid and protein oxidation in raw porcine patties subjected to chilled storage. Meat Sci 89:166–173
60. Dorta E, Rodríguez-Rodríguez EM, Jiménez-Quezada A, Fuentes-Lemus E, Speisky H, Lissi E, López-Alarcón C (2017) Use of the oxygen radical absorbance capacity (ORAC) assay

to predict the capacity of mango (Mangifera indica L.) by-products to inhibit meat protein oxidation. Food Anal Methods 10:330–338
61. Wolfe K, Liu R (2007) Cellular antioxidant activity (CAA) assay for assessing antioxidants, foods, and dietary supplements. J Agric Food Chem 55:8896–8907
62. Liu RH, Finley J (2005) Potential cell culture models for antioxidant research. J Agric Food Chem 53:4311–4314
63. Wolfe KL, Liu RH (2008) Structure−activity relationships of flavonoids in the cellular antioxidant activity assay. J Agric Food Chem 56:8404–8411
64. Mura F, Silva T, Castro C, Borges F, Zuniga MC, Morales J, Olea-Azar C (2014) New insights into the antioxidant activity of hydroxycinnamic and hydroxybenzoic systems: spectroscopic, electrochemistry, and cellular studies. Free Radic Res 48:1473–1484
65. Abboud KY, da Luz BB, Dallazen JL, Werner MFDP, Cazarin CBB, Maróstica Junior MR, Iacomini M, Cordeiro LMC (2019) Gastroprotective effect of soluble dietary fibres from yellow passion fruit (Passiflora edulis f. flavicarpa) peel against ethanol-induced ulcer in rats. J Funct Foods 54:552–558
66. Schneider VS, Bark JM, Winnischofer SMB, Dos Santos EF, Iacomini M, Cordeiro LMC (2020) Dietary fibres from guavira pomace, a co-product from fruit pulp industry: characterization and cellular antioxidant activity. Food Res Int 132:109065
67. Dhingra D, Michael M, Rajput H, Patil RT (2012) Dietary fibre in foods: a review. J Food Sci Technol 49:255–266
68. Robledo-O'Ryan N, Matos MJ, Vazquez-Rodriguez S, Santana L, Uriarte E, Moncada-Basualto M, Mura F, Lapier M, Maya JD, Olea-Azar C (2017) Synthesis, antioxidant and antichagasic properties of a selected series of hydroxy-3-arylcoumarins. Bioorg Med Chem 25:621–632
69. Espinoza M, Olea-Azar C, Speisky H, Rodriguez J (2009) Determination of reactions between free radicals and selected Chilean wines and transition metals by ESR and UV-vis technique. Spectrochim Acta A Mol Biomol Spectrosc 71:1638–1643
70. Waterhouse AL, Laurie VF (2006) Oxidation of wine phenolics: a critical evaluation and hypotheses. Am J Enol Vitic 57:306
71. Zúñiga MC, Pérez-Roa RE, Olea-Azar C, Laurie VF, Agosin E (2014) Contribution of metals, sulfur-dioxide and phenolic compounds to the antioxidant capacity of Carménère wines. J Food Compos Anal 35:37–43
72. Magalhães LM, Segundo MA, Reis S, Lima JLFC, Rangel AOSS (2006) Automatic method for the determination of Folin−Ciocalteu reducing capacity in food products. J Agric Food Chem 54:5241–5246
73. Robards K, Antolovich M (1997) Analytical chemistry of fruit bioflavonoids a review. Analyst 122:11R–34R
74. Singleton VL, Rossi JA (1965) Colorimetry of total phenolics with phosphomolybdic-phosphotungstic acid reagents. Am J Enol Vitic 16:144
75. Prior RL, Wu X, Schaich K (2005) Standardized methods for the determination of antioxidant capacity and phenolics in foods and dietary supplements. J Agric Food Chem 53:4290–4302
76. Benzie IF, Strain JJ (1996) The ferric reducing ability of plasma (FRAP) as a measure of "antioxidant power": the FRAP assay. Anal Biochem 239:70–76
77. Berker KI, Güçlü K, Tor İ, Apak R (2007) Comparative evaluation of Fe(III) reducing power-based antioxidant capacity assays in the presence of phenanthroline, batho-phenanthroline, tripyridyltriazine (FRAP), and ferricyanide reagents. Talanta 72:1157–1165
78. Benzie IFF, Choi S-W (2014) Chapter one - antioxidants in food: content, measurement, significance, action, cautions, caveats, and research needs. In: Henry J (ed) Advances in food and nutrition research, vol 71. Academic, Cambridge, pp 1–53
79. Bolanos de la Torre AAS, Henderson T, Nigam PS, Owusu-Apenten RK (2015) A universally calibrated microplate ferric reducing antioxidant power (FRAP) assay for foods and applications to Manuka honey. Food Chem 174:119–123
80. Phonsatta N, Deetae P, Luangpituksa P, Grajeda-Iglesias C, Figueroa-Espinoza MC, Le Comte J, Villeneuve P, Decker EA, Visessanguan W, Panya A (2017) Comparison of antioxidant

evaluation assays for investigating antioxidative activity of gallic acid and its alkyl esters in different food matrices. J Agric Food Chem 65:7509–7518
81. Jimenez-Alvarez D, Giuffrida F, Vanrobaeys F, Golay PA, Cotting C, Lardeau A, Keely BJ (2008) High-throughput methods to assess lipophilic and hydrophilic antioxidant capacity of food extracts in vitro. J Agric Food Chem 56:3470–3477
82. Chen T-S, Liou S-Y, Wu H-C, Tsai F-J, Tsai C-H, Huang C-Y, Chang Y-L (2010) New analytical method for investigating the antioxidant power of food extracts on the basis of their electron-donating ability: comparison to the ferric reducing/antioxidant power (FRAP) assay. J Agric Food Chem 58:8477–8480
83. Ou B, Huang D, Hampsch-Woodill M, Flanagan JA, Deemer EK (2002) Analysis of antioxidant activities of common vegetables employing oxygen radical absorbance capacity (ORAC) and ferric reducing antioxidant power (FRAP) assays: a comparative study. J Agric Food Chem 50:3122–3128
84. Agriculture C, Affairs F, Zagreb J, Brala A, Levaj B, Bursać Kovačević D (2010) Evaluation of phenolic content and antioxidant capacity of blueberry cultivars (Vaccinium corymbosum L.) grown in the Northwest Croatia. Food Technol Biotechnol 48:214–221
85. Villamena FA (2017) Chapter 6 - UV–Vis absorption and chemiluminescence techniques. In: Villamena FA (ed) Reactive species detection in biology. Elsevier, Boston, pp 203–251
86. Yeo J, Shahidi F (2019) Critical re-evaluation of DPPH assay: presence of pigments affects the results. J Agric Food Chem 67:7526–7529
87. Bandoniene D, Murkovic M (2002) The detection of radical scavenging compounds in crude extract of borage (Borago officinalis L.) by using an on-line HPLC-DPPH method. J Biochem Biophys Methods 53:45–49
88. Wang W, Jiao L, Tao Y, Shao Y, Wang Q, Yu R, Mei L, Dang J (2019) On-line HPLC-DPPH bioactivity-guided assay for isolated of antioxidative phenylpropanoids from Qinghai-Tibet Plateau medicinal plant Lancea tibetica. J Chromatogr B 10:1106–1107
89. Gacche RN, Jadhav SG (2012) Antioxidant activities and cytotoxicity of selected coumarin derivatives: preliminary results of a structure–activity relationship study using computational tools. J Exp Clin Med 4:165–169
90. Magalhães LM, Segundo MA, Reis S, Lima JLFC (2006) Automatic method for determination of total antioxidant capacity using 2,2-diphenyl-1-picrylhydrazyl assay. Anal Chim Acta 558:310–318
91. Wang S, Meckling KA, Marcone MF, Kakuda Y, Tsao R (2011) Synergistic, additive, and antagonistic effects of food mixtures on total antioxidant capacities. J Agric Food Chem 59:960–968

Thermoluminescence the Method for the Detection of Irradiated Foodstuffs

4

Grzegorz Piotr Guzik and Wacław Stachowicz

Abstract

The chapter is related to food irradiation, a method of microbial decontamination of foodstuffs with the use of ionizing radiation, i.e. ^{60}Co gamma rays or 10 MeV accelerated electrons. The method is adapted to dried spices, herbs, and seasonings. The control of irradiated food is achieved with the use of standardized detection methods. Thermoluminescence method is presently considered the leading detection method for irradiated food and is widely adapted in food control laboratories around the world.

The chapter compiles the principles and description of detection procedure of thermoluminescence method as well as the glow curves recorded with minerals isolated from irradiated and not irradiated foodstuffs, the basis for the evaluation of investigated food sample whether irradiated. Discussion on heating rate one of the important operational parameters of TL measurement is carried out. The selection of suitable solvent is discussed in terms of the effectiveness of mineral separation from foods.

The list of results of thermoluminescence analyses obtained with 15 vegetal foodstuffs taken as an example and identified irradiated and not irradiated is enclosed.

The selection method of solvents suitable for mineral isolation from foodstuffs is successfully adapted in food control laboratories in Poland. The results of thermoluminescence analysis of vegetal foodstuffs enclosed were obtained in food control laboratories in Poland as well.

G. P. Guzik (✉) · W. Stachowicz
Laboratory for Detection of Irradiated Food, Institute of Nuclear Chemistry and Technology, Warsaw, Poland
e-mail: g.guzik@ichtj.waw.pl

A. K. Shukla (ed.), *Spectroscopic Techniques & Artificial Intelligence for Food and Beverage Analysis*, https://doi.org/10.1007/978-981-15-6495-6_4

Keywords

Thermoluminescence · Spice · Seasoning · Detection · Irradiate · Solvent · Extract

4.1 Introduction

The treatment of food with ionizing radiation called irradiation or sometimes cold pasteurization is one of the effective methods of microbiological decontamination preventing potential consumer against infection with food-borne diseases.

From 1984 irradiation technique is approved and issued [1] by WHO/FAO Codex Commission and recommended for a common use similarly to thermal pasteurization or deep freezing. The Council of the European Union of European Parliament dated for 1999 [2, 3] formulates basic regulations concerning radiation treatment of food as specification of recommended irradiation sources, suitable dose levels, and maximal dose limit. The labeling of irradiated food is obligatory including foodstuffs containing the admixture of irradiated component only. The assortment of irradiated foodstuffs admitted for distribution in trade is in countries more or less limited while the control of irradiated foodstuffs became obligatory.

Detection of irradiated food is not an easy task. Any foodstuff undergone radiation treatment is not distinguished visually or by taste from not irradiated one while negligible chemical or structural changes expected to occur are not identified with analytical methods for the control of food quality. The development of dedicated analytical methods only delivered promising result. A number of physical, chemical, and biological methods have been proposed and tested. The Committee of Standardization (CEN) in Brussels [2, 4–6] approved 10 from 21 positively tested detection methods as sensitive and reliable enough to be recommended for the routine control of various assortments of irradiated foodstuffs in trade. The selected methods elaborated by the expert in the field have been stepwise issued in the form of European Standards suitable for the common use.

Thermoluminescence is one of the detection methods approved by CEN and published in 1996 as European Standard EN 1788 [4]. The method is presently considered the leading detection method for irradiated food and adapted in the most of food control laboratories around the world. The advantage of the method is high sensitivity, reliability, and suitability for the control of many assortments of food of vegetal origin and seafood. Currently, foodstuffs of vegetal origin undergone radiation treatment are reported to appear in world food market and require irradiation control in many countries. Thermoluminescence as only suitable method capable to meet this requirement becomes today universal detection method adaptable to identify radiation treatment of all assortments of vegetal foods fresh, died, powered, or pre-processed. The specificity of all kinds of vegetal food despite fresh or reprocessed not commonly realized is a constant contamination with minerals from soil like crystalline quartz or feldspar being adjacent to the surface of leaves, roots, etc., of plants. The crystalline lattice of mineral grains incorporated

with plants and subsequently with foods represents potential sides for trapping of radiation energy during radiation treatment. The trapped radiation energy is durably stored inside the crystal lattice of minerals for years and is freed by intentional heating only. The stored energy is released as light defined thermoluminescence.

Thermoluminescence method is currently used for the detection of radiation treatment of fresh and dried spices, herbs, fruits, vegetables, mushrooms, etc., as well as food concentrates and foodstuffs with low content of irradiated ingredient only.

Diet supplement, a recently popular product in the market, is classified as foodstuff by FAO/WHO Codex Alimentarius [1] and normative directives of EU Parliament [2, 3]. From the other side diet supplement is considered a medical product and as such undergoes obligatory microbial decontamination preferentially with the use of ionizing radiation if distributed powdered (tablets, capsules, etc.). Consequently, according to international regulations mentioned above diet supplement undergoes obligatory irradiation control. The essential component of commercial diet supplements produced today are vegetal extracts qualified foodstuff as well. These relatively new products of pharmaceutical industry developed on industrial scale was not applied earlier in the production of diet supplements which contained powdered spices, herbs, fruits, or vegetables controlled by thermoluminescence method whether irradiated [4]. Recently it has been found that less effective control effect of vegetal extracts with thermoluminescence method in the past has been improved by the modification of preparative step of thermoluminescence detection method based on European standard.

4.2 Principles of Thermoluminescence

Thermoluminescence is a form of luminescence released under heating from crystalline materials such as minerals the components of soil. The energy previously absorbed in crystalline lattice of minerals defined ionizing radiation is re-emitted as light. The phenomenon is distinct from black-body radiation. According to Aitken engaged in thermoluminescence dating [7] and Keizars studying natural thermoluminescence from sands containing quartz grains [8], thermoluminescence emission occurs in three subsequent stages.

1. *irradiation*: ionizing radiation naturally emitted from rocks or generated from irradiation sources as beam of high energy photons or accelerated electrons when passing across crystalline materials loses a part of energy which becomes dissipated in crystal lattice and trapped in lattice imperfections of crystals;
2. *storage*: trapped radiation energy becomes stabilized and durably stored due to the lack of sufficient interior energy to escape crystal lattice;
3. *eviction*: heat energy delivered to crystal lattice of minerals from outside stimulates the release of trapped radiation energy from storage sides in the form of light defined thermoluminescence.

Quantum-mechanically interpreted, the energy storage states are stationary and have no formal time dependence but are not stable energetically. Heating of irradiated material frees trapped states to interact with phonons, while lattice vibrations evoked initiate rapid decay to lower-energy states followed by the emission of thermoluminescence photons.

The amount of thermoluminescence is proportional to the original dose of radiation received. In dating of ancient remains TL intensity vs. irradiation dose relationship is employed to estimate the date of burials of investigated objects that have been exposed in the past to ionizing radiation generated from radioactive soil elements and/or were coming from cosmic rays in proportionality to present age. The proportionality is successfully explored in the thermoluminescence dosimeter [9–11], the device measuring radiation dose received by a chip of suitable material carried by a person or placed with an object exposed to radiation. The discussed proportionality cannot be employed, however, for the determination of dose delivered to food by radiation treatment. It is because mineral fraction isolated from foodstuffs is characterized being different and undefined proportion from sample to sample between the content of thermoluminescence active minerals like quartz and feldspar and those not thermoluminescence active amorphous soil components like loams, gneiss, etc., which are always present. It is obvious that proportion between the contents of both kinds of minerals isolated from the same portion (batch) of food in the form of small grains can differ and cannot be evaluated. It is reflected in some statistical dispersion of thermoluminescence measurements which does not influence the reliability of the result of radiation detection. The difference between the measurements is higher if the volume of isolated mineral fraction is lower. It is advised, therefore, to isolate always suitably high portion of mineral fraction from investigated food sample.

4.3 Detection of Irradiated Foods by Thermoluminescence Method

The European Standard EN 1788 titled “Thermoluminescence detection of irradiated food from which silicate minerals can be isolated” is certainly the basic normative document comprising the rules and nuances concerning the applicability of thermoluminescence method in the practice. High sensitivity and reliability proven as well as suitability of irradiation detection in numerous assortments of vegetal food and seafood grounded on positive results of inter-laboratory comparative studies on international level [4] classify thermoluminescence the leading method of irradiation detection for foods (Fig. 4.1).

The content of silicate minerals (Fig. 4.2) is found very low in all foods not higher than 0.1% by weight in the order of milligrams. The maximal volume of fresh or dried food portion which can be measured by thermoluminescence in the reader is limited for technical reason despite the quality of measuring device used. In consequence, the thermoluminescence intensity of original food sample is extremely low and hardly detected. The solution was found in the isolation of mineral fraction

Fig. 4.1 Examples of foodstuffs controlled with thermoluminescence method. Powdered spices (red paprika, *knoblauch* granulate, and *lutein marigold*) in left. Vegetables in whole (garlic and *Hedera helix*) in right

Fig. 4.2 Mineral fractions isolated from dried herbs in whole (left) and from spicy vegetal concentrate (right) on stainless steel TL measuring cups stabilized with silicon spray. Mean dimensions (diameter) of mineral grains ca. 140 nm (left) and ca. 80 nm (right) in diameter

from organic residue of food by applying the density separation method taking advantage of high molecular density of mineral fraction markedly lower from that of organic constituents of food. The advantage of density separation method is that the volume of fresh product from which mineral is separated can be relatively high, facilitating to obtain the volume of mineral suitable for TL measurement. The volume of minerals isolated from foodstuff suitable for TL measurement becomes sometimes low and not sufficient to proceed reliable sample classification especially if food concentrates containing the irradiated component in minority as illustrated in Fig. 4.2 in right.

The intensity of thermoluminescence is expressed as number of bleaches registered per second (counts per second) in photomultiplier, the basic part of TL

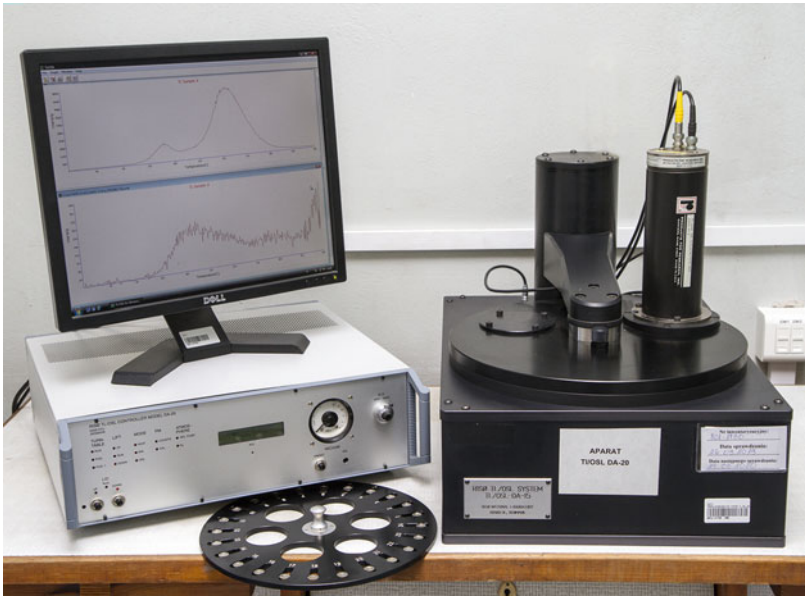

Fig. 4.3 TL reader adapted for the detection of irradiated foods (TL/OSL DA-20 model by RISØ Denmark)

reader as shown in Fig. 4.3. The result of TL measurement is obtained as a record presenting the TL intensity vs. heating temperature in the form of graph assigned Glow 1. The numerical values of TL intensity are also available.

Silicates and/or quartz grains contained in mineral fraction isolated from foodstuff evoke by linear heating thermoluminescence registered by TL reader in the temperature range 150–250 °C and are characterized by the TL peak with the maximum near to 200 °C, as shown in Figs. 4.4 and 4.5. Each of mineral samples preliminary TL measured stabilized with silicon spray on stainless steel measuring cup or plate undergoes subsequent irradiation with 1 kGy of gamma rays. The intention of this treatment is to ascertain the reliability of the result obtained in the first measurement (Glow 1). The glow curve obtained after normalization (Glow 2) resembles that recorded with irradiated sample (Fig. 4.5) despite investigated sample was or was not irradiated before giving rise of Glow 1 curve as shown in Fig. 4.4.

Thereafter, from Glow 1 and Glow 2 records the integrated numerical TL intensities are obtained and the ratios Glow 1/Glow 2 are estimated. TL glow ratios of irradiated foodstuffs are typically greater than 0.1, whereas those obtained from not irradiated samples are lower than 0.1. This is a basic criterion for the classification of investigated food sample whether irradiated or not irradiated, recommended for general use by European standard EN 1788. It has to be noted that in addition the TL intensity of Glow 2 should always exceed the *minimum detection level,* an important factor which has to be estimated before each TL measurement on investigated food

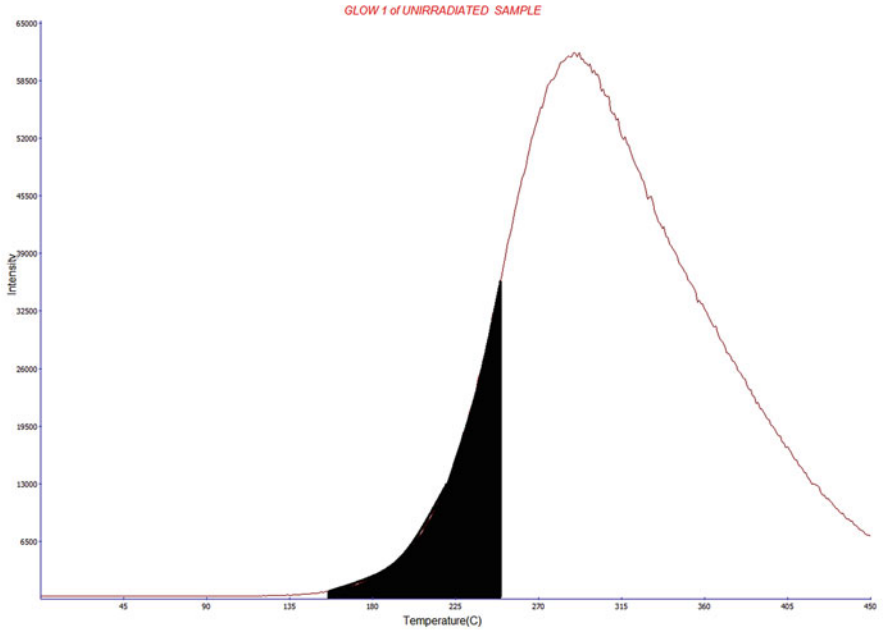

Fig. 4.4 The glow curve (Glow 1) of minerals isolated from not irradiated majoran. The area in black represents TL intensity (C/s) integrated within the heating temperature range from 150 °C to 250 °C. The maximum seen outside the range typical for irradiated samples represents the so-called geologic TL luminescence from radioactive micro components of soil containing uranium or thorium. No maximum specific for irradiated sample seen

sample and represents the numerical value of TL measurement on blind sample (preparative and measuring procedure without mineral sample). Nevertheless, by the identification of radiation treated multicomponent foodstuffs which contain only admixture of irradiated ingredient (presumably aromatic spices or herbs) the glow ratio becomes sometimes lower than 0.1. Under such circumstances the glow ratio criterion must be strengthen by the analysis of the shape of Glow 1 curve. The identification of a peak distinguished from glow curve and having the maximum near to 200 °C becomes the only reliable criterion for the qualification of such sample as radiation treated.

The list of basic measuring parameters (TL reader settings) recommended by European Standard EN 1788 as found satisfactory if adjusted for the TL analysis of foods is given in Table 4.1.

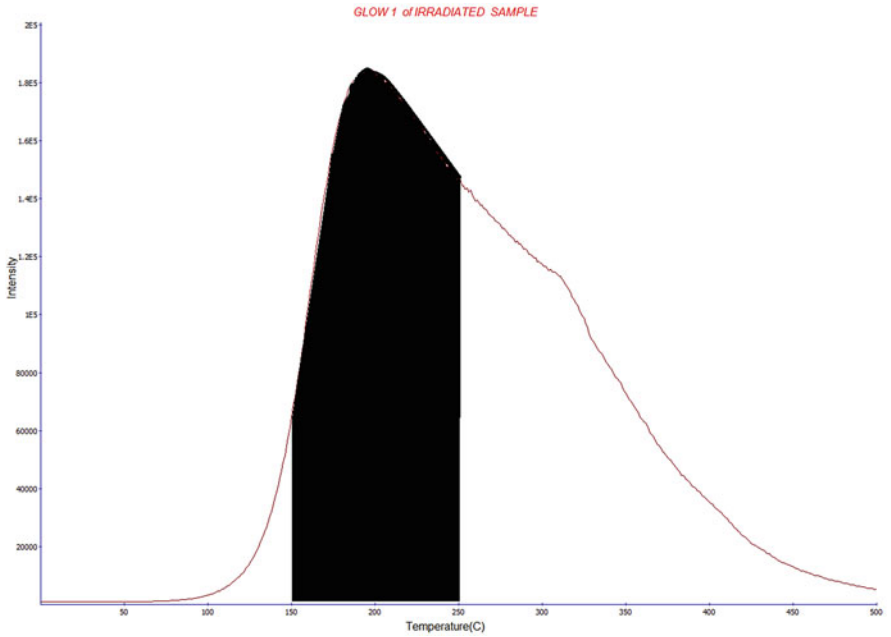

Fig. 4.5 The TL glow curve (Glow 1) of minerals isolated from irradiated majoran. The area in black represents TL intensity (C/s) integrated within the heating temperature range from 150 °C to 250 °C. The maximum near to 200 °C as seen within this temperature range is typical for irradiated samples

Table 4.1 Operational parameters of TL measurements on irradiated food

Parameter	Value
Initial temperature of heating	70 °C
Final temperature of heating	450 °C
Linear heating time	ca. 65 s
Heating rate	6 °C/s

4.4 Aspects of Heating Rate

Heating rate and linear heating time are operational factors which could theoretically influence the sensitivity of TL measurement. Presently adapted universal heating rate of 6 °C/s by experimental fitting (see Table 4.1) seems to meet the requirements.

The relevant literature data [12–15] deliver interesting consideration concerning the heating rate if TL measurement on inorganic materials like minerals isolated from foodstuffs is considered. The shape of round, oval, or shapeless (powdered) grains of minerals and their mean dimensions may influence the surface of the contact between the mineral and stainless steel area of TL heating cup or plate. These are the factors which no doubt influence in some degree the gradient effect

of heat transfer between mineral and heating plate and theoretically the heating rate too.

According to the authors [4, 7] the optimal conditions for the achievement of a favorable thermal contact between powdered sample and the surface of heating plate are:

- the mean dimensions of powder grains between 80 and 140 nm;
- the weight of powdered samples not exceeding 4 mg per one TL measuring cup;
- fixing of the powdered samples on stainless steel cups with silicon spray, preferably ACMOS 70–2406 by ACMOS CHEMIE KG company.

It has to be noted, however, that the above consideration concerns mainly the crystalline materials while mineral fraction isolated from foodstuffs contains silicate minerals (quartz, silicate minerals) indeed but it contains also some of TL inactive amorphous soil originated mineral components disturbing in some degree the heat convention inside mineral fraction.

It has to be noted that various heating rate methods (heat treatment on different samples in a function of temperature) have been proposed by several authors [12–15] for the calculation of activation energy of the processes involved. It is interesting that the results obtained with several TL phosphors showed that TL emission from phosphor samples (area under the glow curve recorded) indicated a shift of the temperature maximum towards higher temperatures [16–18].

It has been also reported that drastic decrease of TL response appears in some materials as a function of heating rate. This behavior has been attributed to thermal quenching effect [16–18].

The heating rate effect on TL glow peaks has been discussed by G. Kitis [19, 20] who considers the heat effect as a dynamic parameter rather than a simple experimental setup variable. His study has been carried out on a single, well separated TL glow peaks, considering the experimental characteristics. The first thing to be taken into consideration is a possible delay between the temperatures monitored by thermocouple fixed on the surface of heating stainless steel cup with the sample. According to M. S. Rasheedy [21, 22], the decrease of the TL intensity with increasing heating rate cannot be explained using the kinetics equations in their usual time-dependent forms.

4.5 Improvement of Mineral Isolation by Using Suitable Solvents

It has been confirmed in the analytical practice addressed to trade [private communication INCT] that the effectiveness and consequently the yields of mineral isolated from foodstuffs like vegetal extracts, depend on the quality and choice of solvent used. The appropriate choice of solvent facilitated the dissolution of investigated food sample. According to European Standard EN 1788 the following solvents are recommended preferentially to be used for mineral separation: (1) distilled or

column purified water, (2) 98% methanol of analytical purity, or (3) 6M water solution of hydrochloric acid. It has been proven experimentally, however, that not only the choice of solvent is important. A more satisfactory result has been obtained by the application of appropriate composition of solvents recommended in European standard EN 1788 [private communication INCT]. In addition the time of keeping the sample submerged in the experimentally selected composition of solvents influences markedly the separation efficiency.

In Table 4.1 the most effective solvents and solvent compositions are listed which have been selected through the laboratory fitting tests as effective in facilitating of mineral separation from herbs, seasonings, and plant ingredients of foodstuffs and pharmaceutics. The important factor influencing the effectiveness of mineral separation from organic remaining was also stated the time of the keeping the crushed herbs, seasonings, and plant ingredients of pharmaceutics submerged in solvent. For some of products one hour was sufficient while for the other ones positive effect of separation appeared after several hours only (see Table 4.2).

4.6 Examples of Irradiation Detection in Different Foodstuffs by Thermoluminescence Method

The results of irradiation control of foodstuffs in INCT laboratory are presented below. The numbers listed are the average of two TL analyses accomplished for each product. The selected set of results presents 10 samples identified irradiated and five samples classified not irradiated. Five of investigated samples were powdered spices, five extracts in the form of powders, and five fresh leaves and fruits of popular herbs. Ten of selected samples were found irradiated while the other five not irradiated.

The results of thermoluminescence measurements on mineral fractions isolated from the investigated samples are comprehended in Table 4.3. Mineral fractions listed were isolated from investigated products by means of experimentally assorted sorbent or composition of solvents while the TL measurements have been accomplished with the use of TL reader, model TL/OSL DA-20 from RISØ TL/OSL System Company, Denmark. All steps of TL analysis were performed in accord with EN 1788 European standard while mineral separation was enriched in the application of appropriate solvent selected experimentally.

The results comprehended in Table 4.3 are divided in three groups—commercially powdered spices, herbs, and seasonings, vegetal extracts, and fresh spices and herbs irradiated in whole.

Table 4.2 Solvents, combination of solvents and time of keeping herbs, seasonings, and plant ingredients of pharmaceutics in solvent effective by the separation of mineral fraction from that kind of products

	Solvent or composition of solvents used					
Group of sample	Demineralized water (%)	Methanol anal. purity (%)	6M HCl (%)	Demineralized water (%)	Methanol anal. purity (%)	6M HCl (%)
	1 h in the solvent			Overnight (10 h) in the solvent		
Seasonings	80	0	80	100	0	100
Plant extracts	100	100	100	–	–	–
Plant ingredients of pharmaceutics	0	0	60	0	0	100

Table 4.3 Results of thermoluminescence measurements on selected herbs, seasonings, and plant ingredients

Product characteristic	Initial mass of product (g)	Mass of minerals (mg)	TL-max glow 1 (°C)	TL-max glow 2 (°C)	Glow 1/Glow 2 ratio[a]	Q[b]
Paprika chipsflakes cut	63.5	0.64	168	195	0.792	+
Red peppergrains	65.3	0.89	203	186	0.4925	+
Paprica sweetpowdered	264.2	1.16	230	182	2.009	+
Paprica greencut fresh	68.4	0.56	176	185	0.130	+
Cultivated garlic *(Allium sativum) cut fresh*	63.4	0.69	198	174	0.212	+
Maidenhair tree (*Ginkgo biloba*) powder extract	115.9	0.93	209	201	0.249	+
Silibina technica per fosfolipidy powder extract	45.6	0.56	179	204	0.607	+
Lutein marigoldpowdered extract	68.5	0.99	176	197	0.114	+
Neighbor fleabane *(Erigeron vicinus)*powdered extract	98.0	0.78	202	189	0.609	+
Butcher's broom (*Ruscus aculeatus*) powder extract	46.5	0.95	215	187	4.593	+
Common ivy (*Hedera helix*) fresh leaves	46.9	1.12	285	201	<0.010	−
Horse-chestnut (*Aesculus hippocastanum*)fresh fruits	65.2	0.65	296	191	<0.010	−
Dog rose (*Rosa canina*)fresh fruits	32.8	0.89	302	189	<0.010	−
Common periwinkle (*Vinca minor)* fresh leaves	56.4	0.65	378	191	<0.010	−
Quince (*Cydonia oblonga)*fresh fruits	44.6	1.04	350	179	<0.010	−

[a]Glow 1 and Glow 2 expressed as the number of bleaches recorded in photomultiplier during 1 s (counts per second—c/s)
[b]Qualification of sample: + irradiated; − not irradiated

Fig. 4.6 Fresh paprika green taken in whole after drying and crushing to pieces (left) In right after subsequent cutting to smaller pieces (right) for better dilution in solvent

The weight of portions of selected products taken for further investigation were from 32.8 g (min) to 264.2 g (max), respectively. Fresh leaves and fresh fruits were dried and cut to smaller pieces suitable for mineral isolation from organic pulp with the use of selected solvent or solvent mixture ensuring effective density separation of both phases (Fig. 4.6).

The examples of thermoluminescence diagrams recorded with irradiated spices and plant ingredients of pharmaceutics studied are shown below (Figs. 4.7, 4.8, and 4.9).

4.7 Comments

Among 15 products controlled 10 were found irradiated. The remaining five samples were classified not irradiated. By accident only the selected powdered spices and vegetal extracts were identified irradiated while spices and herbs in whole—not irradiated. The classification of all samples controlled given in the table is repeatable (two consistent TL measurements done in parallel) and reliable as additionally controlled elsewhere.

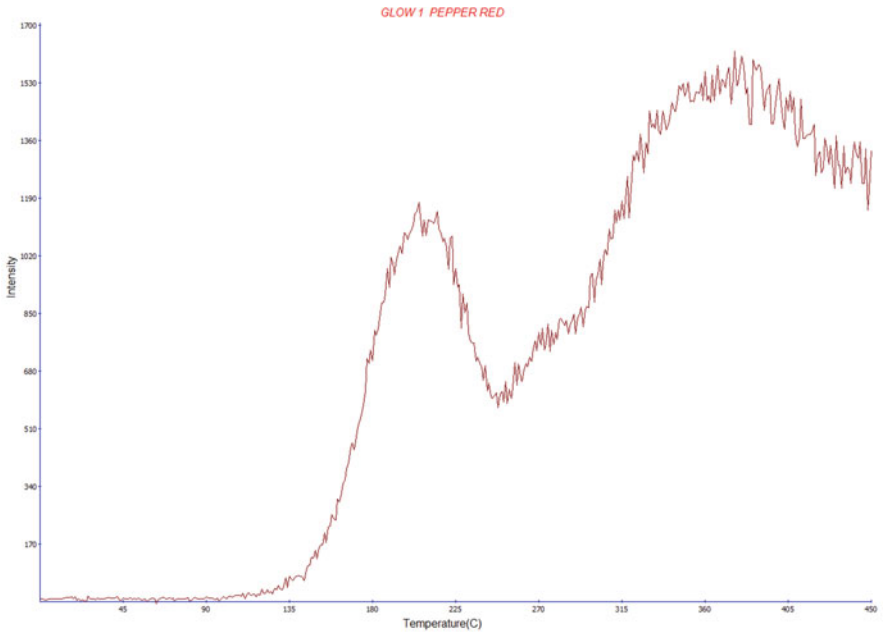

Fig. 4.7 Thermoluminescence record of Glow 1 obtained with mineral isolated from irradiated grains of red pepper. Glow peak with the maximum at 203 °C proves radiation treatment on sample. Broad higher peak with maximum at 370 °C is of geologic origin as derived from radioactive components of soil (U, Th)

4.8 Final Remarks

As known from reliable sources new, economic technologies of microbial decontamination of foodstuffs are recently adapted by food producers and distributors based on the application of combined thermal-irradiation or high pressure-irradiation treatment on foodstuffs. It is announced that such combined disinfecting process of food requires much lower than recommended doses of ionizing radiation. High sensitivity of thermoluminescence detection method, however, confirmed in experimental studies on the variety of foodstuffs irradiated with low doses of ionizing radiation approves the applicability of this method for positive control of foodstuffs undergone new technology too. Nevertheless, special attention has to be paid by irradiation control of foodstuff showing extremely low thermoluminescence intensity which can also appear by the control of foods after prolonged storage.

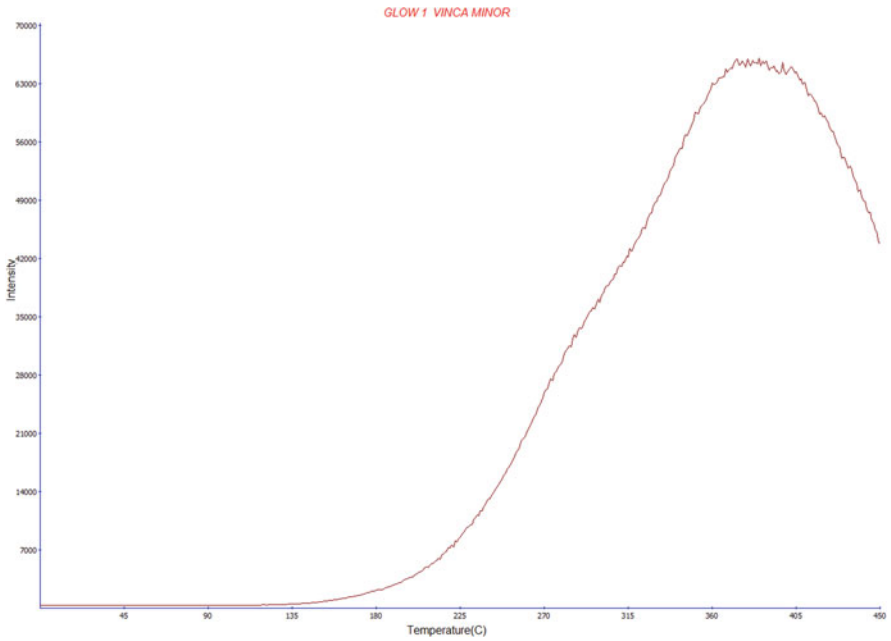

Fig. 4.8 Thermoluminescence record of Glow 1 obtained with minerals isolated from not irradiated fresh leaves of common periwinkle (*Vinca minor*). Broad peak with maximum at ca. 378 °C is of geological origin (see comment above (Fig. 4.7)

Separation of mineral from organic pulp for thermoluminescence analysis of herbs, seasonings, and plant ingredients of pharmaceutics, executed with the use of selected solvents makes possible to identify samples irradiated with the doses of 0.5 kGy and lower. The study undertaken in specialized Radiation Control Laboratories in Poland proved also the successful isolation of mineral fraction from multicomponent foodstuffs and diet supplements in quantities sufficient to proceed reliable TL analysis.

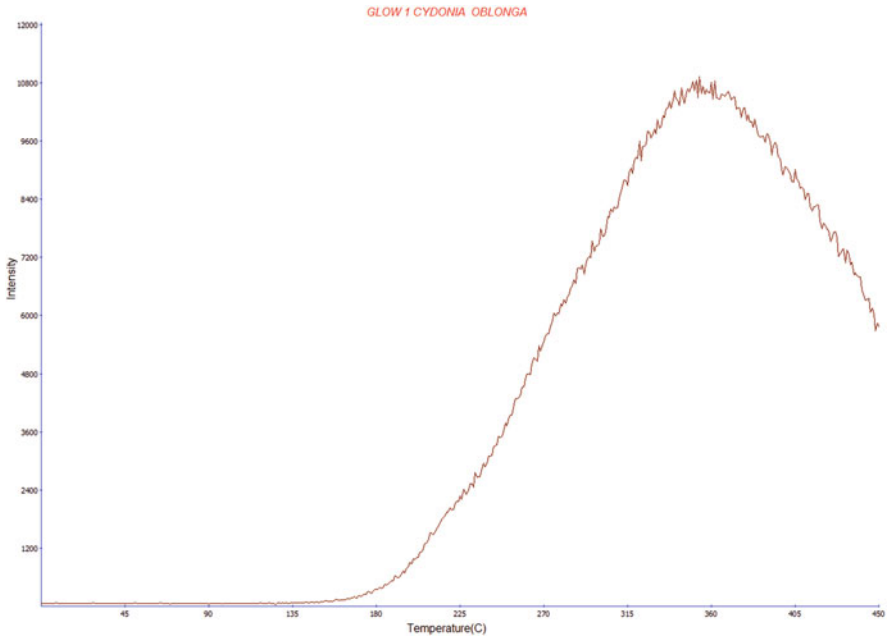

Fig. 4.9 Thermoluminescence record of Glow 1 obtained with minerals isolated from fresh fruit of Quince (*Cydonia oblonga)* not irradiated. Broad peak with the maximum at 350 °C is of geological origin, as above

References

1. Codex General Standard for Irradiated Foods and Recommended International Code of Practice for the Operation of Radiation Facilities Used for the Treatment of Foods, w: Codex Alimentarius vol. XV FAO/WHO Codex Alimentarius Commission, Rome 1984. Codex Stan 106-1984, Rev.1-2003
2. Council of the European Union, European Parliament (1999) Directive 1999/2/EC of the European Parliament and of the Council on the approximation of the laws of the Member States concerning foods and food ingredients treated with ionizing radiation. Publications Office of the European Union
3. Council of the European Union, European Parliament (1999) Directive 1999/3/EC of the European Parliament and of the Council on the establishment of a Community list of foods and food ingredients treated with ionizing radiation. Publications Office of the European Union
4. PN-EN 1788:2002: Foodstuffs - Thermoluminescence detection of irradiated food from which silicate minerals can be isolated. European Committee for Standardisation, Brussels 2002. EN 1788 was published in 1996
5. European Committee for Standardization (2004) Foodstuffs – detection of irradiated food containing fat–gas chromatographic analysis of hydrocarbons. PN-EN 1784
6. European Committee for Standardization (2003) Foodstuffs – Detection of irradiated food containing fat – Gas chromatographic/mass spectrometric analysis of 2-alky/cyclobutanones. PN-EN 1785
7. Aitken MJ (1998) Thermoluminescence dating. ISBN: 0-12-046381-4

8. Keizars KZ, Forrest BM, Rink JW (2008) Natural residual thermoluminescence as a method of analysis of sand transport along the coast of the St. Joseph Peninsula, Florida. J Coast Res 24:500. https://doi.org/10.2112/04-0406.1
9. Kelly P, Braunlich P, Abtani A, Jones SC, de Murcia M (1984) Radiat Prot Dosim 6:25
10. Gorbics SG, Nash AE, Attix FH (1968) Proc. 20d International Conf. on Lum. Dosimetry, Gatlinburg, TN, USA, p 587
11. Vana N, Ritzinger G (1984) Radiat Prot Dosim 6:29
12. Booth AH (1954) Can J Chem 32:214
13. Bochum A (1954) Czech J Phys 4:91
14. Hoogenstraaten W (1958) Philips Res Rev 13:515
15. Chen R, Winer SAA (1970) J Appl Phys 41:5227
16. Kathuria SP, Sunta CM (1982) J Phys Dosim 15:497
17. Kathuria SP, Moharil SV (1983) Phys Dosim 16:1331
18. Gartia RK, Singh SJ, Mazumdar PS (1988) Phys Stat Sol 106:291
19. Kitis G, Spiropulu M, Papadopoulos J, Charalambous S (1993) Nucl Instr Methods B 73:367
20. Kitis G, Papadoupoulos J, Charalambous S, Tuyn JWN (1994) Radiat Prot Dosim 55(3):183
21. Rasheedy MS (2004) Int J Mod Phys B 18:2877
22. Rasheedy MS, Zahram EM (2006) Phys Scr 73:98

Advantages of Multi-Target Modelling for Spectral Regression

5

Sylvio Barbon Junior, Everton José Santana, Amanda Teixeira Badaró, Nuria Aleixos Borrás, and Douglas Fernandes Barbin

Abstract

Spectral methods usually produce a large amount of data, and have been greatly applied to food and agricultural products. These products demand several analyses to determine different parameters, that will further indicate their quality. There have been several approaches reported to deal with multi-target regression in recent years, with different applications demanding a specific approach. Multi-target modelling could provide a useful tool for spectral methods, specially when applied to food products, as it could deal with prediction of different parameters from a single data source. This chapter provides an overview of multi-target regression methods, presenting the performance evaluation metrics and discussing its potential application for spectral data. In addition, recent applications to food products are presented, and the future trends discussed.

Keywords

Multi-output regression · Near infrared spectroscopy · Food quality · Food composition · Adaptation methods · Prediction performance

S. Barbon Junior · E. J. Santana
State University of Londrina, Londrina, Brazil

A. T. Badaró
State University of Campinas, Campinas, Brazil

Universitat Politècnica de València, Valencia, Spain

N. A. Borrás
Universitat Politècnica de València, Valencia, Spain

D. F. Barbin (✉)
State University of Campinas, Campinas, Brazil
e-mail: dfbarbin@unicamp.br

A. K. Shukla (ed.), *Spectroscopic Techniques & Artificial Intelligence for Food and Beverage Analysis*, https://doi.org/10.1007/978-981-15-6495-6_5

5.1 Preliminaries

Regression analysis is a valuable method in statistics. This analysis can be grouped in three basic areas:

- Univariate analysis, which refers to a single variable, and its analysis does not attempt to infer relationships, but to find the pattern in the data itself;
- Bivariate analysis, which refers to an independent variable (the feature of the object to be studied) and a dependent variable (the target or the expected outcome) and attempts to extract relationships between them;
- Multivariate analysis, which refers to three or more variables and attempts to extract relationships among them.

Bivariate analysis can be made by a simple regression model. In other words, in bivariate analysis the dependent variable can be described as function of a single independent variable.

In contrast, if more than one independent variable is involved in the problem, multiple regression models are required. For instance, in multiple linear regression the relationship established between a dependent (Y) and m independent ($X_1, X_2, \ldots, X_m$) variables can be defined as

$$Y = \beta_0 + \beta_1 X_1 + \beta_2 X_2 + \cdots + \beta_m X_m + \epsilon, \tag{5.1}$$

in which $\beta_0, \beta_1, \beta_2, \ldots, \beta_m$ correspond to the regression coefficients and ϵ is a random error term [36].

Another common multiple linear regression model is a polynomial function of j-th order, which, ignoring the possible interaction among factors, can be expressed as

$$Y = \beta_{0k} + \beta_{1k} X_k + \beta_{2k} X_k^2 + \cdots + \beta_{nk} X_k^j + \epsilon_j, \quad 1 \leq j \leq m, \tag{5.2}$$

There are many non-linear functions that can be used in regression: Logistic, exponential, trigonometric, and inverse functions are very usual examples, to name a few.

The regression analysis can be used in two approaches: first, in the use for prediction of a corresponding target, and, second, for causal relationship between the predictor and the target. Usually, regression analysis establishes a correlation between the target variable and the independent variables in the dataset. To develop a causal relationship between the dependent and independent variables, it is necessary to understand the theoretical connection between them [11, 18].

Moreover, regression analysis can be performed by different methods, including machine learning (ML) approaches. ML has allowed to predict the most distinct parameters from the most diverse fields. In traditional supervised ML, an algorithm is used to learn how the input information is related to one output (or target) based

on historical data. Generally, the result of this learning process leads to a model that can be used to predict the output of new samples.

However, in several situations there is more than one target of interest. For instance, if you receive in your laboratory a sample of meat, how many physico-chemical tests would you apply? Normally, it should be carried out physical tests (colour), chemical tests (protein and fat content), and physico-chemical (drip loss, pH). Moreover, many of these parameters are related to each other. Considering this, multi-target regression (MTR) has emerged with the main concern of developing special methods that could be more suitable to problems with multiple continuous targets.

5.2 Multi-Target Regression

5.2.1 Definition

Essentially, MTR deals with problems that are composed by more than one continuous response variable, i.e. multiple continuous targets. There are many examples of possible numerical continuous variables in food analysis, from pH to colour, texture, and protein content. Usually, these problems have the following characteristics [7]:

- An input set X with m features, in such a way that each example i is associated to an input vector $\mathbf{x}_i = (x_{i_1}, x_{i_2}, \ldots, x_{i_m})$;
- An output set Y with d continuous targets, in such a way that each example is associated to an output vector $\mathbf{y}_i = (y_{i_1}, y_{i_2}, \ldots, y_{i_d})$;
- A set of samples D with n pairs of $\mathbf{x}_i$ and $\mathbf{y}_i$, with $1 \leq i \leq n$, i.e. $D = \{(\mathbf{x}_1, \mathbf{y}_1), \ldots, (\mathbf{x}_n, \mathbf{y}_n)\}$.

Figure 5.1 exemplifies a generic MTR problem and states the adopted nomenclature in this work.

In this way, the MTR task is to find a model $\mathbf{h}$ that, for each input vector $\mathbf{x}_i$ produces a prediction of $\hat{\mathbf{y}}_i = \mathbf{h}(\mathbf{x}_i)$ that best approximates the true output vector $\mathbf{y}_i$ [45].

Fig. 5.1 Generic MTR problem

D

$\mathbf{X}$	X_1	X_2	$\cdots$	X_m
$\mathbf{x}_1$	x_{1_1}	x_{1_2}	$\cdots$	x_{1_m}
$\mathbf{x}_2$	x_{2_1}	x_{2_2}	$\cdots$	x_{2_m}
$\vdots$	$\vdots$	$\vdots$	$\ddots$	$\vdots$
$\mathbf{x}_n$	x_{n_1}	x_{n_2}	$\cdots$	x_{n_m}

$\mathbf{Y}$	Y_1	Y_2	$\cdots$	Y_d
$\mathbf{y}_1$	y_{1_1}	y_{1_2}	$\cdots$	y_{1_d}
$\mathbf{y}_2$	y_{2_1}	y_{2_2}	$\cdots$	y_{2_d}
$\vdots$	$\vdots$	$\vdots$	$\ddots$	$\vdots$
$\mathbf{y}_n$	y_{n_1}	y_{n_2}	$\cdots$	y_{n_d}

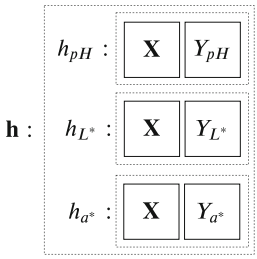

Fig. 5.2 Single-target method

There are several ways of finding **h**; the most intuitive is building independent models for each output. Take as an example a dataset with $\mathbf{X} = \{\mathbf{x}_1, \ldots, \mathbf{x}_n\}$ corresponding to the spectral information and **Y** with three output variables: pH and colour L^*, and a^*. In this way, h_{pH} could be created considering **X** and $Y_1 = Y_{pH}$, h_{L^*} could be created considering **X** and $Y_2 = Y_{L^*}$, and h_{a^*} could be created considering **X** and $Y_3 = Y_{a*}$. The final models h will be, then, composed by the models h_{pH}, h_{L^*}, and h_{a^*}, as illustrated in Fig. 5.2.

This method is known as single-target regression (ST) since it looks independently to each target to build a separate model at once. Traditional ML regression algorithms belonging to different families can be used to create these models: linear regression, random forests [8], support vector regression machines [16], gradient boosting machine [19], decision tree, k nearest neighbour, etc.

One may note that some of the output variables of a problem might be correlated. Looking back at our example, pH and colour have some correspondence. In this case, it is reasonable to assume that exploiting the dependencies among the targets when creating the models could lead to better predictions.

Considering this, several MTR methods were specially designed to capture the correlation among the targets and aiming at developing improved models. There are two general ways of doing that: by means of algorithm adaptation or problems transformation. Figure 5.3 shows one possible characterisation of the classes of methods existing in MTR. This classification is based on [7] and is extended to include the later works present in the current MTR literature.

In different works, different implementations of the MTR methods were used based mainly in Java and R programming languages. These implementations can be found in Mulan,[1] Clus,[2] Mulan-extended,[3] Multi-target Framework,[4] and glmnet R package.[5]

[1] http://mulan.sourceforge.net.

[2] http://dtai.cs.kuleuven.be/clus/.

[3] https://github.com/lefman/mulan-extended.

[4] http://www.uel.br/grupo-pesquisa/remid/?page_id=145.

[5] https://cran.r-project.org/web/packages/glmnet/index.html.

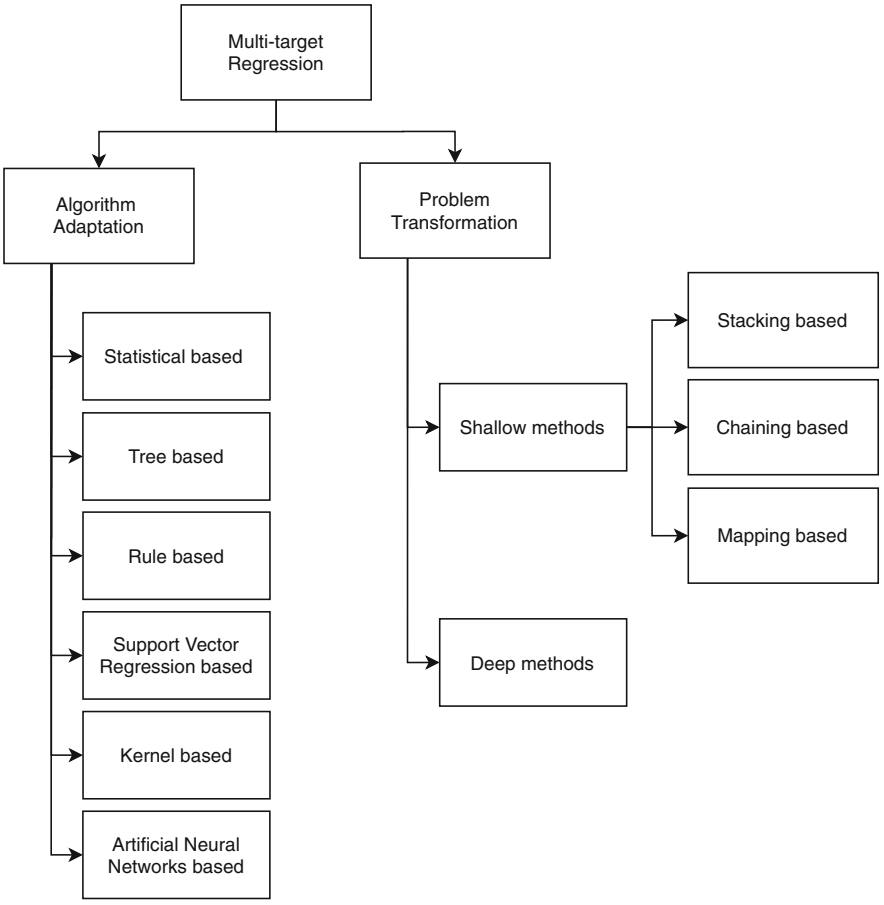

Fig. 5.3 MTR methods classification

5.2.2 Algorithm Adaptation Methods

Algorithm adaptation methods are based on algorithms and techniques which are used for problems with a single output. Most of these methods produce a single model h that predicts all the targets simultaneously and can capture the relationships among the targets. Since they generally generate a unique model, this approach is considered to be more concise than transforming the problem.

5.2.2.1 Statistical-Based Methods

Statistical methods can be seen as the first proposals to predict multiple targets simultaneously. Multivariate regression analysis for problems with more than one dependent variable is a particular case of MTR.

Other more complex methods also belong to this class. For instance, reduced-rank regression [21] imposes a rank of constraints to the matrix of estimated coefficients.

Multi-output contour regression [1], another statistical method, uses a combination of linear regressions and quantile mapping to reduce the error and obtain joint relationships among the targets.

5.2.2.2 Tree-Based Methods

Tree-based MTR methods are another class of algorithm adaptation. These methods tend to generate smaller trees than individual trees for each target. Struyf and Džeroski [46] suggested the construction of multi-objective regression trees (MORTs) by imposing constraints of size and accuracy.

For this, it initially builds a large tree and after that prunes it. Figure 5.4 exemplifies a very simplified MORT. One of the greatest differences between a traditional regression tree and a MORT is that the latter has a vector in its leaves, with each element of this vector corresponding to one target.

Both [26,27] applied bagging (sampling training examples with replacement) and random forests (bagging combined to random sampling of attributes during training) to build MORTs. The multi-objective random forest (MORF), corresponding to

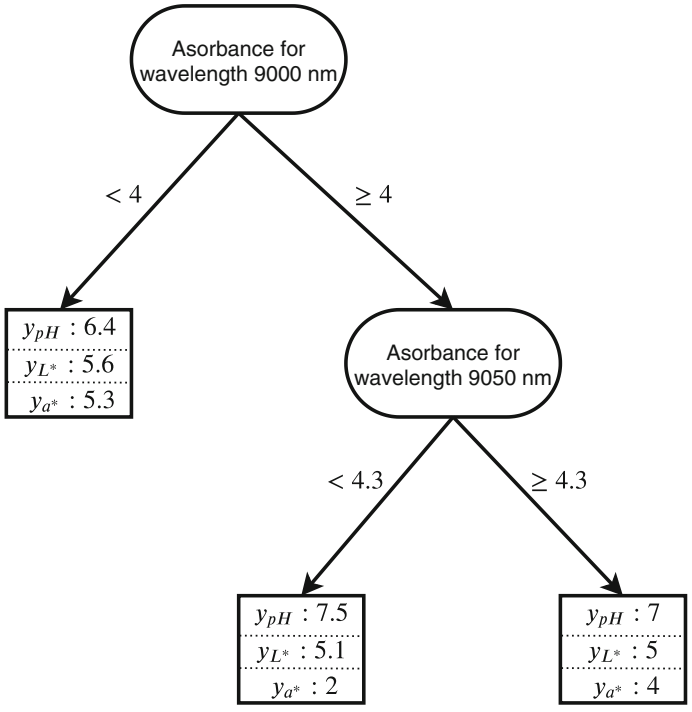

Fig. 5.4 Illustration of a MORT

random forest of MORTs, increased the predictive performance but decreased the interpretability of the problem.

5.2.2.3 Rule-Based Methods

Rule methods were also developed for multi-target learning. Fitted rule ensembles (FIRE) [2] adapts and transforms the result given by an ensemble of trees in the format of rules. After that, it optimises the number of rules.

FIRE was further developed in [3]. In this work, the rules were associated with linear functions, and the weight of each rule to the final estimated value is adjusted by a gradient-directed optimisation algorithm.

5.2.2.4 Support Vector Regression Machine Methods

Support vector regression (SVR) machine is also the basis of some methods due to characteristics of performance and low sensitivity to input size. One example is multi-output least squares support vector regression machines [51], which adapts the least squares support vector regression machine (LS-SVR) to deal with the multi-output case, capturing, in this way, the underlying cross relatedness among the targets.

Other methods, such as multi-output twin support vector regression (M-TSVR) and multi-output parameter-insensitive twin support vector regression (M-PITSVR) [30], attempt faster learning by using up-and-down-bound functions. These functions are solved by smaller-sized programming problems.

5.2.2.5 Kernel-Based Methods

Kernel methods were also released to improve the results of MTR. Multi-output learning via spectral filtering [4] applied regularised kernel methods to the learning of vector-valued functions. For this, it performed a filtering in the spectrum of the kernel matrix defined for each type of problem.

5.2.2.6 Artificial Neural Networks Methods

Artificial neural networks (ANNs) can also be adapted to be used for MTR. In fact, the definition of architecture with the number of output neurons equal to the number of targets can be seen as an algorithm adaptation method. Figure 5.5 shows an example of a traditional ANN applied to our study case.

Multi-layer multi-target regression (MMR) [52] has an architecture composed of input, hidden, and output layers. In these methods, matrix elastic nets are used to obtain inter-target correlations. It also takes advantage of a kernel trick to explore non-linear relationships.

Deep multi-target regression [40] uses a deep architecture to model the inter-target and inter output correlation. It shares a chain of layers with all the targets, which allows exploring the commonalities among them. There is also a chain of non-shared layers that are associated with each target, trying to represent their specificities.

Fig. 5.5 ANN illustration

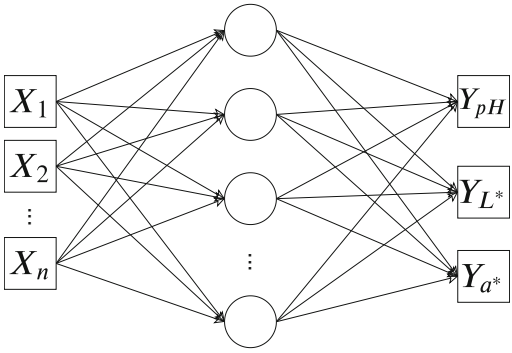

5.2.3 Problem Transformation Methods

In problem transformation, the data is modified for using the ML algorithms in their original versions. Generally, the problem is subdivided into d simpler problems. Until this point, it is very similar to ST, in such a way that some authors consider ST a particular case of problem transformation. However, methods that follow this approach modify the input training data in several different ways to explore the targets' correlation. We can split the transformation methods into two main groups: shallow and deep methods according to the number of subdivisions in a perspective of layers for iterative recombination of problem transformations.

5.2.3.1 Shallow Methods

Shallow methods subdivide the problem in a single or reduced number of recombinations. This kind of method can be divided into three types, based on stacking, chaining, or statistics.

Stacking is an ensemble technique often used by MTR methods. It consists of building multiple models to obtain intermediate predictions and building new models (meta-regressors) that consider those predictions. This technique has as premise that the models in a further training phase can correct the error from a previous phase. Stacked single target, multi-target augmented stacking, and multi-target stacked generalisation are examples of stacking methods.

Chaining methods, such as ensemble regressor chains, multi-output tree chaining and support vector regression via correlation regression chair, consider target orders when creating the models. The first attempt in this branch, regressor chain, created a single chain in the exact order the targets figured in the dataset. However, it was found a performance sensitivity in relation to this order. Then, other methods were created trying to overcome this drawback.

Finally, mapping-based method, e.g. random linear target combinations, maps the source input to new variables to generate a matrix of coefficients related to the inter-correlation among the targets.

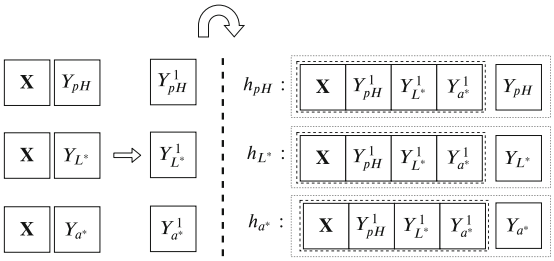

Fig. 5.6 SST training illustration

SST

Stacked single target (SST) [45] is one of the most used methods. First, it builds one independent regressor for each target, as in ST. After that, it predicts the values of the targets using these models. These predictions ($\mathbf{Y}^1$) are concatenated to $\mathbf{X}$, forming a new input data $\mathbf{X}^2 = \mathbf{X}|\mathbf{Y}^1$. After that, one model is created for each of the targets again. The predictions of the meta-regressors ($\mathbf{Y}^2$) are the final predictions. In this sense, it produces d models in the first phase and other d models in the second phase. Figure 5.6 illustrates the training of SST.

MTAS

Multi-target augmented stacking (MTAS) [42] uses more than one regression algorithm for each target in the first phase. Considering r the number of used regression algorithms, it produces $r \times d$ regressors in the first phase. After that, it predicts the values of the targets using these models. Before concatenating these predictions, they are assessed in terms of contribution to the explanation of the problem. Only the useful predictions are then aggregated to the input set for the second phase training. In this phase, one regression algorithm is chosen to generate the meta-regressors, producing one model for each target. Again, d models are produced as final models. Figure 5.7 illustrates the training of MTAS considering $r = 2$: linear regression (LR) and random forest (RF).

MTSG

Multi-target stacked generalisation (MTSG) [43] is very similar to MTAS, as shown in Fig. 5.8. The main difference between them occurs during the second phase training. MTSG does not use the $\mathbf{X}$ set as part of input data. It means that only the useful predictions obtained by the models in the first phase will be considered as input for the meta-regressors.

ERC

Ensemble of regressor chains (ERC) [45] defines distinct permutations of the targets order (which defines the chain) and then builds regressors sets. In each set, the models are trained sequentially, following the chain. A first model is built considering only X and the first target in the chain; The second model is built considering X, the first target, and the second target in the chain. This procedure is

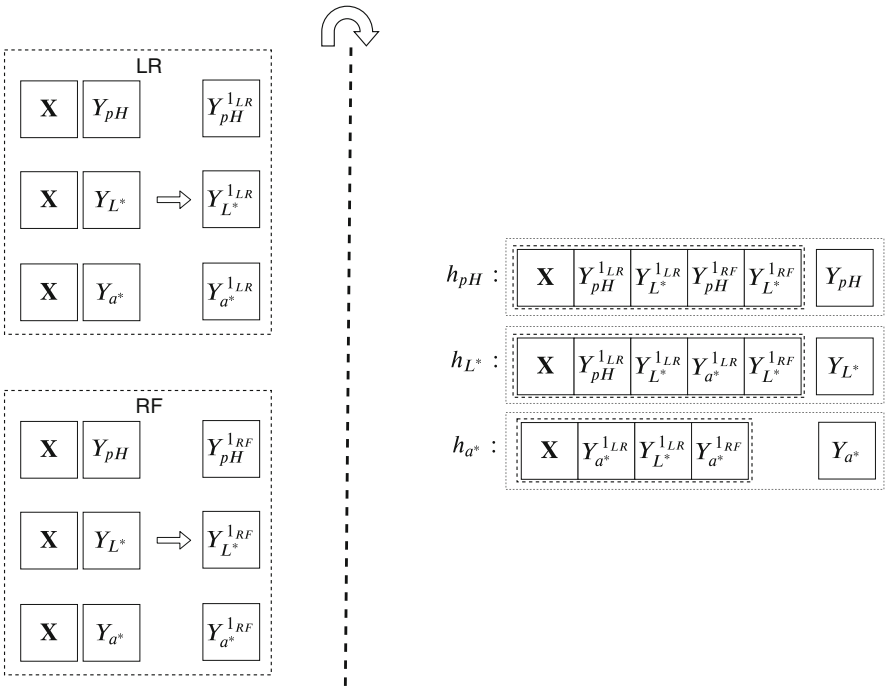

Fig. 5.7 MTAS training illustration

repeated until the end of the chain. The final output of the method for each target will be the average of predictions of all regressors trained for that target in the different chain sets.

Figure 5.9 shows how would be the training for the dataset example mentioned in the beginning of this chapter. Since there are 3 targets, there are $3! = 6$ distinct permutations of the targets. If the number of targets is greater than 3, the number of chains used to train is limited to 10, which are randomly chosen.

MOTC

Multi-output tree chaining (MOTC) [33] creates a chain in the form of a tree. This tree is built by evaluating the correlation of the targets. The models are then built from leaves to the root. When compared to ERC, MOTC uses less training time and memory. One advantage of these methods is the interpretability, in the form of a graph, on the number of times a given target was used to explain the other.

Figure 5.10 illustrates the interpretability promised by MOTC: it is possible to extract how many times pH, L^*, and a^* were used to explain each other. If there is no connection between two targets, it means that they were not used to explain each other directly. The edge values are related to the strength of the correlation.

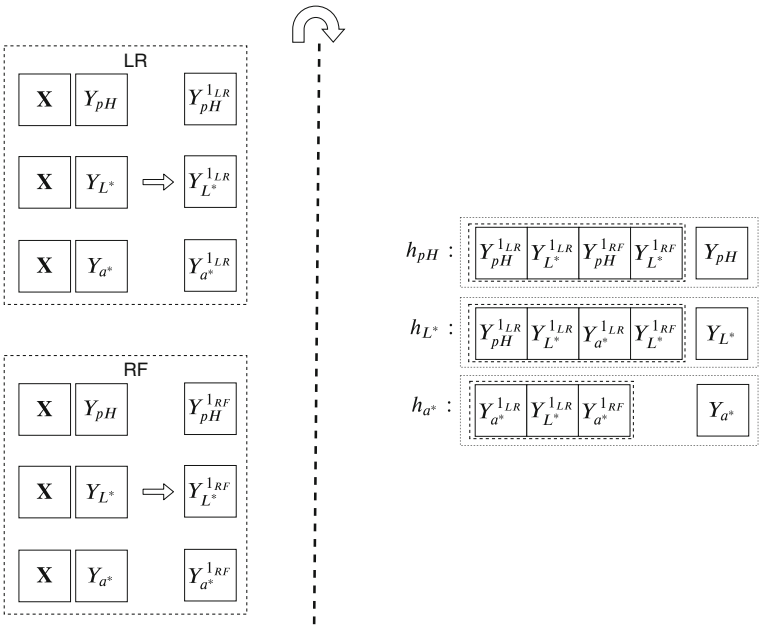

Fig. 5.8 MTSG training illustration

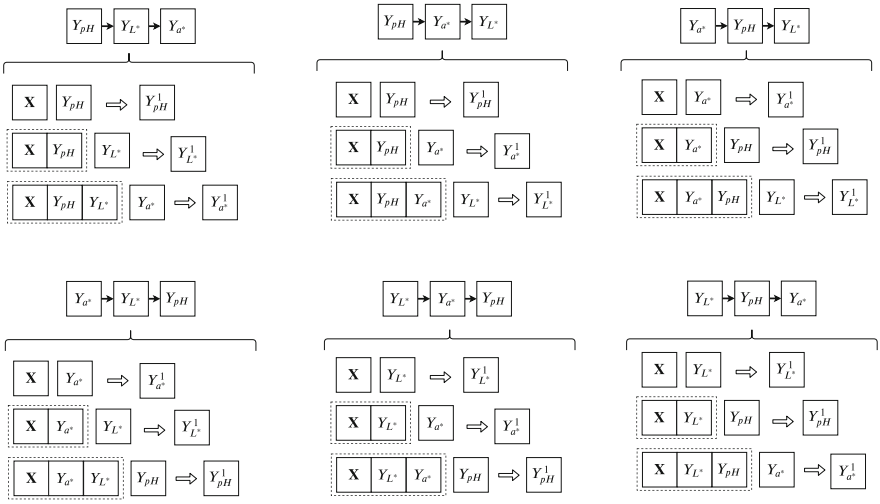

Fig. 5.9 ERC training illustration

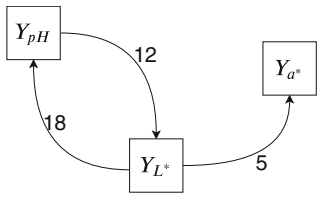

Fig. 5.10 MOTC output graph

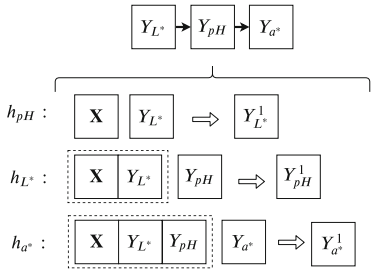

Fig. 5.11 SVRCC training diagram

SVRCC

Melki et al. [35] proposed SVR correlation chains (SVRCC). This method creates a single chain that extracts the maximum inter-target correlation. In this way, the targets will be sorted in decreasing order, starting with the most correlated and ending with the least correlated.

Figure 5.11 shows an example in which Y_{L*} is the most correlated target, followed by Y_{pH} and lastly Y_{a*}.

RLC

Random linear target combinations (RLC) [48] is an ensemble method which maps the original input variables to q new variables. For this, it creates a random coefficient matrix $\mathbf{C}$ of size $d \times q$ and obtains the product of $\mathbf{Y}$ and $\mathbf{C}$, generating a matrix $\mathbf{Y}'$ of size $n \times q$.

The problem is divided as in ST. Predictions of these new variables are obtained ($\mathbf{Y}'^1$) and then an inversion of the combination is applied to obtain predictions of the original targets ($\boldsymbol{Y}^1$).

5.2.3.2 Deep Methods

DRS

Deep regressor stacking (DRS) [41] can be seen as an extension of SST to multiple layers of regressors. In a first phase, it creates d regressors using a single regression algorithm. After that, the predictions $\mathbf{Y}^1$ are obtained and concatenated to the original input $\mathbf{X}$, forming $\mathbf{X}^2$. Then, in a second phase, d regressors are obtained considering $\mathbf{X}^2$ and Y. New predictions $\mathbf{Y}^2$ are obtained and concatenated to $\mathbf{X}^2$, forming $\mathbf{X}^3 = \mathbf{X}^2|\mathbf{Y}^2$. In this way, consecutive training phases are executed until a predetermined number of layers (λ) is reached. Figure 5.12 shows the

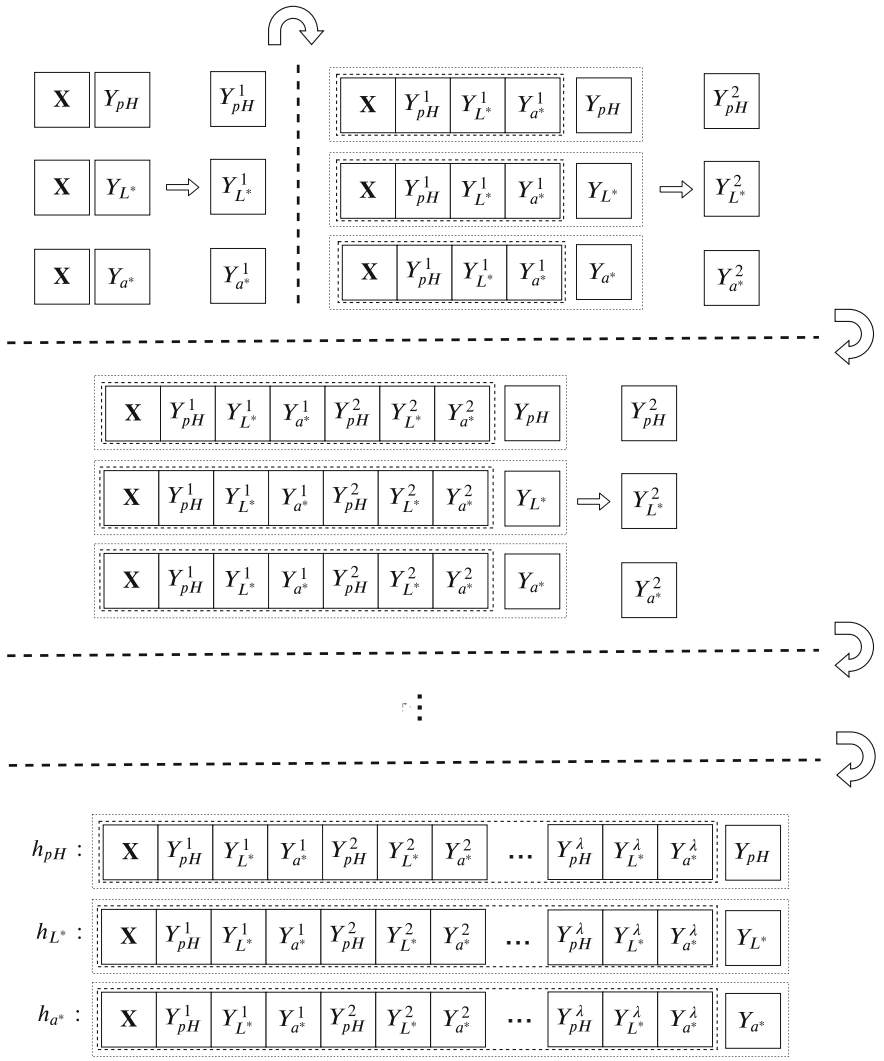

Fig. 5.12 DRS training illustration

training mechanism of DRS. In the last training phase, the input set consists of the predictions of all previous layers, i.e. $\mathbf{X}^\lambda = \mathbf{X}|\mathbf{Y}^1|\mathbf{Y}^2|\ldots|\mathbf{Y}^{\lambda-1}$.

DSTARTS

Deep structure for tracking asynchronous regressor stack (DSTARS) [34] also builds multiple layers, as DRS. However, only correlated targets are concatenated to the input set at each training phase. Another difference is that the stop of training is determined by the method itself according to a user predefined improvement factor.

Thus, DSTARS explores different levels of inter-dependencies among the targets based on the dataset seeking to find the best composition of stacked regression models to decrease the prediction error.

It is important to note that DSTARS relies on certain hyperparameter choices, including the sampling strategy used to separate the data, error improvement hyperparameter, and threshold.

5.3 Near Infrared Spectral Analyses

Spectroscopy implies in energy absorption from chemical bonds present in organic molecules. Multivariate analysis has been used together with near infrared spectroscopy (NIRS) and near infrared hyperspectral imaging (NIR-HSI) techniques for spectral data interpretation. Multivariate data analysis includes a branch of exploratory, non-supervised and supervised, qualitative and quantitative techniques [25].

5.3.1 Modelling Spectral Regression

5.3.1.1 Qualitative or Classification Techniques

Among the techniques of exploratory analysis found in the literature, principal component analysis (PCA) is the most used. Considering a NIR or NIR-HSI dataset, which contains hundreds of variables, there is a lot of irrelevant information that do not contribute or can jeopardize data interpretation. Therefore, methods such as PCA are able to compress these variables to a smaller number, which carries all the information necessary to explain the variance among samples. These new variables, called principal components (PCs), are a combination of the original variables, and, usually, just few of them are necessary to identify the differences between the studied samples. Moreover, PCA is an unsupervised method, so no prior information is required. This is a great advantage of this technique and explains why PCA usually is used as a first step in data modelling [32].

The linear and non-linear qualitative methods used in multivariate analysis include linear discriminant analysis (LDA), partial least squares discriminant analysis (PLS-DA), k-nearest neighbour (k-NN), artificial neural networks (ANNs), support vector machine (SVM), and so on. The main idea of these supervised techniques is to discriminate between classes of samples. When performed in a spectral dataset, these methods search for the similarities between the spectrum of each sample in order to develop a model that is able to correctly discriminate samples according to the predetermined group. In the food field, this qualitative analyses can be used, for instance, to determine samples origin, variety, pure and adulterated samples, among many other applications.

Apart from these methods, soft independent modelling of class analogy (SIMCA) is also widely used in qualitative determinations. The main difference between this method and the others is the capacity of classifying a sample as belonging to more

than one class or none of them, while the other methods discriminate between the established classes [32]. Therefore, qualitative modelling gives the possibility of determining many outputs with the same dataset. For example, a dataset containing the spectral information about corn grains from different varieties, harvest year, and country. With this same dataset, models can be developed to discriminate or classify these samples within the respective classes.

5.3.1.2 Quantitative or Prediction Techniques

On the other hand, linear and non-linear quantitative methods for multivariate analysis provide the possibility of prediction of different parameters, such as protein and fat content, percentage of adulteration, and so on. Partial least squares regression (PLSR), principal component regression (PCR), multiple linear regression (MLR) are some quantitative techniques used for this propose. Their main idea is to establish a relationship between independent variables (e.g. spectral information) and a dependent variable (e.g. chemical parameter).

As in qualitative determinations, the same dataset can provide the information for many predictions. For example, the measurement of meat quality involves the determination of parameters such as protein, fat, colour, pH, moisture, and others [17]. By relating the spectral information regarding meat samples and the reference values of the parameters to be determined, one model can be developed for the prediction of each property. The performance of these models is evaluated based on the relationship between the predicted and the reference value [32, 39]. Therefore, the inference about the conformity or the quality of some product can take the determination of more than one parameter, consequently, the development of more than one model.

Currently, partial least square regressions (PLS) is the most common method used for prediction of parameters of interest. The use of linear techniques has shown to be good enough for most of the determinations based on spectral data. However, due to some changes that may occur in sample properties, there may be an increase in the complexity of the data and the appearance of non-linearities, which cannot be modelled by linear models. In this context, machine learning (ML) includes many algorithms that are able to handle complex and non-linear data [9, 22, 28].

5.3.1.3 Multi-Target Regression

Recently, MTR has played an important role in machine learning and has been widely applied in various fields. Considering the fact that spectroscopy has been used for prediction of many outputs using the same dataset, and MTR implies the prediction of many outputs, MTR would be a great deal for spectral data interpretation [15, 22].

The algorithms used in MTR can be categorised in two groups: algorithm adaption methods and problem transformation methods. Algorithm adaption methods use the single target regression algorithms to directly solve MTR tasks. Therefore, prediction of an unknown sample is possible by the development of one single model. The main advantage of this approach, but still a challenge, is the possibility

of exploring the relationship not only between the inputs and outputs, but also the existence of a correlation between targets [50].

On the other hand, the problem transformation methods basically transform MTR in individual single target regression problems. Although these single target methods are well-known scenarios, by developing different models, the reference values regarding other targets are included in the calibration of the desired target, causing an accumulated error that may reduce the MTR performance. Moreover, this approach does not consider the correlation between the outputs. In other words, the prediction of n outputs of a given unknown sample would take the development of n single models, each one for its specific target without considering their relationship [35, 50].

In the literature, some works can be found in different fields regarding the use of MTR, such as the prediction of healthcare resource utilisation [12], drug efficacy [29], stock market [13], and quality prediction in a mining process [15]. However, not much is found regarding the development of MTR with spectral data.

5.4 NIR Spectral Analysis in Food Samples

Near infrared spectroscopy has been used in the assessment of different features in food samples, performed by the association of NIR spectra with the parameter of interest in the product.

However, when it comes to food products, the complexity of food matrices can be a challenge for this technique. Food products are very heterogeneous materials, and taking one measurement from one point of the sample might not be enough to represent the whole sample. To deal with this impasse, it is interesting to have spatial information of the whole sample. Hence, spectral techniques that are able to give also spatial information as near infrared hyperspectral imaging is a great alternative.

The quality and safety of food products are essential requirements for producers, consumers, and food regulatory agencies. The assessment of food quality and safety includes the evaluation of sensory (e.g. texture, colour) and chemical (e.g. protein, fat) parameters, authentication of adulteration (e.g. adulteration by cheaper products), contamination (e.g. toxin, allergens), and any other aspects that can affect the consumers health or even the product acceptance.

This search for high-standards in food quality led to the development of analytical tools that are able to confirm if the product is able or not to be in the market. Currently, many tools are available for food analysis such as the conventional wet chemical methods, mass spectrometry (MS), high performance liquid chromatography (HPLC), and so on. Although these methods are commonly used and provide high quality information, they are mostly time-consuming, destructive, and some of them even hazardous [47, 49], with the added handicap that it only applies to a small portion of the batch. Therefore, the development of methods that are able to assess food quality and safety without these drawbacks is required.

In this context, vibrational techniques such as near infrared spectroscopy (NIRS) and near infrared hyperspectral imaging (NIR-HSI) have been reported to be promising tools in many sectors, specially in the food field. These techniques have proven to be an good alternative to the traditional methods of analysis, since it is fast, non-destructive, appropriate to be applied in/on-line, chemical-free, and so on [31].

5.4.1 NIRS and NIR-HSI in Food Products

NIR spectroscopy and NIR-HSI have demonstrated to be very efficient in the determination of many parameters in the most varied types of products.

5.4.1.1 Determination of Quality Parameters

The assessment of quality parameters in grains and flours includes the determination of protein, carbohydrate, fat, moisture contents, among other parameters. Chickpea flour (also called *besan*) is used as ingredients for other products, making chickpea an important staple food, specially in South Asia. In this context, [23] studied the possibility of using a lab-built predispersive filter-based NIR spectrometer (700–2500 nm) for rapid characterisation of quality parameters in *besan*. The authors determined protein, carbohydrate, fat, and moisture contents using partial least square regression (PLSR), principal component regression (PCR), interval partial least squares (iPLS), and synergy interval partial least squares (siPLS). PLSR and PCR models were developed based on full wavelengths and had R^2 over 0.96 and RMSEP below 0.05 for all parameters. After that, wavelength selection was performed and iPLS and siPLS models were developed. RMSEP of these reduced models were determined and compared to the RMSEP of full spectra. Wavelengths from 2100 to 2345 nm were able to predict moisture content with RMSEP of 0.005 by iPLS. SiPLS models were able to predict carbohydrate, fat, and protein contents and reduce by 0.41%, 0.1%, and 1.1%, respectively, when compared to the models built with full wavelengths. Hence, this work showed the feasibility of using NIR spectroscopy for rapid determination of quality parameters in chickpea flour.

Protein content is one of the most important parameters for the determination of wheat quality. Aiming to determine the protein distribution in whole wheat kernels, [10] used a near infrared hyperspectral imaging system (980–2500 nm). The authors studied varied wheat samples that were analyzed by NIR-HSI and by the Dumas combustion method as the reference value of protein content. Partial least squares regression models were developed with the information of the single kernel spectra. The protein content determined by Dumas method ranged from 6.2 to 19.8%. PLSR models were able to predict the protein content with a coefficient of determination of 0.79 and root mean square error of 0.94%, showing the feasibility of using NIR-HSI for protein quantification in whole wheat kernels.

5.4.1.2 Sensory Attributes

Sensory attributes play an important role in product acceptance. Therefore, the development of a method that is able to quantify the sensorial properties is very interesting. In this sense, [20] applied near infrared reflectance spectroscopy in different samples of cheese (cow, ewe, goat) to evaluate different sensory attributes, such as surface features (presence of holes), salty and buttery taste, texture (hardness, chewiness, creamy), flavour (rancid aroma), and other sensory attributes (pungency, retronasal sensation). The reference values of sensorial properties were defined by trained panellists. Modified partial least squares (MPLS) regression was used to quantitatively evaluate the attributes. The models performance was evaluated by comparing the results of NIR spectral data and the reference feature of calibration samples with those of samples left out for external validation by means of Student's *t*-test. The significance levels obtained were between 0.84 and 0.01 for the rancid flavour and chewiness, respectively. The results for residuals were between 0.9 (detection of holes) and 0.4 for sensory attributes creamy, chewiness, and retronasal sensation. Root mean standard error (RMSE) values were 1.0 and 0.4 for holes and creamy, respectively. The results obtained by NIR spectroscopy were comparable to those obtained by the panel experts, showing the potential of NIR in determination of sensory attributes in cheese.

Coffee is one of the most consumed beverages worldwide, and the determination of sensory attributes in coffee is part of its quality determination. Usually, this analysis is performed by a "cupping test", which depends on the expertise of trained testers. Although these testers have developed an acute sensibility for these evaluations, the analysis is still very subjective. Therefore, [5] evaluated the use of near infrared spectroscopy for the assessment of sensory attributes in commercial roasted and ground coffee samples. The reference values of powder fragrance, drink aroma, acidity, bitterness, flavour, body, astringency, residual flavour, and overall quality used for the development of PLSR models were obtained by the "cupping test". The performance of the models was evaluated based on many parameters of merit, including coefficient of correlation, RMSEP, and limits of detection and quantification. The coefficients of correlation were between 0.73 and 0.84, RMSEP between 0.09 and 0.29, limits of detection between 0.06 and 0.72, and limits of quantification between 0.19 and 2.17. These results showed the possibility of using NIR and chemometrics for prediction of sensorial properties of coffee without drink preparation.

5.4.1.3 Adulteration

Adulteration of food products is commonly practiced around the world. Most of these adulterations are hardly detected, due to the similarity between the product and the adulterant. Regarding minced meat, this is even hard because the variation of morphological characteristics is eliminated during mincing process. Therefore, [24] used a hyperspectral imaging system (400–1000 nm) as a fast and non-destructive technique to detect adulteration in minced beef meat with horse meat. PLSR models were developed with spectral information of samples at different levels of

adulteration. The coefficient of determination and the standard error of prediction were 0.98 and 2.23%, respectively. After that, the regression coefficients were evaluated to select important wavelengths (515, 595, 650, and 880 nm) in order to develop prediction maps for the evaluation of the adulteration level in each pixel of the hyperspectral images. The results demonstrated that HSI has a great potential as a rapid screening technique for determination of adulterated minced meat.

Paprika is a spice widely used as food additive in processed foods, acting as dye and flavour agent. Due to this, paprika powder is very susceptible to adulteration, which is not easy to detect. Recently, [38] tested a portable NIR spectrometer for rapid detection of paprika adulteration. The authors adulterated different paprika samples (sweet, smoked, and spicy) from different suppliers, adding different amounts of acacia gum, annatto, and potato starch. Data analysis was performed using classification models (partial least squares discriminant analysis—PLS-DA) and prediction models (partial least squares regression—PLSR). PLS-DA was performed to identify samples as adulterated or non-adulterated and the type of adulterant. All the models performed well, with specificity over 90% and error rate below 2%. After, PLSR models were used to predict the level of adulteration in paprika samples. Additionally, reduced models based on selected wavelengths were developed. The model performance had values of $R^2 = 0.87$ and RMSEP = 1.74 for prediction of adulteration with acácia gum, $R^2 = 0.97$ and RMSEP = 1.74 for annatto, and $R^2 = 0.95$, and RMSEP = 2.12 for potato starch. The authors demonstrated that NIR spectroscopy can be applied as a screening technique for detection of adulteration in paprika.

5.4.1.4 Contamination

Wheat is the major cereal consumed around the world, and, as any cereal, is very susceptible to fungal contamination. Ochratoxin A (OTA) is a mycotoxin commonly found in cereals and its level is controlled by many regulatory agencies in order to avoid the excessive intake by consumers. In this context, [44] evaluated infected wheat samples with a hyperspectral imaging system. Principal component analysis was applied on spectral data and important wavelengths were selected (1280, 1300, and 1350 nm) based on the highest factor loadings. Information regarding these wavelengths (six statistical and ten histogram features) was extracted and used as inputs to linear, quadratic, and Mahalanobis discriminant classifiers. Healthy and fungal-infected kernels were correctly classified with an accuracy higher than 90% for all the three classifiers. Pair-wise, two-way, and six-way classification models were developed and the quadratic discriminant provided classification accuracy higher than the linear and Mahalanobis classifiers. Moreover, apart from these wavelengths, one specific wavelength (1480 nm) was detected in samples contaminated with Ochratoxin A. These samples were identified with an accuracy of 100%, showing the ability of NIR hyperspectral imaging system to differentiate between wheat samples in different fungal infection stages and with different levels of Ochratoxin A.

Recently, [14] used Fourier Transform near and mid-infrared spectroscopy (FT-NIR, FT-MIR) for evaluation of wheat samples contaminated with OTA. Partial least

squares discriminant analysis (PLS-DA) and principal component-linear discriminant analysis (PC-LDA) models were performed on spectral data to differentiate between highly contaminated and low contaminated wheat samples (limit set at 2 μg/kg OTA). Overall, the models were able to discriminate samples with accuracy above 94% for both techniques, regardless the classification model. A rate of 6% of misclassifications were obtained for both spectral techniques and both classification models. These results indicated that both spectroscopy techniques offer a promising alternative for a cheap and easy-to-use screening tool for discrimination of OTA contaminated wheat samples.

5.4.1.5 Identification

The meat industry and consumers are greatly concerned about the quality and safety of meat products. These parameters include a series of evaluations regarding composition, authenticity (e.g. fresh meat), adulteration, and so on. Moreover, the identification of meat parts and processed products can play an important role in product authentication. In this context, [37] explored the possibility of using a portable near infrared spectrometer (900–1700 nm) for the identification of chicken parts (breasts, thighs, and drumstick). Since the traditional methods of analysis can successfully deal with this task, physical–chemical analysis (pH, $L^*a^*b^*$ colour, protein, fat, moisture, and ash contents) was also carried out, but some disadvantages as time and use of chemicals are evident. Then, the authors associated NIR spectral data and machine learning (ML) techniques in order to develop a rapid and noninvasive technique for chicken parts identification. Principal component analysis was used as screening step, and support vector machine (SVM) and random forest (RF) algorithms were performed for classification of chicken parts. The models were able to differentiate breast from thighs and drumstick samples with an accuracy of 98%, showing the feasibility of using a portable NIR spectrometer for rapid discrimination of chicken parts and the potential of using this technique in the meat industry.

Recently, [6] evaluated the potential of near infrared (NIR) spectroscopy (400–2500 nm) as a rapid technique to discriminate turkey cuts (wing, leg, drumstick, breast, and skin) and processed turkey meat products (blanquette, cooked ham, turkey breast, and smoked breast). Principal component analysis (PCA) was performed on spectral data in order to explore the samples spectral information and as a tool for selecting relevant wavelengths for linear discriminant analysis (LDA). The effect of chemical and physical information of turkey meat and processed products could be observed on PCA score plots. LDA models developed with raw data were able to discriminate turkey cuts with an accuracy over 80% and processed products with an accuracy over 71%, suggesting that NIR spectroscopy is a promising tool for evaluation of raw turkey meat and ready-to-eat turkey products.

Although it was reported here a wide range of applications of NIR spectral methods in food samples, there has been few of them using MTR. It can be seen that several of the applications used several independent models to predict different attributes from samples, using the same information as predictors, the spectra. Thus, MTR could find an interesting niche in food applications, combined with NIR spectroscopy or imaging.

5.4.2 Multi-Target Regression Applied to Food Samples

Characterising food products is an extensive process performed from production to consumption, identifying nutritional content, product quality, and at even health risks to consumers. Physico-chemical analysis can reveal a great part of food characteristics, exposing hydration properties, rheological behaviour, texture properties, surface properties, capacity for formation and stability, surfactant agents, optical and thermal properties.

Several food properties present linear and non-linear inter-correlation, providing an opportunity to employ MTR methods. Boosted by the capacity of NIR and NIR-HSI, recent projects have been taking advantage of MTR methods to improve the predictive performance of food analysis.

In this section, two projects addressing meat and flour applications of MTR over NIR spectra are deeply discussed.

5.4.2.1 Chicken Meat

Nutritional analysis in poultry science usually requires carcass chemical analysis to estimate the nutritive value of meat. Thus, the quality of chicken meat is connected to physico-chemical features ordinarily assessed in the breast muscle. Santana et al. [42] proposed a new method, called multi-target augmented stacking (MTAS), to predict several attributes (colour features, pH determination, chemical composition, water holding capacity, cooking loss, and tenderness) in poultry breast muscles. MTR methods were compared to evaluate the efficiency of spectral data in the prediction of poultry meat parameters, as Fig. 5.13 shows.

To support the hypothesis of MTR application, the authors extract the linear and non-linear correlation of poultry parameters using Pearson correlation and random forest importance, respectively. Several parameters from a different type of characteristics exposed to be high-correlated, sustaining the usage of MTR methods. Further, in this work, the authors proposed a new method combining the MTRS stacking-based idea with the addition of multiple base learners. Thus, the MTAS takes advantage of the different levels of correlation and integration among target variables, assuming that each pair of parameters need to be modelled differently.

The NIR signal was pre-processed and the first seven principal components (PC) were used to characterise each sample. The authors compared the performance of:

- Multi-target regressor stacking (MTRS)
- Ensemble of regressor chains (ERC)
- Multi-target augmented stacking (MTAS)
- Deep regressor stacking (DRS)

To predict many poultry meat quality parameters, including moisture, protein, lipids, ashes, pH, colour, and texture, the authors compared support vector machine (SVM), random forest (RF), and classification and regression tree (CART) as regressors. As result, the work explored not only the advantages of using MTR in

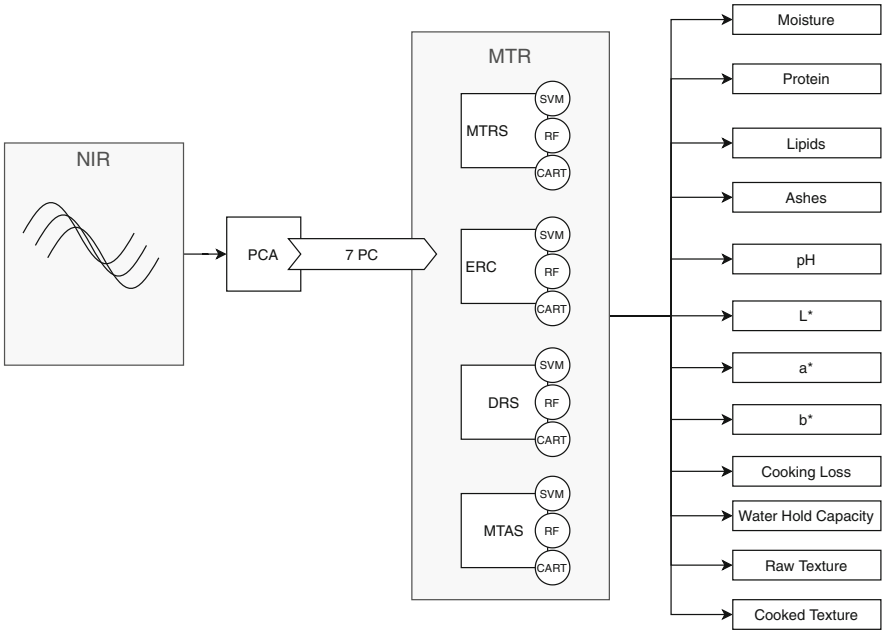

Fig. 5.13 Overview of proposed approach in [42]

NIR data, but also the different interactions between the outputs. The results showed the proposed method, MTAS, was very successful, and it achieved an increase of 7.9% in the models performance.

5.4.2.2 Flour

Several variables affect the quality of bread wheat flour, e.g. varietal differences, cultivation practices, and environmental effects. These factors, in turn, influence the regional and year to year variations and the climatic circumstances, which influence the quality of wheat flour, estimated throughout the trading. Recently, [22] tested MTRs and machine learning algorithms as a strategy to improve the prediction performance of quality parameters in wheat flour (hectolitre weight, falling number, protein content, alveographic indexes, and farinograph stability), based on near infrared (NIR) spectral data.

The authors used Pearson correlation coefficient to calculate the inter-correlation among all parameters. Protein content and alveographic index W were the most correlated. On the other hand, hectolitre weight and falling number presented no-correlation, but all of the parameters had at least one average correlated parameter. NIR reflectance spectra was acquired using a Bruker MPA Multi Purpose FT-NIR Analyzer, with an integrating sphere and a RT-PbS detector in the 12,500–3600 cm^{-1} range.

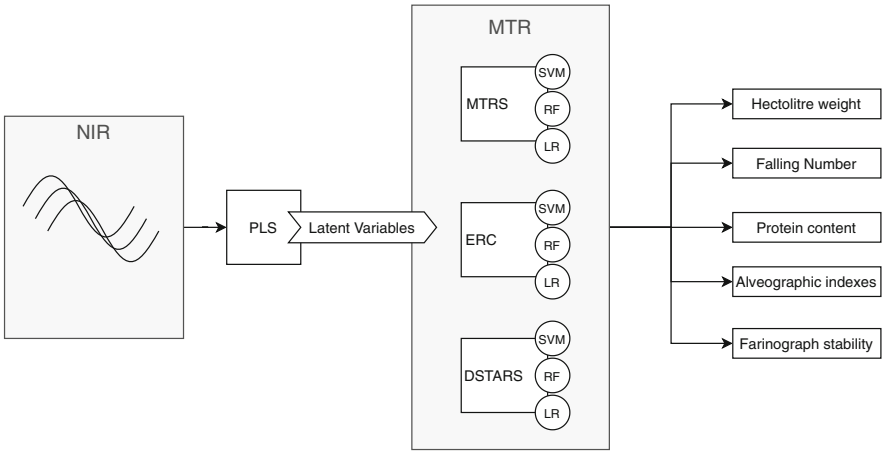

Fig. 5.14 Overview of proposed approach in [22]

Using traditional NIR signal pre-processing (i.e. scaling and mean-centering), the authors extracted the latent variables of PLS from the dataset to predict the wheat flour parameters. It was compared the performance of several multi-target methods:

- Multi-target regressor stacking (MTRS)
- Ensemble of regressor chains (ERC)
- Deep structure for tracking asynchronous regressor stack (DSTARS)

Three distinct machine learning algorithms were compared as: support vector machine (SVM), random forest (RF), and linear regression (LR). In Figure 5.14 it is possible to observe the overview of the proposed approach in [22].

The authors reported that MTR allowed an increase of 7.9% in the performance of prediction models for quality parameters of wheat flour. Further, two contributions for the analysis of spectral data have been achieved, as the advantages of non-linear modelling by using latent variable from PLS and RF, and the possible advantages of multi-target prediction in general. Considering the results exposed in [22], we recommend the use of MTR over PLS modelled by ML algorithm. This alternative is capable to deal with drawbacks of PLS by non-linear ML modelling. Particularly, RF delivers further information from RF relevance and requires less hyperparameters to be used.

5.5 Future Trends

In the current chapter, we present a comprehensive discussion on the state of the art of multi-output regression. It is presented an overview and comparison of the main techniques reported in the literature, with respect to prediction accuracy based on

the evaluation metrics, computational complexity, and interpretation of results. The chapter then focuses on performance of MTR to spectral data, and its application to food quality and composition measurements.

Before considering the most promising usage and future implementations of MTR methods, their drawbacks need to be discussed to pave the way for the future proposal. The most recent problem transformation methods have already overcome the former MTR methods (i.e. MTRS and ERC) when considering predictive performance. On one hand, the shallow methods have a similar computational complexity of MTRS and ERC, but some studies exposed a strict relation between problem and regressor. Thus, the demand for tuning and choosing optimal hyperparameters for machine learning regressor is more relevant than MTR method for many of problems. On the other hand, deep methods are computationally expensive, in several cases, the improvement obtained is not significant enough due to cost.

When using algorithm adaptation, the architecture and deep knowledge required to modify an algorithm pose some additional challenges to this type of solution. This fact is indicated by the growing usage of problem transformation applications.

An interesting area for future works would be to compare different approaches of MTR to spectral data obtained from food matrices. Researchers that work on the subject could make data publicly available for further tests, or new data could be acquired with this purpose. It could allow prediction of several attributes at once, which is a promising application for complex matrices such as food and agricultural products.

Another interesting application will be grouping the different approaches available according to prediction performances, identifying the most useful methods for each type of product, based on their performances for that given sample based on the multiple targets of interest.

Definitely predictive performance improvement is mandatory when selecting a MTR solution based on NIR spectra from food. Nevertheless, recent studies suggested more comprehensive and uncomplicated methods to interpret the intercorrelation of targets, helping to understand relationships between physic chemical attributes of the food product. Further, it is expected that visual models from MTR can help interpretation of the obtained predictive pattern by food specialists.

Acknowledgments This study was financed in part by the Coordenação de Aperfeiçoamento de Pessoal de Nível Superior—Brasil (CAPES)—Finance Code 001 and Technological Development (CNPq) of Brazil—Grant of Project 420562/2018-4 and Fundação Araucária (Paraná, Brazil). The authors gratefully acknowledge the financial support from the São Paulo Research Foundation (FAPESP) project 2015/24351-2, 2017/17628-3, 2019/06842-0.

References

1. Abraham Z, Pang-Ning T, Julie W, Shiyuan Z, Malgorzata L et al (2013) Position preserving multi-output prediction. In: Joint European conference on machine learning and knowledge discovery in databases, pp 320–335

2. Aho T, Ženko B, Džeroski S (2009) Rule ensembles for multi-target regression. In: 2009 9th IEEE International Conference on Data Mining, pp 21–30
3. Aho T, Zenko B, Dzeroski S, Elomaa T (2012) Multi-target regression with rule ensembles. J Mach Learn Res 13:2367–2407
4. Baldassarre L, Rosasco L, Barla A, Verri A (2012) Multi-output learning via spectral filtering. Mach Learn 87(3):259–301
5. Baqueta MR, Coqueiro A, Valderrama P (2019) Brazilian coffee blends: a simple and fast method by near-infrared spectroscopy for the determination of the sensory attributes elicited in professional coffee cupping. J Food Sci 84(6):1247–1255
6. Barbin DF, Badaró AT, Honorato DCB, Ida EY, Shimokomaki M (2020) Identification of turkey meat and processed products using near infrared spectroscopy. Food Control 107:106816
7. Borchani H, Varando G, Bielza C, Larrañaga P (2015) A survey on multi-output regression. Wiley Interdiscip Rev Data Min Knowl Disc 5(5):216–233
8. Breiman L (2001) Random forests. Mach Learn 45(1):5–32. https://doi.org/10.1023/A:1010933404324
9. Brereton RG (2003) Chemometrics: data analysis for the laboratory and chemical plant. Wiley, Hoboken
10. Caporaso N, Whitworth MB, Fisk ID (2018) Protein content prediction in single wheat kernels using hyperspectral imaging. Food Chem 240:32–42
11. Cook RD, Weisberg S (1982) Criticism and influence analysis in regression. Sociol Methodol 13:313–361
12. Cui L, Xie X, Shen Z, Lu R, Wang H (2018) Prediction of the healthcare resource utilization using multi-output regression models. IISE Trans Healthcare Syst Eng 8(4):291–302. https://doi.org/10.1080/24725579.2018.1512537
13. da Silva JAPR, Santana EJ, Mastelini SM, Barbon S Jr (2018) Stock portfolio prediction by multi-target decision support. In: Proceedings of the XIV Brazilian symposium on information systems, pp 1–8
14. De Girolamo A, von Holst C, Cortese M, Cervellieri S, Pascale M, Longobardi F, Catucci L, Porricelli ACR, Lippolis V (2019) Rapid screening of ochratoxin a in wheat by infrared spectroscopy. Food Chem 282:95–100
15. Dogan A, Birant D, Kut A (2019) Multi-target regression for quality prediction in a mining process. In: 2019 4th international conference on computer science and engineering (UBMK), pp 639–644
16. Drucker H, Burges CJC, Kaufman L, Smola AJ, Vapnik V (1997) Support vector regression machines. In: Advances in neural information processing systems, pp 155–161
17. ElMasry G, Barbin DF, Sun D-W, Allen P (2012) Meat quality evaluation by hyperspectral imaging technique: an overview. Crit Rev Food Sci Nutr 52(8):689–711
18. Freedman DA (2009) Statistical models: theory and practice. Cambridge University Press, Cambridge
19. Friedman JH (2001) Greedy function approximation: a gradient boosting machine. Ann Stat 29:1189–1232
20. González-Martín MI, Severiano-Pérez P, Revilla I, Vivar-Quintana AM, Hernández-Hierro JM, González-Pérez C, Lobos-Ortega IA (2011) Prediction of sensory attributes of cheese by near-infrared spectroscopy. Food Chem 127(1):256–263
21. Izenman AJ (1975) Reduced-rank regression for the multivariate linear model. J Multivar Anal 5(2):248–264
22. Junior SB, Mastelini SM, Barbon APAC, Barbin DF, Calvini R, Lopes JF, Ulrici A (2019) Multi-target prediction of wheat flour quality parameters with near infrared spectroscopy. Inf Process Agri 7:342–354
23. Kamboj U, Guha P, Mishra S (2017) Characterization of chickpea flour by near infrared spectroscopy and chemometrics. Anal Lett 50(11):1754–1766

24. Kamruzzaman M, Makino Y, Oshita S, Liu S (2015) Assessment of visible near-infrared hyperspectral imaging as a tool for detection of horsemeat adulteration in minced beef. Food Bioprocess Tech 8(5):1054–1062
25. Kemsley EK, Defernez M, Marini F (2019) Multivariate statistics: considerations and confidences in food authenticity problems. Food Control 105:102–112
26. Kocev D, Vens C, Struyf J, Džeroski S (2007) Ensembles of multiobjective decision trees. In: European conference on machine learning, pp 624–631
27. Kocev D, Džeroski S, White MD, Newell GR, Griffioen P (2009) Using single- and multi-target regression trees and ensembles to model a compound index of vegetation condition. Ecol Model 220(8):1159–1168
28. Li H, Liang Y, Xu Q (2009) Support vector machines and its applications in chemistry. Chemometr Intell Lab Syst 95(2):188–198
29. Li H, Zhang W, Chen Y, Guo Y, Li G-Z, Zhu X (2017) A novel multi-target regression framework for time-series prediction of drug efficacy. Sci Rep 7(1):1–9
30. Li Y, Sun H, Yan W, Zhang X (2020) Multi-output parameter-insensitive kernel twin SVR model. Neu Netw 121:276–293
31. Liu D, Zeng X-A, Sun D-W (2015) Recent developments and applications of hyperspectral imaging for quality evaluation of agricultural products: a review. Crit Rev Food Sci Nutr 55(12):1744–1757
32. Manley M (2014) Near-infrared spectroscopy and hyperspectral imaging: non-destructive analysis of biological materials. Chem Soc Rev 43(24):8200–8214
33. Mastelini SM, da Costa VGT, Santana EJ, Nakano FK, Guido RC, Cerri R, Barbon S (2019) Multi-output tree chaining: an interpretative modelling and lightweight multi-target approach. J Signal Process Syst 91(2):191–215
34. Mastelini SM, Santana EJ, Cerri R, Barbon S (2020) DSTARS: a multi-target deep structure for tracking asynchronous regressor stacking. Appl Soft Comput 91:106215
35. Melki G, Cano A, Kecman V, Ventura S (2017) Multitarget support vector regression via correlation regressor chains. Inf Sci 415:53–69
36. Montgomery DC, Runger GC (2010) Applied statistics and probability for engineers. Wiley, Hoboken
37. Nolasco P, Marivel I, Badaró AT, Barbon S Jr, Barbon APAC, Pollonio MAR, Barbin DF (2018) Classification of chicken parts using a portable near-infrared (NIR) spectrophotometer and machine learning. Appl Spectrosc 72(12):1774–1780
38. Oliveira MM, Cruz-Tirado JP, Roque JV, Teófilo RF, Barbin DF (2020) Portable near-infrared spectroscopy for rapid authentication of adulterated paprika powder. J Food Composi Anal 87:103403
39. Porep JU, Kammerer DR, Carle R (2015) On-line application of near infrared (NIR) spectroscopy in food production. Trends Food Sci Technol 46(2):211–230
40. Reyes O, Ventura S (2019) Performing multi-target regression via a parameter sharing-based deep network. Int J Neu Sys 29(9):1950014–1950014
41. Santana E, Mastelini S, Barbon S Jr (2017) Deep regressor stacking for air ticket prices prediction. In: Anais do XIII simpósio brasileiro de sistemas de informação, pp 25–31
42. Santana EJ, Geronimo BC, Mastelini SM, Carvalho RH, Barbin DF, Ida EI, Barbon S Jr (2018) Predicting poultry meat characteristics using an enhanced multi-target regression method. Biosyst Eng 171:193–204
43. Santana EJ, dos Santos FR, Mastelini SM, Melquiades FL, Barbon S Jr (2020) Improved prediction of soil properties with multi-target stacked generalisation on EDXRF spectra. Preprint arXiv:2002.04312
44. Senthilkumar T, Jayas DS, White NDG, Fields PG, Gräfenhan T (2016) Detection of fungal infection and ochratoxin a contamination in stored barley using near-infrared hyperspectral imaging. Biosyst Eng 147:162–173
45. Spyromitros-Xioufis E, Tsoumakas G, Groves W, Vlahavas I (2016) Multi-target regression via input space expansion: treating targets as inputs. Mach Learn 104(1):55–98

46. Struyf J, Džeroski S (2005) Constraint based induction of multi-objective regression trees. In: International workshop on knowledge discovery in inductive databases, pp 222–233
47. Su W-H, He H-J, Sun D-W (2017) Non-destructive and rapid evaluation of staple foods quality by using spectroscopic techniques: a review. Crit Rev Food Sci Nutr 57(5):1039–1051
48. Tsoumakas G, Spyromitros-Xioufis E, Vrekou A, Vlahavas I (2014) Multi-target regression via random linear target combinations. In: Joint European conference on machine learning and knowledge discovery in databases, pp 225–240
49. Wu D, Sun D-W (2013) Advanced applications of hyperspectral imaging technology for food quality and safety analysis and assessment: a review—part I: fundamentals. Innov Food Sci & Emerg Technol 19:1–14
50. Wu G, Tian Y, Liu D (2018) Privileged multi-target support vector regression. In: 2018 24th international conference on pattern recognition (ICPR), pp 385–390
51. Xu S, An X, Qiao X, Zhu L, Li L (2013) Multi-output least squares support vector regression machines. Pattern Recognit Lett 34(9):1078–1084
52. Zhen X, Yu M, He X, Li S (2017) Multi-target regression via robust low-rank learning. IEEE Trans Pattern Anal Mach Intel 40(2):497–504